Quantitative and Portable Instrumentation for the Screening and Assessment of Pharyngeal Dysphagia

A Thesis Submitted to the University of Kent
for the Degree of Doctor of Philosophy
in Electronic Engineering

By

Martin Peter Joseph Henderson

May 2018

UNIVERSITY OF KENT

Quantitative and Portable Instrumentation for the Screening and Assessment of Pharyngeal Dysphagia

By

Martin Peter Joseph Henderson

Supervisors:
Dr. Gianluca Marcelli
Mr. Steve Kelly

A Thesis Submitted to the University of Kent
for the Degree of Doctor of Philosophy
in Electronic Engineering

May 2018

Corrections Added

January 2019

This thesis is dedicated to my wife, Abi, and to my daughter, Saskia.

Thank-you Abi, for your patience throughout this process,
and thank-you Saskia for the joy you bring me.

Acknowledgements

Firstly, I would like to thank Gianluca Marcelli and Steve Kelly for their guidance throughout the process of course of my PhD project. This thesis would not have been possible without their careful supervision.

My thanks go also to the technical staff of the School of Engineering and Digital Arts, particularly David O'Donnell, for their assistance in the fabrication of the various mechanical and electronic systems documented in this thesis.

Lastly, I would like to thank Ladan Najafi for her encouragement and support in writing up, and for giving me the space and time to complete this thesis.

Abstract

Dysphagia, the dysfunction of swallowing, is a common complication of neurological conditions, and presents increased risk of morbidity, mortality, and may critically reduce the subject's quality of life.
The early detection of dysphagia is essential to maintaining the subject's health, while accurate diagnosis of the physiological source of dysphagia is essential for successful treatment. 'Silent' dysphagia, where there are no outward symptoms, is a particular concern, as many screening processes rely on patients self-reporting difficulties.

A gap exists in available instrumentation, between simple techniques, which are subjective and require experience to employ, and highly sophisticated instruments, which are invasive to the patient and resource intensive. This thesis addresses this by exploring the possibility of developing instrumentation techniques which present the potential for portable, non-invasive solutions, which are relatively inexpensive and require dramatically less expertise to employ, enabling more effective dysphagia screening procedures to be introduced to clinical practice.

This thesis develops the means for measuring laryngeal motion by the use of a non-invasive throat-mounted sensor in four stages: firstly, a mathematical and a physical model of the larynx are constructed to develop our understanding of the relationship between laryngeal motion and sensor signals; secondly, swallowing sensor data was captured from 23 healthy participants; thirdly, the data from the participants was analysed to evaluate alternative data processing techniques, and to develop an understanding of practical factors deriving from inter-personal variations in physiology; finally, a prototype instrument was constructed, based on specifications evolved from our analysis.

Initial testing of the prototype instrument has demonstrated the validity of the concepts employed in its design: it is straight-forward to use, compact, portable, non-invasive, and can be used to quantitatively measure laryngeal elevation in a repeatable fashion.

Contents

List of Figures

Glossary

aspiration Bolus material partially or completely entering the trachea.. 2, 3, 18, 19

bolus A small, rounded mass for swallowing, containing either solids, liquids or both. x, xi, 2–5, 15, 16, 18–20, 55, 57, 58, 60, 69, 83–86, 93

deglutation The process of swallowing. 2, 9, 38, 66, 96, 123

I2C Inter-Integrated-Circuit bus - a digital communication bus typically used to connect peripheral integrated circuits (such as sensors) to a central processor unit. 61

pharynx The space at the back of the throat linking the oral and nasal cavities, the entrance to the airway, and the UES. 3, 20, 69

swallowing apparatus A composite term for the parts of the anatomy which aid in deglutation. 3

swallowing behaviour The manner in which the swallowing apparatus is operated, e.g. reflexes, timing of physiological events, speed of laryngeal elevation, patterns of muscle activation, etc.. 16, 40, 83, 84, 120, 126–129

Acronyms

ADC Analog to Digital Converter. 61

ANOVA anaylysis of variance. 101, 103

AP anterior-posterior. 15, 17, 18, 27, 32, 33

EMG Electromyography. 20

FEES Fiberoptic Endoscopic Evaluation of Swallowing. 18, 19, 117, 122

IMU Inertial Measurement Unit. 13, 22, 33, 45, 46, 54, 109, 122, 125

LES Lower Esophagal Sphincter. 4

LP laryngeal prominence. 3, 41–43, 46, 48, 49, 55, 58, 74–76, 79, 81–83, 88, 93–95, 99–101, 104–107, 113, 114, 122, 125, 126, 128

LSM Laryngeal Strap Muscles. 3, 41

MDD Medical Device Directive. 29, 128

MEMS micro electro-mechanical system. 22, 24

PID Participant IDentification number. 56, 57, 63

sEMG Surface Electromyography. 20, 117, 124

SI superior-inferior. 15, 27, 32, 33

UES Upper Esophageal Sphincter. xiv, 3, 4, 16, 116

VFSS Videofluoroscopic Study of Swallowing. 15, 18, 117, 122

Nomenclature

μ	Coefficient of friction
ϕ	Rotational velocity
ρ	Pearson's correlation coefficient
θ	Tilt angle
θ_α	Tilt angle calculated using an accelerometer
θ_γ	Tilt angle calculated using a gyrometer
c_x	Horizontal coordinate of the sensor centre-point
c_y	Vertical coordinate of the sensor centre-point
e	Error - the difference between a measured value and the theoretical true value.
$e_{\theta.\alpha}$	Error in the tilt computed using an accelerometer
$e_{\theta.\gamma}$	Error in the tilt computed using a gyrometer
G	Gravitational pull, an acceleration approximately equal to $9.81ms^{-2}$
l	The length of the sensor
x	horizontal axis acceleration (absolute axis) – used as approximation of AP axis
x'	accelerometer X axis output (relative axis)
y	vertical axis acceleration (absolute axis) – used as approximation of SI axis
y'	accelerometer Y axis output (relative axis)

Chapter 1

Introduction

1.1 Thesis Overview

This thesis presents interdisciplinary research which applies engineering principles to the evaluation and design of instrumentation intended for clinical screening, diagnosis, and evaluative processes.

The topic of the research is pharyngeal dysphagia, and the main technologies developed upon are accelerometry and gyrometry.

The methods used in this thesis include mathematical modelling, physical modelling, regression analysis, and exploratory research featuring healthy participants.

Several important discoveries regarding the application of accelerometry and gyrometry to the measurement of laryngeal elevation are presented. The design of an instrument based on our findings, and the construction and testing of a prototype based on this design are also presented.

Recommendations for future research, and guidance for future work that may develop on the technologies studied in this body of work are presented in the discussion.

1.2 Motivation for Research: Dysphagia

Dysphagia, or the dysfunction of swallowing, is a major cause of morbidity, mortality and malnourishment [1]. Hospital stays are lengthened by dysphagia and quality of life is greatly reduced [1]. Dysphagia presents commonly as a complication of neurological conditions [2]–[5]. The Royal College of Physicians advise that it is "essential" to the care of stroke patients that dysphagia is detected as early as possible [6]. The greatest danger presented by dysphagia is food or drink entering the airway. This is termed aspiration, and commonly results in chest infections, such as pneumonia [4], [5]. It may be argued that the goal of dysphagia treatment is to minimise risk of aspiration.

Silent aspiration is a particular concern to clinicians [7]. It has been a past assumption that ingestion of food and drink into the airway would necessarily cause discomfort, and result in coughing or choking, however studies have shown that up to 39% of dysphagic stroke patients, 77% of dysphagic traumatic brain injury patients, 78% of dysphagic patients with intellectual or motor disabilities and 96% of children with developmental dysphagia aspirated silently [7], [8] – these are routinely missed by many of the simple tests and screening tools available to clinicians.

1.2.1 Deglutation: The swallowing process

To understand the approach taken in this work, it is important to have an understanding of the swallowing process and swallowing apparatus.

Deglutation is the term for the entire swallowing process, in which a bolus travels from the lips to the stomach. As deglutation involves a series of separate processes, it is usually divided into three phases: oral, pharyngeal and esophageal. The oral phase begins at the lips, ends when the bolus enters the pharynx, and is mostly

concerned with *preparation* of the bolus for transport. This phase involves salivation, chewing, and manipulation of the bolus with the tongue. The pharyngeal phase begins as the bolus enters the pharynx, and ends when the bolus passes the Upper Esophageal Sphincter (UES). This phase mostly involves *protection* of the airway. The esophageal phase begins as the bolus enters the UES, ends when the bolus enters the stomach, and is simply a process of the bolus being pushed along as efficiently as possible.

1.2.2 The anatomy of swallowing

The swallowing apparatus used in each swallowing phase, together with its function, is outlined below. The relative position of parts of the anatomy referenced below can be seen in figure 1.1.

Oral phase In the oral phase, the teeth, lower jaw, and masseter muscle are used for chewing [9], which has the function of breaking solids into smaller pieces [9]. The orbicularis oris muscles are responsible for keeping the bolus in the mouth [9], [10]. The salivary glands produce saliva, which lubricates the bolus, and contains enzymes which begin the digestion process [9]. The tongue is used to move the bolus around the mouth, and to push the bolus into the pharynx once it is sufficiently smooth and lubricated [9].

Pharyngeal phase The epiglottis and vocal folds act to protect the airway (trachea) from ingress of the bolus [9], [11] (i.e. aspiration.) The larynx, cricoid, hyoid bone, connecting tissue, and Laryngeal Strap Muscles (LSM) assist in widening the pharynx, moving the entry to the airway and pushing the bolus towards the UES [11], [12]. The laryngeal prominence (LP) is visible beneath the skin and can be used to see and feel (palpate) the laryngeal elevation [9].

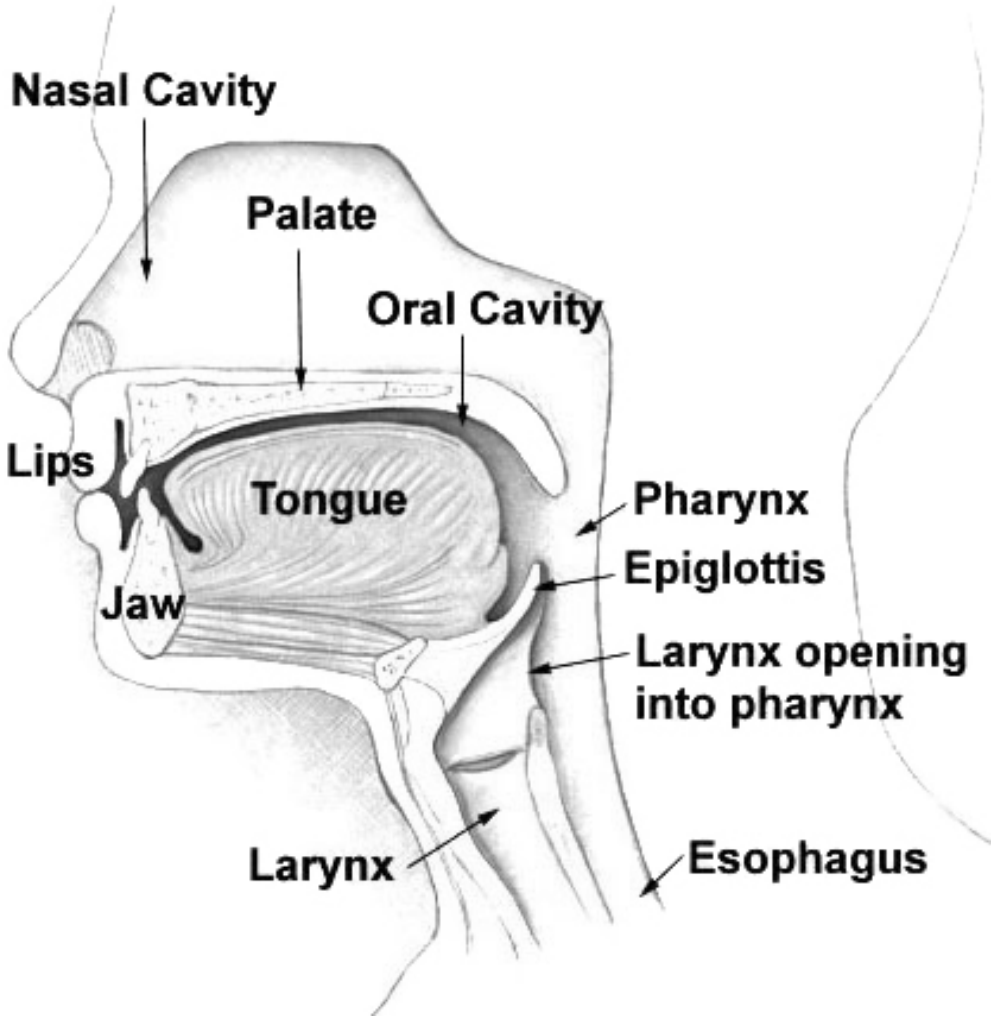

Figure 1.1: *An illustrated cross-section of the head and neck. By Arcadian [Public domain], via Wikimedia Commons.*

Esophageal phase The UES opens to allow the bolus to progress [11]. The esophagus is a fibromuscular tube [9], [10], which constricts in waves to push the bolus along towards the stomach [10], [12]. The Lower Esophagal Sphincter (LES) closes to prevent stomach acid from entering the esophagus, and opens to allow the bolus to enter the stomach [10], [12].

1.2.2.1 Dysphagia Etiology

Dysphagia is essentially the result of disruption to any of the mechanisms described above, which may be as a result of injury, disability, age [13], disease, or stroke [3]. There is disagreement on whether age-related swallowing impairment should be regarded as dysphagia, or as a normal result of age, so as to reserve the term for more severe impairment [14]. The term 'presbyphagia', meaning *old-age swallowing*, is used to aid this distinction [15]. Dysphagia that originates from disruption to the nervous system is commonly referred to as neurogenic dysphagia [11], [16]. Dysphagia is also a common result of pharyngeal or esophageal cancer [17], as tumours may block the passage of a bolus, or reduce the efficiency of airway-protection mechanisms. In addition, surgery to remove such tumours, as well as other head-and-neck procedures (for example, glossectomy) may also result in dysphagia due to the disruption of swallowing anatomy [18].

1.2.3 The Purpose(s) of Dysphagia Instrumentation

Dysphagia instrumentation has multiple distinct purposes, falling roughly into three categories:

Screening A pre-diagnosis process designed to provide a high degree of confidence that the patient is at *low* risk of dysphagia, allowing them to leave the care pathway. Those that are not cleared by the screening process are referred for a full assessment. As the usual intention of screening is to spare diagnostic resources, it is important that the screening process is either quicker, cheaper, or requires less expertise to carry out, than a full diagnosis. Preferably, the screening procedure will be all three.

Diagnosis A process designed to determine, in as much detail as possible, the na-

ture and cause of a patient's complaint. A patient who has been referred to a dysphagia specialist with suspected dysphagia must be examined in greater detail, using sophisticated instruments and techniques, so that the most appropriate treatment or intervention may be prescribed.

Monitoring, or Progress Tracking To determine if the patient's condition is improving or deteriorating over time, the symptoms of dysphagia are quantified and recorded. Ideally, instrumentation assists in the quantification of symptoms. There must also be adequate consistency in the measurements for the clinical significance of changes to be judged by the clinician.

Both screening and monitoring are best served by quantitative measurements, so that they can be carried out by non-specialist clinicians. Imaging and other types of non-quantitative instrumentation types may be appropriate for diagnosis, as it is carried out by experts.

1.3 Dysphagia Screening

There is currently a gap in appropriate instrumentation for assessing dysphagia, between the simple, subjective techniques that may be used to detect warning signs, and the complex, expensive, invasive techniques which require specialist interpretation, but provide the clinician with a sufficiently comprehensive view of their patient's deglutation to perform a diagnosis [19].

Single clinical features, such as gagging have low sensitivity and specificity [2], [4], and are inconsistent across studies [2], [4]. As a result, best practice for screening is currently an aggregation of simple tests conducted in a standardised way (called swallowing screening tools (SSTs)), but the fact that no SST has achieved consensus [2] is indicative of the lack of efficacy of such tools. There is, however, evidence

that use of a SST produces significantly better outcomes than no tool at all [20].

1.3.1 Theory of Screening

Effective screening processes are necessary to ensure that, firstly: health problems are detected early, before they develop into disease [2], [21], [22], and secondly: specialists' time, or expensive resources, are not wasted by application to large numbers of people who do not need intervention [2], [21], [22].

A screening process must first identify as high a proportion of those who are at risk as possible (achieving high sensitivity,) then eliminate as many of those at risk who require no further treatment as possible (achieving high specificity,) with as little requirement of specialist resources as possible (achieving cost-effectiveness).

1.3.2 Ethics in Screening

To be ethical, screening must be applied in such a way as that the benefit to the patient – in terms of increasing the likelihood of successful intervention – outweighs the harm to the patient – in terms of worry caused by false positives, unnecessary interventions and indeed undergoing the screening procedure itself, if it involves the use of invasive techniques [21].

1.3.3 Specifications for a Screening Instrumentation Technique

It is well established which sections of the population are at most risk of dysphagia: stroke victims [2], [3], those with neuro-degenerative conditions [4], [5], [11], learning disabilities [23], and cerebral palsy [24]. It is also well established that repeated and unexplained bouts of pneumonia, other chest infections and reduced nutrition are

also indicative of dysphagia [2], [9], [20], [25].

Current limitations of screening lie in narrowing down patients from those who have been identified as at-risk, mainly due to limitations in available instrumentation techniques [2], [11], [22], [25].

As it is important that a screening process can be carried out by as wide a range of healthcare professionals as possible, instrumentation for this purpose must require minimal training to be used effectively [22]. As it is important that a screening process is carried out widely, it is important that the equipment necessary is not overly expensive. It is similarly important that the instrumentation is minimally invasive [26] and preferable that it is portable [26]. Finally, it is vital that it takes quantitative measurements, as, for the performance of a screening process to be consistent, it is the designers of the screening process – who should be experts in their field – who make decisions on thresholds for further investigation; judgement calls should not be required of those carrying out the screening tests, who (as stated above) may be minimally trained, and not experts in dysphagia.

The work documented in this thesis was therefore carried out with the aim of developing instrumentation techniques which meet the above requirements, and are suitable for providing a quantitative measure which may aid calculation of an individual's risk of dysphagia, as well as assist in identifying the cause thereof.

1.4 Research Rationale and Objectives

The development of instrumentation that is portable and non-invasive, that requires minimal training to use, that is relatively inexpensive to manufacture, and can be used to take quantitative measurements of deglutation physiology, is of vital importance to the future of assessment, screening, diagnosis and monitoring of dysphagia.

Of further concern is the detection of silent aspiration, as many existing screening tools rely on visible or self-reported discomfort and difficulty with swallowing, for example choking and coughing – such signs are absent in patients with severe paresis of the larynx, potentially leaving such individuals undiagnosed for a critical length of time, allowing secondary pneumonia and other complications to occur.

Accelerometry has been used as the basis of a number of experimental bedside clinical examination systems, but has not been adopted more widely, as there are significant unanswered questions regarding what is actually being measured.

The objectives of the work described in this thesis are therefore:

1. To examine the underlying physiology of the pharyngeal phase of deglutation
2. To model the relationship between laryngeal motion and the sensor's output
3. To better explain and interpret the accelerometer's signals
4. To prepare the grounds for the development of a viable instrument for assessment and screening of dysphagia

1.5 Thesis Organisation

Chapter 2: Literature Review reviews relevant literature to establish the state of art.

Chapter 3: Methodology defines the models used to describe how laryngeal motion is measured by the sensors and describes the methods and materials used to capture data from human participants.

Chapter 4: Results presents the results from experiments following the methods described in chapter 3.

Chapter 5: Further Analysis and Instrument Design contains analysis of the results from chapter 4 in the context of objective 4 of this body of work (see section 1.4 of this chapter), and charts the development to-date of a prototype instrument.

Chapter 6: Discussion discusses the results from chapter 4 and analysis from chapter 5 in the context of the literature reviewed in chapter 2, to develop on emergent themes, make further recommendations, and conclude the thesis.

1.6 Contributions

The contributions of this thesis to new knowledge lie within the realms of physiological modelling, engineering analysis and instrument design, and have clinical implications for the assessment of dysphagia. The specific contributions are as follows:

1. The development of a simulation model which describes the basic motion of the larynx during deglutation, and simulates the effect of laryngeal prominence size, and speed of laryngeal elevation, on a throat mounted sensor (chapter 3)

2. The development of a mechanical model of the human throat, which simulates laryngeal elevation, and allows for a sensor to be mounted on the model's skin (chapter 3)

3. The development of a data capture system, which records accelerometer and gyrometer signals, and displays them in real time (chapter 3)

4. It is demonstrated that a throat-mounted sensor will tilt in response to laryngeal elevation (chapter 4)

5. It is demonstrated that the size of a subject's laryngeal prominence will directly impact the peak of accelerometry signals (chapter 4)

6. It is established that the tilt of a sensor positioned immediately superior to the laryngeal prominence increases linearly with elevation of the larynx, given that the length of the sensor is greater than the peak laryngeal elevation (chapter 4)

7. The principle that the combination of two inertial measurement units with knowledge of a subject's laryngeal prominence size is sufficient to accurately measure laryngeal elevation over time (chapter 5)

1.6.1 Talks and Conference Presentations

- *Quantitative and Portable Instrumentation for Dysphagia* was presented [27] at the International Graduate Forum on Advanced Instrumentation and Measurement Technology 2014, annexed to the 5th International Symposium on Test Automation Instrumentation in Beijing.

- The developing work was presented yearly in group seminars to the University of Kent Instrumentation, Control and Embedded Systems Research Group.

1.6.2 Conference Posters

- *The use of Gyrometry to correctly interpret accelerometry in dysphagia* was accepted as abstract [28] to the 5th European Society for Swallowing Disorders Congress 2015 in Barcelona, and presented in poster format.

- *Quantitative and qualitative instrumentation for dysphagia* was accepted as abstract [29] to the 5th UK Swallowing Research Group Conference in London, and presented in poster format.

1.6.3 Manuscript

- A research paper manuscript titled *Cross-disciplinary approach to quantifying the effects of individuals physiology on laryngeal accelerometry* has been written, pending submission for publication.

Chapter 2

Literature Review

In this chapter, we examine the literature relevant to the topic of this thesis, to establish the state of art and the evidential basis for our methods. Due to the inter-disciplinary nature of the topic, we cover the basic knowledge required for both the technical and clinical reader to follow the work presented and discussed in this thesis. The chapter begins with the physiological, proceeds with the clinical, before focusing on the technical aspects of laryngeal dysphagia instrumentation.

In sections 2.1 to 2.3 we examine the clinical side, in order to establish what is known about the condition of dysphagia. We briefly look at the history of the study of swallowing disorders, before focusing on silent aspiration, which presents a particular challenge to the screening and assessment of dysphagia.

Section 2.5 lists the instrumentation techniques used in current clinical practice, as well as those under active research in the literature. As accelerometry is selected as the basis for the work in this thesis, the theory of the family of device that accelerometers belong to, Inertial Measurement Unit (IMU), is introduced in section 2.6.

In section 2.7, the detail of research into laryngeal accelerometry is critiqued,

while in section 2.8 the regulatory concerns for the development of medical devices is introduced.

The chapter is concluded in section 2.9 with a summary of findings, which serve as a justification for the approach presented in chapter 3: Methodology.

2.1 Study of Swallowing Disorders

Swallowing disorders have been the subject of scientific study for several hundred years, over which period the approach to and categorization of dysphagia has undergone several changes. While references to dysphagia can be found in lists of maladies from as early as 1768 [30], it appeared to be viewed in literature as a (possibly fatal) symptom of another condition [31]–[33] rather than a condition to be studied in itself. Cases which report dysphagia as the primary condition of study appear in literature in the 1940's, such as a case reported by Thorpe [34], which is cured by tonsillectomy. Categorization of dysphagia around swallowing phase appears in literature from around 1960 [35], [36], as does literature regarding oral, pharyngeal, and esophageal dysphagia separately, and as a primary condition [37], [38].

Research into dysphagia tends to be targeted towards patient groups who share a particular diagnosis (e.g. cerebral-vascular accident, motor-neurone disease), which makes it difficult to gain a complete view of its incidence in the general population; indeed there is a far greater quantity of literature regarding dysphagia in stroke patients than of any other patient group.

Huckabee, Lamvik and Jones investigated pharyngeal mis-sequencing as a mechanism causing dysphagia, and criticised the undue focus on weakness only, especially in the prescription of effortful swallowing as a compensation technique where it is inappropriate [39].

2.2 Silent Aspiration

Silent aspiration is the term for ingestion of a bolus, or part of a bolus, into the airway with no outward symptoms – i.e. no gagging, coughing or choking. There is significant concern that many early assessment procedures are insensitive to silent aspiration, as they rely greatly on self-reported difficulty swallowing, and simple observation of a clinician, for example in the water-swallow test. A retrospective study by Smith et al. [8] of Videofluoroscopic Study of Swallowing (VFSS) from 1101 patients, with diverse diagnoses, visiting two acute care hospitals over a two year period, found that of the included patients who aspirated (467 patients, 43%), 59% (276 patients) aspirated silently. Other studies provide estimates for the incidence of silent aspiration which range from 28% to 94%, for varying populations [7], [8].

The mechanisms by which silent aspiration occur are known to include muscle weakness (affecting the efficiency of protection mechanisms,) reduced sensation in the pharynx (preventing the triggering of protective reflexes and/or impairing or delaying the swallowing reflex,) and impaired ability to produce a reflexive cough [7].

2.3 Laryngeal Motion During Swallowing

Failure to elevate the larynx was identified as a cause of dysphagia as early as 1912 [40], when Hill and Hope discuss whether a case study's failure to swallow was due to a spasm of the oesophagus, or paresis of the larynx, and conclude from x-ray examination that "the food stuck in the pharynx and did not enter the œsophagus," due to "no effort [being] made to pull the larynx upwards and forwards and away from the spine."

Zoratto [41] measured the motion of the larynx and hyoid in two dimensions (superior-inferior (SI) and anterior-posterior (AP)) in 20 female and 23 male patients

with neurogenic dysphagia, describing the typical displacement of the larynx as 10 mm in the superior direction, and 10 mm in the anterior direction.

Cook et al. [42] measured the transit times of 2 to 20 ml boluses in 21 healthy male subjects using a combination of manometry, videofluoroscopy and EMG. The study found that timings are dependent on bolus size – larger boluses pass the oral phase, and begin the esophageal phase, quicker than small boluses – and that the average transit time for the pharangeal phase was 0.6 s. The specific timing of laryngeal elevation was not included in the study. Dantas et al. [43] conducted a similar study with 10 healthy males, which measured an average pharangeal phase transit time of 0.43 s for liquid boluses and 0.53 s for paste boluses.

Mendell and Logemann [44] looked at the kinetic timings of swallowing-related structures including the larynx, finding that age, bolus size and bolus texture all affect the timings of movements of the measured structures.

Study of hyoid movement is has been included in some studies [41] and the focus of others [45]. The general consensus found in literature is that during pharyngeal deglutation, a number of processes involving the larynx, hyoid and muscles in the region work together (in healthy swallowing behaviour) to seal the airway, open up the UES, and propel the bolus swiftly through the pharynx and into the esophagus; where there is a deficit in one of the complementary processes, strengthening of the other processes may be effective in compensating.

Dysphagia tends to be manifest where there is a deficit in multiple processes simultaneously – which is the natural history for neuro-degenerative diseases, stroke, many learning disabilities, cerebral palsy, and other conditions associated with dysphagia. Dysphagia also occurs where there is a physical disruption of the swallowing apparatus, as is common with throat and esophageal cancers, and where there has been surgery to the throat leaving alteration of the anatomy and/or significant scar

tissue.

2.4 Laryngeal Dimensions

Kahane [46] studied how the larynx changes in size and shape in children of 9 to 18 years of age, noting divergence between boys and girls being detectable from puberty, and that the female larynx reaches maturity more quickly than the male. Litman [47], in a study of children of ages 0 to 14 years, concluded that male and female dimensions were "essentially the same" over this age range. The focus of both of these studies is on the general shape of the larynx, the length of the larynx, and the size of the vocal folds. Litman found that the larynx grows from a conical shape to a rectangular shape as the child grows. Both demonstrated a linear increase in the length of the larynx up to the age of 12 years.

In adults, the larynx is significantly larger in males than females, with an average length of 44 mm in males and 36 mm in females, and an average AP diameter of 36 mm in males and 26 mm in males [10].

The literature features studies of cadavers, and does not include measurements that can be taken in a non-invasive manner.

2.5 Dysphagia Instrumentation Techniques

The state of art for instrumentation available to clinicians for use in the evaluation of dysphagia is outlined in this section.

In reviewing the breadth of instrumentation techniques, Steele observed that the different options essentially each measure different aspects of swallowing, and compared the state of art to the Indian parable of the six blind men and the elephant [48], in which each of six blind men examine a different part of an elephant

and then proceed to argue about the true nature of the elephant, as none can see the whole picture, only the trunk, tail, knees, etc. It is for this reason that it is important to understand the limitations of each technique, as well as the strengths.

2.5.1 Videofluoroscopy

Videofluoroscopic Study of Swallowing (VFSS) succeeded cinefluoroscopy in the '70s as the gold standard for diagnosis of dysphagia and related throat conditions [49]–[53].

Videofluoroscopy is the construction of video from a rapid series of x-rays. VFSS is videofluoroscopy of the throat, recorded while the subject swallows a radiographically dense medium, such as a barium sulphate solution. The progression of the bolus can be viewed by the clinician on the VF video.

VFSS is normally configured to provide the clinician with a side-on (lateral) view of the patient's head and throat, however front-on VF (AP axis) is sometimes used, but this is far less common.

VFSS is considered valuable for rehabilitation, as it provides immediate feedback; this is valuable for making decisions and educating the patient [49]. In particular, VFSS is useful for detecting excess residue and aspiration [49], [51].

The drawbacks of VFSS are that it is expensive, requires specialist operation, and is not suitable for repetitive follow-up testing [11], [49], particularly for paediatric patients, due to a significant radiation dosage [16], [54].

2.5.2 Fiberoptic Endoscopic Evaluation of Swallowing

Fiberoptic Endoscopic Evaluation of Swallowing (FEES) is an evaluation procedure in which an endoscope is inserted along the nasel passage to gain a top-down view of the oro-pharangeal cavity during swallowing. FEES is commonly used as an

alternative to VF in clinical practice [51], [52], although the two instrumentation techniques are complementary, and differ in sensitivity to elements of dysphagia [52], [55].

FEES provides the clinician with a top-down view of the vocal folds, epiglottis and oesophagus, but no view at all of the oral phase of pharyngeal phase. Penetration into the upper airway can usually be seen, and FEES is the "test of choice" for studying residue left in the pharynx [51], but aspiration into the lungs can only be inferred; no confirmation of aspiration can be made using FEES alone.

A major weakness of FEES is that at the moment of swallowing, if the patient has any swallowing reflex at all, the convulsions in the pharynx cause the image to lose focus [55] and effectively disappear during the pharyngeal phase, meaning that the clinician is only certain of a clear view before and after the bolus passes through the pharynx, and may therefore miss a crucial event.

2.5.3 Auscultation

Auscultation, or the use of a stethoscope to listen to physiological sounds, is a very basic technique used to evaluate dysphagia, but one of the few tools available to clinicians in long-term care [26], [56]. As the vocal folds close, they produce an audible 'click' sound [26]; if this can be heard, it indicates that the subject is protecting their airway from ingression of the bolus. Absence of this sound is a warning sign that they may suffer from dysphagia. In addition, an exhalation should be heard soon after the swallow, and it should sound clear of fluids [56].

The subjectivity of this technique is clear [26], as clinicians report that recordings of breath sounds during swallowing do not sound like what they are used to hearing through a stethoscope [57], due to differences in frequency response [57]. Clinicians have similarly reported difficulty identifying swallowing sounds where

throat-mounted accelerometers have been used to record sound.

Literature supports the use of auscultation to evaluate swallowing, but cautions that it should be used in conjunction with other instruments [58].

2.5.4 Palpation

Palpation of the throat, or the use of fingers to feel the larynx during swallowing is a crude technique used to evaluate strength of elevation of the larynx [55], [59]. The larynx can be felt to elevate sharply as the bolus transits the pharynx. Anomalous laryngeal movement (such as sideways movement) can be easily detected [59], which is indicative of UES function impairment [59].

2.5.5 Electromyography

Electromyography (EMG) is the detection of muscle activation using electrodes. Where the electrodes are attached non-invasively to the skin, this is referred to as Surface Electromyography (sEMG). While not yet widely used for assesment of dysphagia in a clinical setting [11], there are some commercial solutions available.

Typically, electrodes are placed on the skin covering the laryngeal strap muscles to evaluate the swallowing reflex.

While EMG can be used to infer muscle recruitment, it requires knowledge of the strength of the muscles involved to use EMG to measure force of activation. EMG is best thought of as a measure of *intent* and *perceived effort* regarding muscle use, as a subject with relatively weak muscles will commonly record greater EMG activity than a subject with relatively strong muscles, while the muscle is exerting the same force on an external object [60].

Proponents of sEMG argue that it should be the first step in differential diagnosis of neurogenic dysphagia [11].

2.5.6 Accelerometry

Accelerometry of the larynx is the application of an accelerometer to the skin covering the larynx to indirectly measure motion of the larynx. The information obtained using this technique is comparable to palpation, as both techniques ultimately infer physiology from surface movement. Unlike palpation and simple auscultation, however, accelerometry data can be recorded and interpreted separately and objectively.

Proponents of accelerometry argue that it is non-invasive, portable and inexpensive [54], [61]–[63], detects swallowing sounds [64], and is quantifiable [54].

Detractors argue that accelerometry is poorly understood [65], and that existing systems lack sensitivity [22].

A review in 2015 [22] found that the vast majority of studies using accelerometry to assess dysphagia concerned themselves exclusively with post-stroke adults, limiting the generalisability of results.

Attempts have been made to construct classifiers for distinguishing healthy swallows from dysphagic swallows [61].

2.5.7 Other Dysphagia Assessment Tools

2.5.7.1 Water Swallow Test

The water swallow test is commonly used for screening, as it is simple to administer, with little risk to the patient, and is suitable for use with paediatric patients [66]. The patient is asked to swallow 3-oz of water; if the patient coughs or chokes during the task, then they are considered to have failed the water swallow test, and assessed as at risk of dysphagia [53]. The test is found to have good sensitivity, but poor specificity [67], [68].

2.5.7.2 Questionnaires

Questionnaires which combine symptoms which correlate with dysphagia, such as the Sydney Swallow Questionnaire [69], [70] and Burke Dysphagia Screening Test [53], can be effective dysphagia screening tools [71], with the added benefit that they can allow the patient to self-report their symptoms.

2.6 Inertial Measurement

Accelerometers and Gyrometers are known as inertial measures (or Inertial Measurement Unit (IMU),) as they exploit the physical property of inertia in small masses to measure their respective quantities of acceleration and rotational velocity [72].

The work reported in this thesis is concerned primarily with investigation of the use of inertial measures as a method of detecting and measuring laryngeal elevation, so it is appropriate that a summary of their functions be included here:

2.6.1 Theory of Accelerometers

The design and testing of MEMS accelerometers are specified by IEEE standard 1293-1998 (R2008) [73]. Accelerometers contain a small mass (the proof-mass), suspended between proximity sensors. As the sensor unit is accelerated, the proof-mass resists the change in velocity and is thus displaced relative to the sensors. This displacement is a function of the acceleration, so the acceleration can be calculated as the inverse of this function. Modern accelerometer are typically micro electro-mechanical system (MEMS), in which the proof-mass is cut from the silicon substrate and used as one pole of a capacitor. The acceleration of the sensor unit is a function of the capacitance between the proof-mass and electrodes mounted on glass wafers either side [72] (as shown in figure 2.1.)

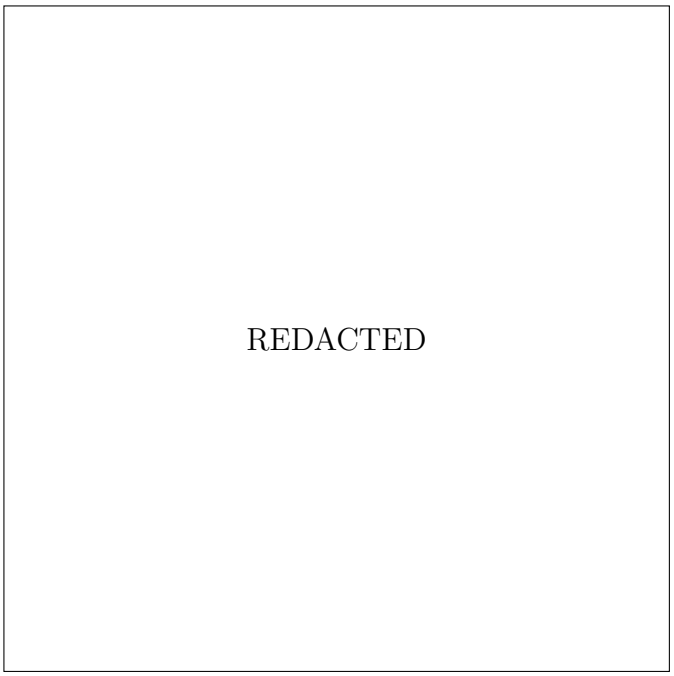

Figure 2.1: *Exploded view of a 1D MEMS Accelerometer. Adopted from Prasad (2011) [72]*

As capacitance is inversely proportionate to the distance between the capacitor's two plates (in this case the proof-mass forming one plate, and each electrode the other,) only acceleration along the axis between the top and bottom electrode through the proof-mass will produce a signal. Oblique accelerations will produce a signal attenuated according to the cosine of the angle between the acceleration and the axis of the accelerometer. Two- and three-dimensional accelerometers are formed by duplicating the MEMS structure at right-angles. A three-dimentional accelerometer is necessary to determine the direction and magnitude of arbitrary accelerations.

2.6.2 Theory of Gyrometers

Gyrometers (also called electronic gyroscopes) measure rotational velocity. While 'gyroscope' is more commonly used, the author prefers the term 'gyrometer', as

it better describes the device's function – the suffix *-meter* (from Ancient Greek $\mu\acute{\epsilon}\tau\rho o\nu$, "measure") is used to denote a measuring device; the suffix *-scope* (from Ancient Greek $\sigma\kappa o\pi\acute{\epsilon}\omega$, "examine, inspect, look to or into, consider") is used to denote a viewing device – and is more commonly used by manufacturers of such devices. The design and testing of MEMS gyrometers are specified by IEEE standard 1431-2004 [74]. A proof-mass is suspended in a plane (xy) perpendicular to the axis of rotation (z,) and vibrated along one axis (x) while the amplitude of vibration along the other axis in-plane (y) is measured. Transference of the vibration from x to y, due to the Coriolis effect, is proportional to the rotational velocity around z [75], as shown in figure 2.2 as the gap between xy and $\xi\eta$.

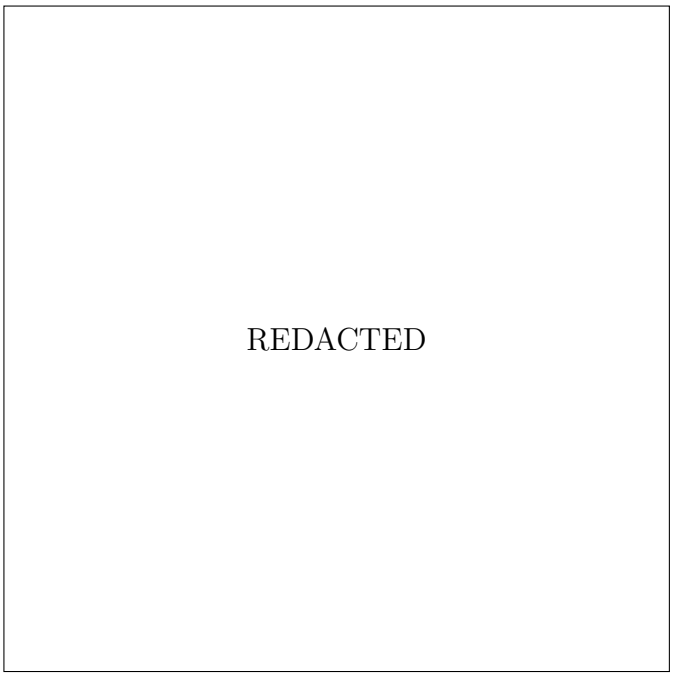

Figure 2.2: *Theoretical model of a single z-axis vibratory gyroscope consisting of a proof mass m suspended in the xy plane. Adopted from Trusov (2011) [75]*

2.6.3 LSM9DS0 Inertial Measurement Unit

In the work detailed in this thesis, a LSM9DS0 integrated accelerometer and gyrometer is used, and, where the specific implementation is relevant, references to accelerometers and gyrometers (or in combination as the 'sensor') are to be understood as refering specifically to a LSM9DS0, which is mounted on a 16mm diameter, circular-shaped circuit board. The LSM9DS0 has an on-chip sampler, communicates using an I^2C interface, and has a sampling rate of up to 1.6kHz (accelerometer) and 760Hz (gyrometer) [76].

2.7 Critique of Laryngeal Accelerometry in the Literature

2.7.1 Laryngeal Accelerometry

O'horo et al. conducted a review of bedside diagnosis of dysphagia in 2015 [22], and reported there to be a "preponderance" of accelerometry studies centred on post-stroke adults, causing them to question whether the systems studied can be generalised to other forms of dysphagia.

Reddy et al. [63] observes that healthy subjects produce a consistent accelerometer pattern, whereas in dysphagic subjects, the pattern is either absent, or delayed. Reddy argues that as accelerometry provides a tool for continuing patient assessment and demonstrating the clinical improvements, by correlating the accelerometry peak with laryngeal elevation. In addition, Reddy emphasises that laryngeal accelerometry is non-invasive, which would make its use preferable to invasive instrumentation techniques of equivalent clinical utility.

Firmin et al. [77] compared the performance of several non-invasive experimental

systems for detecting dysphagia, and found the accelerometer and electrolaryngograph to be"distinctly more useful" than an ear-probe or a neck-mounted microphone in identifying swallowing events. The electrolaryngograph, which measures vocal fold vibration using electrical impedance across the larynx, is not used clinically for assessment of dysphagia as adjustment of the device to measure laryngeal elevation "requires a care in adjustment, which makes it difficult to apply in a clinical environment."

Reddy conceded in 2000 that "the underlying physiological events that give rise to the acceleration signal are poorly understood" [78].

While Gupta investigates the effectiveness of the accelerometer peak in predicting laryngeal elevation [79], the underlying mechanism by which laryngeal elevation 'accelerates' the sensor positioned "at the level of the thyroid cartilage" [78] is neither proposed nor tested. The direct correlation between the accelerometer peak and laryngeal elevation is disputed by Zoratto, who observed that peak acceleration does not coincide with peak hyolaryngeal elevation [41]. The sensor in literary studies is fixed only to skin, and therefore free to rotate as the skin flexes, so it seems apparent to the author that the acceleration signal, reported as $1G$ for healthy participants in the literature [78]–[80], may be at least partially caused by rotation. This could be readily investigated by the inclusion of an integrated gyrometer. Whether rotation of the sensor occurs has important implications: the mechanisms by which greater rotation occurs become implicit indicators for lower risk of dysphagia – this has yet to be scrutinised.

The literature has demonstrated that laryngeal accelerometry can be clinically useful [62], [77], [78], [80]–[85]; its physiological basis must be clarified, however [41], [78].

Multiple Axes Zoratto [41] correlated the trajectories of the hyoid and larynx, measured using videofluoroscopy, with accelerometry signals, and argued that, as there is a signal in both the AP and SI directions that correlates with excursion and elevation of the structures respectively, that SI motion must correlate with SI accelerometry and AP motion with AP accelerometry. This is a misconception: as the accelerometer rotates, the axis labelled 'AP' will become increasingly unaligned with the anterior-posterior axis orthogonal to the throat. To give an extreme example, the 'AP' accelerometer may rotate to the point that it is measuring SI acceleration. In Zoratto's results, excursion and elevation are measured to occur simultaneously, as is the AP and SI accelerometry peaks, which means that the causality of the two axes cannot be easily separated. Zoratto does not, in her methodology, detail any means of preventing rotation in the throat-mounted accelerometer, and neither do any other authors of relevant literature for dual-axial [62], [83], [86]–[94], or tri-axial accelerometry [84], [95], [96] applied to dysphagia. Greco et al. prevent rotation from having an impact on results by using the root-sum-square of the three accelerometer axes [84], which has the effect of making the sensor non-directional.

Head Movement Sejdić et al. and Lee et al. identify head movement as a source of noise in accelerometry data, characterised by high-amplitudes and low frequencies in accelerometry signals [62], [86], [92], for which Sejdić proposes a filter based on a spline least square approximation of the base signal. It is common in literature for dysphagia accelerometry systems to use band-pass filters (with a low cut off frequency of 0.1 - 30 Hz across studies, and a high cut-off of 300 - 3000 Hz across studies) in hardware [41], [78], [80], [86], however the reasoning behind this – particularly the reason for specific filter parameter values – is not explained beyond a reference to "de-noising". Possible mechanism(s) by which head movement

is detected by the accelerometer is not explored in literature. There is also no discussion on the likely impact that such a filter will have on the validity of the filtered data.

Segmentation and Classification Multiple studies have looked at the development of automatic segmentation algorithms [62] for identifying the start and end of swallows, and of classifiers [81], [82], [97], [98], which discriminate between healthy and dysphagic swallows using analysis techniques such as wavelet decomposition. None of these studies address the uncertainty regarding the physiological source of swallowing signals (as identified above,) nor do the authors consider that dysphagia itself has multiple possible physiological causes, and that it is therefore likely that it may result in a plurality of pathological signal patterns.

2.7.2 Laryngeal Gyrometry

A search which used keywords *dysphagia, gyrometer, gyrometry, gyroscope* returned no relevant results. When searching for references in the entire text, 144 papers were returned which contained dysphagia *and* a reference to gyrometry, but none of these applied a gyrometer to the throat in their methodology. Typically, the topic of the papers were to investigate the use of a gyrometer in measuring either head tilt [99], or posture [100]. As such, application of gyrometry to the throat to study movement of the larynx is, to the knowledge of the author, entirely novel.

2.7.3 Multi-modal Systems

Combinations of technologies have been used in several small studies [77], [101], [102], which unanimously conclude that sensitivity and specificity are both improved by the combination of data from multiple sources.

2.8 Regulation of Medical Devices

It is important to consider the requirements of all applicable standards at the earliest stages of design, as it may be difficult and costly to bring a design into compliance later in the development cycle. These requirements are referenced in chapter 5, where we introduce our instrument design, and in chapter 6, where we discuss approaches to instrument design.

Medical device design, manufacture, sale and use are regulated in the EU under the Medical Device Directive (MDD) (Council Directive 93/42/eec concerning medical devices) and harmonised standards enacted by member states *(author's note: this directive has been repealed and superseded by the Medical Device Regulation (European Parliament and Council Regulation 2017/745) [103], as of April 2017. Directive 93/42/eec was active at the time of commencement of writing this thesis.)*.

Medical devices are defined by the directive as:

> "'medical device' means any instrument, apparatus, appliance, material or other article, whether used alone or in combination, including the software necessary for its proper application intended by the manufacturer to be used for human beings for the purpose of:
>
> – diagnosis, prevention, monitoring, treatment or alleviation of disease,
>
> – diagnosis, monitoring, treatment, alleviation of or compensation for an injury or handicap,
>
> – investigation, replacement or modification of the anatomy or of a physiological process,
>
> – control of conception,

and which does not achieve its principal intended action in or on the human body by pharmacological, immunological or metabolic means, but which may be assisted in its function by such means" [104]

Electrical Safety International standard series IEC 60601 is applicable to electrical medical equipment, covering considerations and standards for the electrical safety of medical devices.

Battery powered equipment specifically must provide the following protections:

- Protection against reverse battery connection [105]
- Protection against overcurrent from shortage of battery voltage, and all derived (regulated) voltages [105].

In addition, all possible hazard conditions (e.g. wrong battery type) must be tested, demonstrating no danger to the patient.

Equipment which connects to a mains supply (even just for charging a battery) must either have a protective earth (Class I) or a double insulated casing (Class II) [105], [106], and demonstrate that it presents no danger to the patient in the event of a hazard originating from the power supply, or a fault in the part of the circuit (the Mains Part) powered by the mains supply [105], [106].

The sensor and connected circuitry is classified as the applied part of the equipment, and, as it does not require electrical conduction to the patient to function, should be adequately insulated, and must meet the requirements for type BF Applied Parts. In particular, the circuitry connected to the sensor must be electrically insulated from the Mains Part [105].

Fitness for Purpose In addition to safety, it is incumbent on the manufacturer of medical devices to demonstrate that the device does what it is meant to. Medical

devices which are used for measurement must perform to a minimum degree of accuracy, and to within the manufacturer's stated tolerance [104]. To comply with requirements regarding fitness for purpose, the purpose and intended use of the medical device must be documented clearly and in detail at the start of the design phase.

Quality Control To demonstrate both safety and fitness for purpose, the manufacturer must use a quality system to manage design, development and manufacturing processes, and to be responsive to process and equipment failures [104].

Classification For the purpose of regulation, medical devices are divided into four classes of increasing risk: Class I, Class IIa, Class IIb and Class III. Risk is decided based on a set of rules that consider factors such as invasive or non-invasive, transience of use, and whether the device supplies radiation.

In addition, Class I devices that have a measurement function are designated as 'Class Im', and devices which are placed on the market in a sterile condition are categorised as 'Class Is'. Unlike standard Class I devices, these two categories require a notified body to be involved in CE marking.

2.9 Summary and Analysis of the Literature

Care pathways for dysphagia would benefit greatly from portable, non-invasive, quantitative instrumentation of the larynx. In particular, an expected outcome would be higher detection rates of silent aspiration, enabling early intervention and reducing risk of pneumonia in affected patients.

Accelerometry has been identified as an instrumentation technique with significant potential to form the basis of a portable, non-invasive and quantitative in-

strument for assessment of dysphagia, with wide research support for its efficacy in discriminating between healthy and dysphagic subjects. Laryngeal accelerometry is not, however, widely used in a clinical setting, as the physiological basis for its signals are poorly understood. As a result, it is difficult to say what physiological factors the accelerometer systems presented in literature do and don't take into account. It is not known which types of dysphagia the systems are sensitive to, nor is it clear if anatomical differences in subjects affect the decision made by the presented classifiers. In chapter 3, the effects of inter-personal differences in physiology on accelerometry signals are studied to bring clarity to this topic.

To further prepare the reader for the approach set out in chapter 3: Methodology, some key beliefs which underpin much of the literature as a subtext are briefly examined.

There is a (mostly) unstated axiom in literature that head movement is detected by a throat-mounted accelerometer as a low-frequency acceleration. There is little evidence presented that this is the case, however researchers have consistently designed filters to remove low frequencies in accelerometry systems, which suggests that this effect is real, but undocumented. No causal explanation has been offered for this effect, and no analysis has been presented of how high-pass filters may distort accelerometry data. In chapter 3, the means for testing the veracity of this idea are set out.

In the literature regarding multi-axis accelerometry, the assertion that *SI movement of the larynx (i.e. laryngeal elevation) causes SI movement of the accelerometer, which is detected as acceleration on the accelerometer axis which is SI aligned; AP movement of the larynx (i.e. laryngeal excursion) causes AP movement of the accelerometer, which is detected as acceleration on the accelerometer axis which is AP aligned.* is also treated as axiomatic despite a complete absence of evidence to

support it.

While it has been demonstrated that laryngeal excursion and elevation occur simultaneously, and that AP and SI aligned accelerometers output characteristic signals simultaneously with the combined laryngeal motion, there is no evidence presented in literature to demonstrate that the sources of signals from the two accelerometer axes are unconnected – a valid interpretation of the data, as presented, could be that the signals of both accelerometer axes are interrelated, and have a common source, which could be laryngeal excursion alone, laryngeal elevation alone, or a combination of both.

The inference of performance and behaviour of physiological processes in the throat from sensor data is not justified in literature, as the mechanisms which link the two (physiology and sensor data) have not been established. With regards to laryngeal accelerometry, the rotational component of the accelerometer output has not been studied. Gyrometry would be the natural choice of sensor to study the free rotation in space of a device; fortuitously, IMUs which incorporate accelerometer and gyrometer units in the same integrated circuit are commonly available. In chapter 3, an integrated gyrometer is used to study the rotation of a throat-mounted accelerometer during swallowing.

Chapter 3

Methodology

This chapter describes the methods designed to develop novel dysphagia instrumentation techniques, based on accelerometry and gyrometry.

The chapter begins with section 3.1, which describes the general approach taken by the author to achieve the four objectives set out in chapter 1, section 1.4. Section 3.2 seeks to explain some of the findings in the literature by proposing the mechanisms behind them. Section 3.3 introduces two models used to explore the implications of the proposed mechanisms. Firstly, a simulation model of laryngeal elevation is defined, then a mechanical model of the larynx is presented. The procedure for capturing data from the mechanical model is described in section 3.4. Section 3.5 presents the methodology for experiments with human participants which consists of making anatomical measurements and the capture of swallowing sensor data. Section 3.6 describes the data capture system (hardware and software) developed to record swallowing sensor data in the experiments described in sections 3.4 (mechanical model) and 3.5 (human participants). The scheme designed to ensure ethical handling of human participant information is described in section 3.7. Finally, the techniques used to process the data and extract features is detailed in

section 3.8.

3.1 General Approach

The weaknesses of previous approaches applied to the development of laryngeal accelerometry were touched upon in chapter 2. In particular, there has been a tendency to attempt to evaluate an experimental instrument without first defining what that instrument is intended to measure. There are obvious misconceptions in how an accelerometer functions, which is evident in both the design of experiments and discussion of the results; for example, accelerometer axes have been assumed to be aligned to physiological axes, even when the device is rotating independently to the subject. It is the author's intention to address these issues by establishing the basic mechanisms that are relevant to accelerometer and gyrometer measurements of laryngeal motion. Following this, the variability in human physiology is considered: for an instrument to be clinically useful, it must perform its function for young and old, male and female, of large or slight build; for this reason swallowing data was captured from a wide variety of healthy volunteers so that problems with our instrumentation techniques may be discovered and addressed, leaving us with confidence in our instrument design.

3.2 Larynx-to-Sensor Causality

In this section, the basic mechanisms by which sensor signals are determined by swallowing physiology (both anatomical and behavioural) are set out, with supporting evidence presented, where available, from literature. Further evidence supporting these mechanisms is presented in chapter 4.

3.2.1 Sensor Rotation

It is well established that the effect of a gravitational field on an accelerometer can not be ignored [107]. In a system where the orientation of an accelerometer does not change (generally referred to as *strap-down configuration*), the gravitational acceleration vector can be discounted from the accelerometer axis or axes that are non-zero in the vertical reference axis. In a system where the accelerometer is free to rotate, however, the gravitation acceleration will shift in alignment from one axis to another, creating a signal with a magnitude of $\leq 2G$, and a frequency determined by the speed of rotation.

As a sensor applied to the throat is not prevented from rotating, but instead conforms to the contours of the skin, it seems likely that low-frequency accelerometry signals are due to the sensor tilting – this principle is referred to in this thesis as the *sensor rotation hypothesis*.

The frame of reference we use for this is shown in figure 3.1.

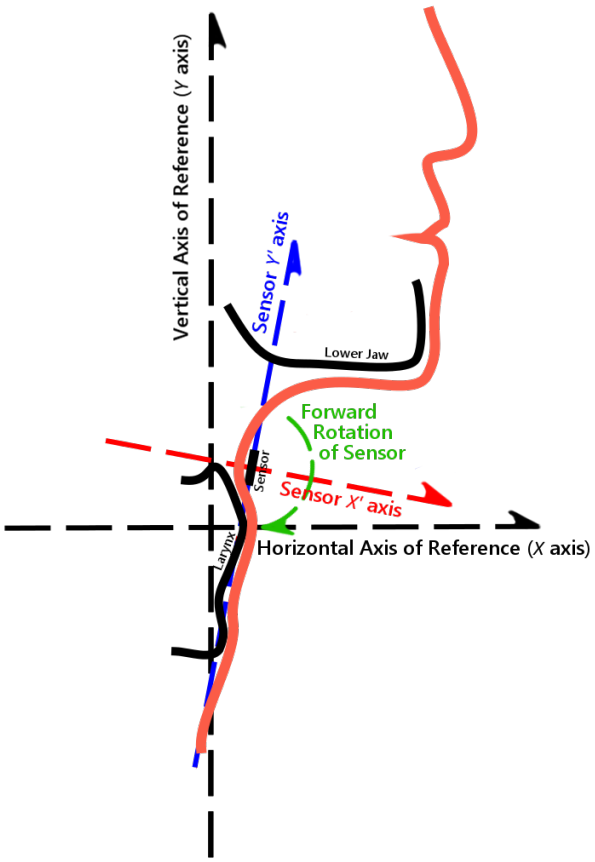

Figure 3.1: *An illustration of the relationship between the two frames of reference. The reference axes x and y are shown in black; the sensor x' axis is shown in red; the sensor y' axis is shown in blue; the positive direction of sensor rotation is shown in green. As the sensor rotates, the rotational displacement between the reference axes and sensor axes will change.*

3.2.2 Axial Coherence

As established in section 2.6.1, it is the nature of accelerometers that acceleration of the device produces a signal proportionate to acceleration *in the direction* that

the accelerometer axis is oriented *at the time* of the acceleration. Rotation of the accelerometer must be taken into account – it cannot be simply assumed that acceleration along a given sensor axis corresponds to motion of the larynx along a given physiological axis where the sensor is not rigidly mounted to the larynx. In this thesis, the gyrometer component of the sensor is used to qualify the accelerometer data.

3.2.3 Speech and Swallowing Sounds

Vibration originating from physiological events, for example: air passing between the vocal folds or the epiglottis closing, is conducted to the skin where it may be picked up by a stethoscope, microphone or accelerometer. The vibration is attenuated by the distance between the source of the vibration and the detector, and the softness of the intervening tissue.

3.3 Modelling of Sensor Reaction to Laryngeal Motion

In this section we introduce our simulation model (section 3.3.1) and our mechanical model (section 3.3.9), explaining the purpose and walking the reader through the design and implementation of each in turn.

3.3.1 Introduction of the Simulation Model

In pursuit of objective 2 (see section 1.4), a set of equations were derived to describe the relationship between laryngeal motion and a throat-mounted sensor. Using these equations, the motion of the larynx during deglutation was simulated, as was the

output of a throat-mounted sensor. The software written to run this simulation is referred to in this thesis as the *simulation model*.

The simulation model outputs the simulated sensor signals, which are modulated by parameters such as the dimensions of the simulated larynx, the maximum elevation of the larynx, and the speed of laryngeal elevation.

3.3.2 Simulation Model Development

The original concept for the simulation model was of a three-dimensional computer-generated representation of the larynx, the skin covering the larynx, and the sensor. The larynx and the sensor were to be modelled as rigid bodies of uniform density, while the skin was to be modelled as a flexible, elastic membrane, described by molecular dynamics.

After a short period of development, a view was taken that this was not an efficient way of modelling the relationship between the laryngeal motion and the sensor output.

The following approach was taken to focus development efforts on modelling which directly informs instrument design:

- Describe only the dynamics which are relevant to interpretation of the sensor's output

and

- Leave out detail that is not likely to have a significant effect on the sensor output

With reference to the second point; considering the symmetrical nature of the human throat, left-right movement of the larynx or the sensor is likely to be negligible, as is rotation on the transverse and coronal planes. With this in mind, a two-dimensional

model of the larynx, skin, and sensor was used. This can be understood with reference to figure 3.1 from section 3.2.

Instead of attempting to perfectly describe the dynamics of the interaction between the larynx and the skin, and the skin and the sensor, the static position and orientation of the sensor was calculated based on the larynx being stationary at a few discrete elevations. Intermediary positions of the sensor were then interpolated.

This approach was used to create a simulation model that is constructed from a few simple formulae, but nevertheless captures the essence of how features in the sensor data emerge from particular physiological processes, and how those features are modulated by variations in anatomical measurements and variations in swallowing behaviour.

3.3.3 Description of the Simulation Model

The simulation model is composed of the larynx, the skin, the sensor. The position and behaviour of these parts is governed by these rules:

1. The larynx moves along a single, vertical axis.

2. The skin conforms to the shape of the larynx at all times.

3. The skin slides over the larynx, i.e. the vertical position of the skin is independent from the vertical position of the larynx.

4. The skin is dragged by movement of the larynx, i.e. the vertical position of the skin is proportional (subject to a coefficient of friction) to the vertical velocity of the larynx.

5. The sensor is modelled as a straight line segment, with a centre point c and a length l.

6. The sensor is fixed to the skin, i.e. the vertical position of the sensor is determined by changes to the vertical position of the skin, and the horizontal position of the sensor is a function of the horizontal position of the skin at the centre and each end of the sensor.

These rules were used to construct formulae to calculate the static position of the centre and angle of the sensor, for a given laryngeal elevation. Dynamic effects, such as inertia and harmonics were discounted from the model at this stage of development.

The output of the sensor is calculated from its position and angle over time: see section 3.3.6 for the details of the formulae used in this calculation.

3.3.4 Simulation Model Larynx Shape

A very simple model of the larynx shape is used, based on straight-lined sections (see figure 3.2). The exact length and angle of the segments depends on the laryngeal prominence (LP) size.

The concept of *excursion* used in this chapter is defined here as an anterior displacement of the skin from the vertical line that would mark the position of the skin were there no larynx – a nominal $0mm$ excursion line. The symbol η is used to refer to an excursion in our equations; in practice, the excursion at two particular points on the skin – where the top and bottom edge of the sensor reside – are sufficient for our simulation model, and are referred to as η_1 and η_2 respectively.
The definitions of the sections:

- The first section (marked A in figure 3.2) is above (superior to) the larynx where the Laryngeal Strap Muscles (LSM) connect the larynx to the lower jaw. It is modelled as a flat surface at 0 mm excursion, which is used as reference for the excursion of the other sections.

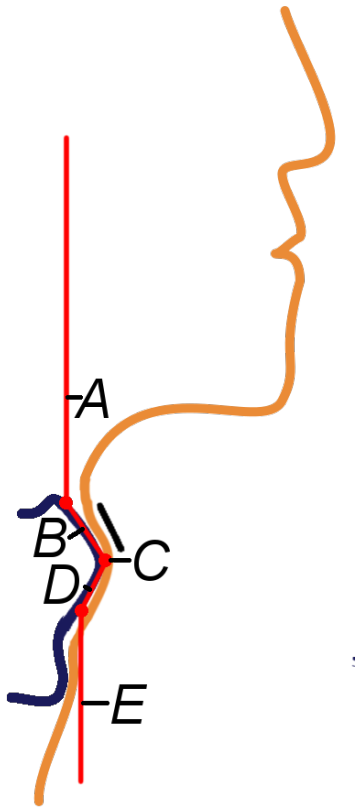

Figure 3.2: *The shape of the larynx, divided into sections.*

- The roughly flat area of the larynx between the LP and the thyroid gland (marked E in figure 3.2) is modelled as a second flat section, at 1 mm excursion. The size of the LP is an input to the model.

- The final two sections (marked B and D respectively, in figure 3.2) connect the LP (marked C in figure 3.2) to the bottom (inferior-most point) of section A and the top (superior-most point) of section E.

The equations that determine the shape of the larynx, expressed as functions of the coordinate y on the vertical axis, with $y = 0$ at the level of the LP:

A The flat section above the LP:

$$A(y) = 0mm \tag{3.1}$$

B The gradient connecting the LP to A:

$$B(y) = \text{LP size} - \frac{\text{LP size}}{8mm}y \tag{3.2}$$

C The peak of the LP:

$$C(y) = \text{LP size} \tag{3.3}$$

D The gradient connecting the LP to E:

$$D(y) = \frac{(1mm - \text{LP size})}{8mm}y + \text{LP size} \tag{3.4}$$

E The flat section below the LP:

$$E(y) = 1mm \tag{3.5}$$

1 mm was used here as an estimated natural excursion of the flat part of the larynx, and 8mm used as a rough estimate for the length of the slope above and below the LP.

These functions are brought together into a single piece-wise function, equation 3.6, describing $H(y)$, the excursion at vertical coordinate y, given that the larynx is at rest (i.e. not elevated.)

$$H(y) = \begin{cases} A(y) & \text{if } y > 8mm \\ B(y) & \text{if } 0mm < y <= 8mm \\ C(y) & \text{if } y = 0 \\ D(y) & \text{if } -8mm < y <= 0mm \\ E(y) & \text{if } y <= -8mm \end{cases} \tag{3.6}$$

3.3.5 Excursion of the Skin

The excursion of the skin at any given point along the vertical axis is given by the shape of the larynx, according to rule 2 from section 3.3.3. As the larynx is elevated, the excursion at any given point on the skin will change to conform to the point on the larynx that has moved to the vertical coordinate of the point in question on the skin.

For the purpose of calculating sensor output, we are only interested in the excursion at the top of the sensor (η_1) and the excursion at the bottom of the sensor (η_2). Figure 3.3 illustrates how η_1 and η_2 change as the larynx is elevated, and equation 3.7 provides the formulae for calculating η_1 and η_2 as a function of the laryngeal elevation, length of the sensor, l, and vertical coordinate of the centre of the sensor, c_y (see section 3.3.6 for the details of how c_y is calculated).

$$\eta_1 = H(c_y + \frac{l}{2} - elevation) \tag{3.7a}$$

$$\eta_1 = H(c_y - \frac{l}{2} - elevation) \tag{3.7b}$$

Our implementation of the simulation model positions the sensor immediately superior to the LP at rest; however the sensor can be positioned higher or lower by adjusting the c_y term in equation 3.7.

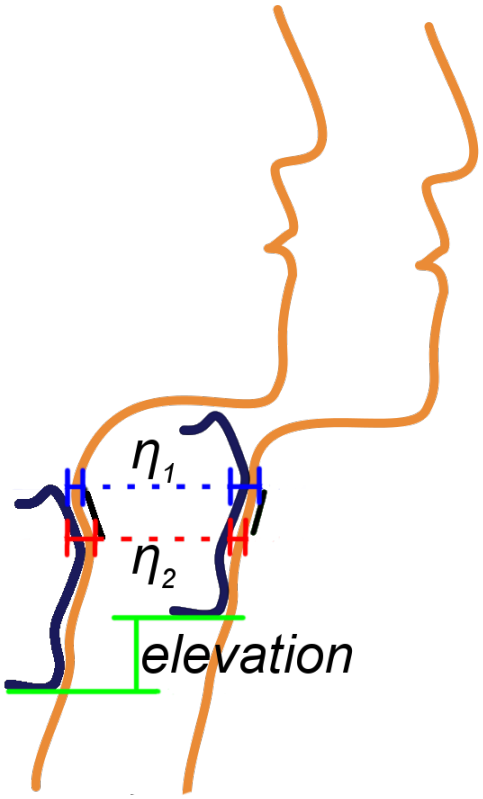

Figure 3.3: *An illustration of η_1, in blue, η_2, in red, and laryngeal elevation, in green. The larynx is shown at rest (left) and elevated (right).*

3.3.6 Simulation Model Sensor Position and Angle

As the sensor is an Inertial Measurement Unit (IMU), its output is a representation of its motion. To simulate the sensor output, its motion must therefore first be calculated; To calculate its motion, the position and angle of the sensor for each time-slice must be calculated.

The horizontal and vertical position of the centre point of the sensor (which is also its centre-of-mass) is referred to as c_x and c_y respectively. c_x is calculated as the centre point between η_1 and η_2, to follow rule 6 from section 3.3.3. c_y is calculated as proportional to the velocity of laryngeal elevation, to follow rules 4 and 6 from section 3.3.3. Equation 3.8 contains the formulae used to calculate the coordinates

of the centre point of the sensor, where μ is the coefficient of friction between the skin and the thyroid cartilage.

$$c_x = \frac{(\eta_1 + \eta_2)}{2} \tag{3.8a}$$

$$c_y = \mu \frac{\text{change in laryngeal elevation}}{dt} \tag{3.8b}$$

The angle between the sensor and the reference vertical axis (referred to as the tilt of the sensor,) θ, is calculated according to the formula given by equation 3.9.

$$\theta = \arctan(\frac{l}{\eta_1 - \eta_2}) \tag{3.9}$$

The relationship between η_1, η_2, and θ is visualized in figure 3.4, where it can also be seen that η_1 and η_2 are dependent on LP, and are elevation-shifted copies of each other.

It can be seen that in our model, for a laryngeal elevation of between 0 and l mm, the tilt of the sensor is close to linear. This is an important finding for the purpose of instrument development, as it means that within the bounds of this domain, laryngeal elevation can be inferred directly from sensor tilt.

3.3.7 Simulation Model Sensor Output

The output of the accelerometer for each of its axes is the second time derivative of the centroid position *along the relevant axis.* This means that the average orientation of the IMU for each sampling period must first be calculated (see equation 3.10a), then the instantaneous velocity can be projected onto the x' and y' axes (see equation 3.10b). From there, the accelerometer output is simply the time-derivative of v (see equation 3.10c).

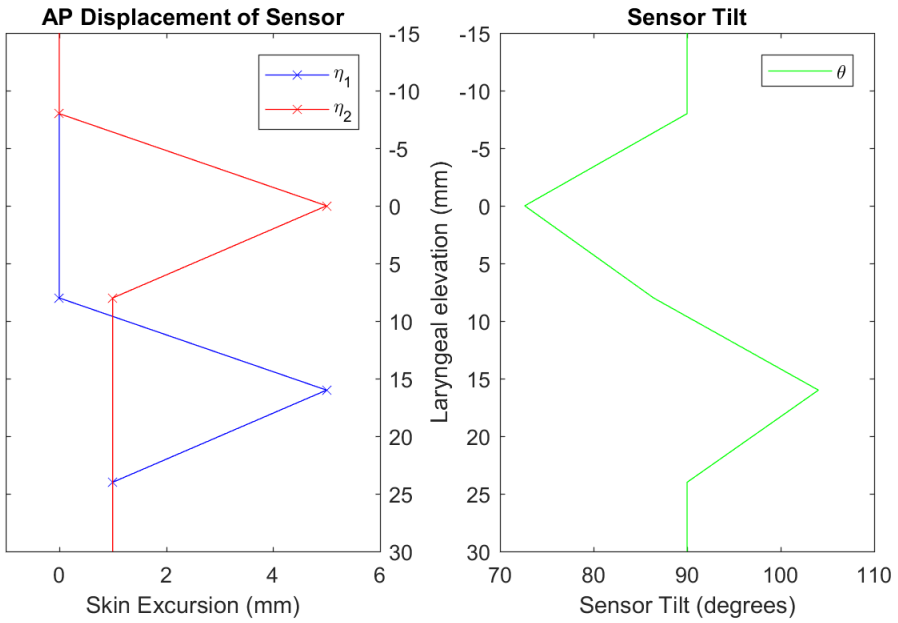

Figure 3.4: *A visualization of the relationship between the anterior excursion of the larynx body at two points on the throat (left) and the angle (tilt) of a sensor positioned between those two points (right), as the elevation (vertical position) of the larynx changes.*

Equations 3.10 and 3.11 are adapted for discrete time systems, where T_s is the sampling period (sometimes called the integration period in technical documents,) i.e. $T_s \equiv t_n - t_{n-1}$.

The mean tilt over the sample period is calculated

$$\overline{\theta}_{t_{1:2}} = \frac{(\theta_{t_1} + \theta_{t_2})}{2} \tag{3.10a}$$

The frame of reference is transposed to that of the sensor and velocity calculated

$$\begin{bmatrix} v_{x',t_{1.5}} \\ v_{y',t_{1.5}} \end{bmatrix} = T_s \left(\begin{bmatrix} c_{x,t_2} - c_{x,t_1} \\ c_{y,t_2} - c_{y,t_1} \end{bmatrix} \cdot \begin{bmatrix} \cos\overline{\theta}_{t_{1:2}} & -\sin\overline{\theta}_{t_{1:2}} \\ \sin\overline{\theta}_{t_{1:2}} & \cos\overline{\theta}_{t_{1:2}} \end{bmatrix} \right) \tag{3.10b}$$

The acceleration is calculated from the velocity and summed with the gravitational acceleration

$$\begin{bmatrix} a_{x,t_2} \\ a_{y,t_2} \end{bmatrix} = T_s \left(\begin{bmatrix} v_{x,t_{2.5}} - v_{x,t_{1.5}} \\ v_{y,t_{2.5}} - v_{y,t_{1.5}} \end{bmatrix} \right) + G \begin{bmatrix} \sin\theta_2 \\ \cos\theta_2 \end{bmatrix} \tag{3.10c}$$

The gyrometer output, ϕ, is calculated as the time-derivative of the orientation angle, θ (see equation 3.11).

$$\phi_{t_{1.5}} = T_s(\theta_{t_2} - \theta_{t_1}) \tag{3.11}$$

Note that each successive time-derivation of the trace causes a time-shift of a half-sample and reduces the sample size by one.

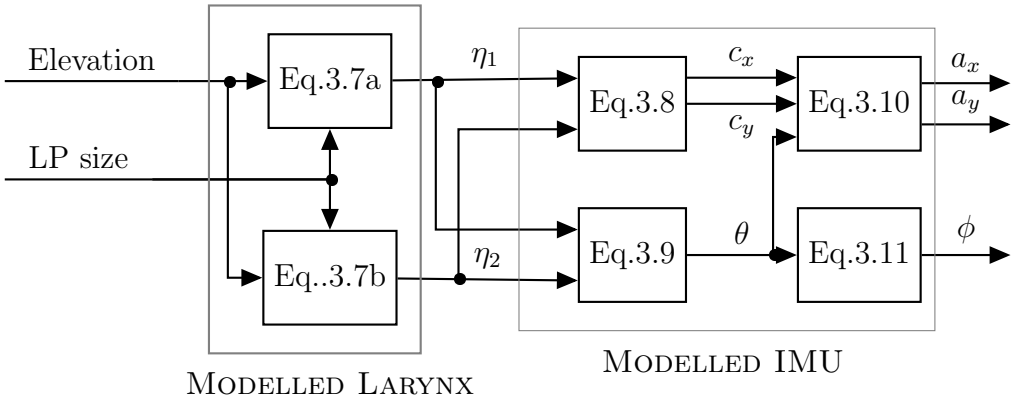

Figure 3.5: *Block diagram of the simulation model.*

The equations above can be seen to feed into one another following the structure shown in figure 3.5, where the motion of the larynx is simulated based on the laryngeal elevation and LP size, the sensor signals (based on two accelerometer axes and one gyrometer axis) are simulated based on the horizontal positions of the top and bottom of the sensor, and the horizontal positions of the top and bottom sensor are consequential of the modelled laryngeal motion.

3.3.8 Simulation Model Swallowing Behaviour

In our model of laryngeal motion, the larynx rests at 0 mm elevation, moves quickly to 10 mm elevation, pauses for 1 second, then returns to 0 mm elevation. How quickly the larynx is elevated is adjustable: in section 4.1, the output of the simulation model is presented for a number of combinations of elevation speed and LP size.

3.3.9 Introduction of the Mechanical Model

The mechanical model was used to provide complementary data to the simulation model, introduced in section 3.3.1. Where the simulation model presents a greatly simplified representation of the mechanisms by which sensor output patterns are derived from laryngeal motion, the mechanical model, existing as it does in the real world, presents an accurate representation of these mechanisms. However, where the simulation model provides complete control over input parameters such as LP size and laryngeal elevation speed, the mechanical model provides just two settings for each of these.

The swallowing process as a whole cannot be separated from other physiological processes, for example breathing and speech, as the breathing apparatus and speech apparatus share many components with that of swallowing. This makes it extremely challenging to say whether a feature in sensor data is relevant to swallowing or not.

To identify the features in sensor data that can be used to measure laryngeal elevation, we use the mechanical model to reproduce laryngeal motion in isolation.

3.3.10 Description of the Mechanical Model

As we have established, the mechanical model models the throat and re-creates laryngeal elevation behaviour for two sizes of LP. To reproduce laryngeal elevation,

the following components are required:

1. A larynx shape

2. A skin covering

3. A vertical axis which the larynx shape moves freely along (elevation)

In consideration of the skin; the make-up of human skin is complex and multi-layered, and the modelling of it non-trivial. We considered that it is only necessary to model the properties of the skin which affect the transference of motion from the larynx to the sensor: the important properties of the skin being its flexibility, elasticity and thickness. It can be seen from simple observation that the human larynx passes beneath the skin with minimal friction, and that the shape of human skin conforms readily to that of the rigid bodies beneath it, with the exception of where there is excess skin. The thickness of skin varies by age, sex and location of the body, between 0.05 mm at the thinnest (eyelids) to 1.5 mm at the thickest (palms of hands and soles of feet) [108]. 1 mm is a typical skin thickness across most of the body.

Natural latex rubber was judged to have flexibility and elasticity similar enough to human skin, and has the benefit of being easily moulded to an appropriate form. As a latex rubber object is formed by the progressive addition of new layers, it is trivial to determine its thickness during manufacture. The following constraints were set to the design of the mechanical mode, to make it as representative of human physiology as possible:

1. The larynx shape must be rigid

2. The larynx shape must be elevated by a total minimum of 5cm

3. The skin covering must be made of latex rubber with a mean thickness of 1mm

4. The larynx shape must slide smoothly beneath the skin covering

5. The skin covering must be held taut regardless of the elevation of the larynx shape

3.3.11 Mechanical Model Implementation

The larynx shapes were cut from 2cm thick sheets of hard plastic – wide enough that the sensor (diameter 16 mm) rests entirely against the shaped surface – following closely the profile of a typical larynx. The shapes are identical apart from the LP size (see figure 3.6.)

The vertical axis was constructed from a rack-and-pinion drive mounted on an aluminium frame. An optical position encoder was constructed to monitor the position of the axis, and the pinion was driven by a electric motor. The position encoder used three IR LED–photodiode pairs, each positioned over a greyscale track.

One track is a black-to-white gradient, which is read in software as a value of between 0 and 1023; this value is directly proportionate to the laryngeal elevation, but influenced by environmental factors, such as the room lighting, and therefore not appropriate for absolute positioning. Instead, this track is used for controlling the speed of the motor.

The second track is white over the active range of the larynx: -5 to +20 mm, stepping to black outside of this range. This track is used for locating the edges of the active range of the model and calibrating the values read from the first track.

The third track is black, apart from a white band at 0 mm. This track is used for zeroing the motor.

A control system was implemented on a microcontroller board, which controlled the motor speed by modifying the input to the motor based on the values read from the optical encoder.

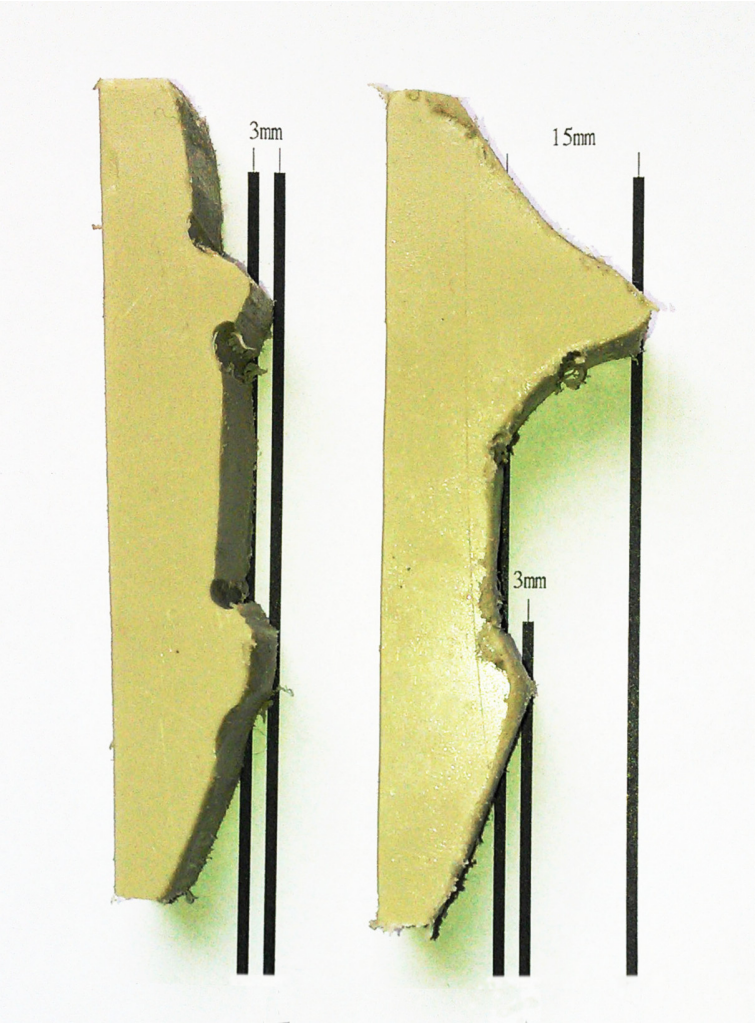

Figure 3.6: *Larynx shapes cut from plastic sheets: LP sizes 3mm (left) and 15mm (right).*

A swallow was defined in the microcontroller's programming as the larynx shape being raised at a pre-defined speed from resting position to a set top position, then immediately back to the resting position at the same set speed.

The latex skin covering was fixed to the aluminium frame and lubricated with talcum powder and machine oil to prevent it being dragged by the larynx shapes as they are elevated.

The constructed model is shown in figure 3.7.

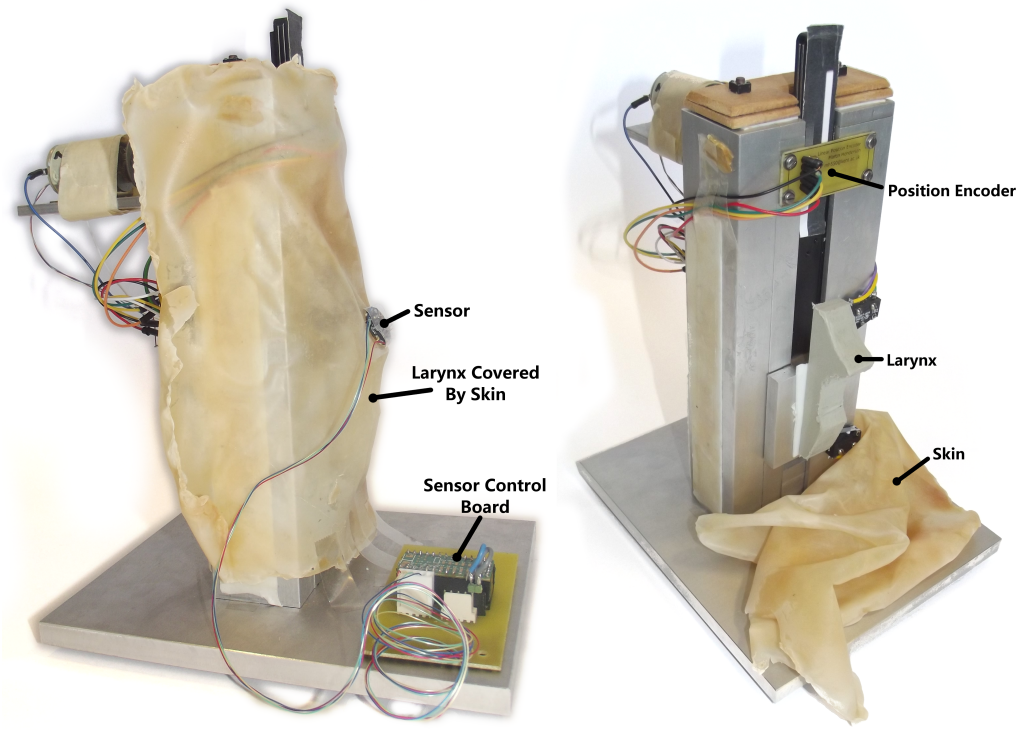

Figure 3.7: *The mechanical model, with the skin covering, sensor and sensor board (left), and showing the larynx shape and position encoder (right).*

Limitations of Mechanical Model The movement of the mechanical model is limited in the following ways:

- The larynx moves along a single axis, and does not rotate in any direction.
- The larynx has a range of $50mm$.
- The larynx can be elevated at a maximum speed of $40mm/s$.

3.4 Mechanical Model Experimental Methods

Data was captured from a sensor placed on the mechanical model, while the model's larynx was elevated and lowered. In this section, the methods for these experiments is presented. The materials used are set out in section 3.4.1; The experimental

procedure is set out in section 3.4.1.

3.4.1 Materials

The following materials were used for data capture in experiments using the mechanical model:

Mechanical Model The mechanical model, as described in section 3.3.10.

Laptop A laptop computer was used to record data.

Data Capture Software A bespoke suite of software was developed to visualise sensor data in real-time, and to record it to disk. See section 3.6.1 for more detail.

Sensor A LSM9DS0 inertial motion unit (IMU) which is composed of an accelerometer (tri-axis) and a gyrometer (tri-axis) was used as the sensor in all experiments.

Sensor Control Board A microcontroller board was constructed to configure and synchronise multiple sensors, and to format the data from the sensors and transmit it to the laptop.

3.4.2 Experimental Procedure

The procedure for recording data from the model was designed to be as analogous as possible to the experimental procedure with participants, which is presented in section 3.5.

1. Position sensor(s) in the appropriate position.

2. Enter "model" as the name of the subject, into data capture software.

3. Enter LP size and speed settings into data capture software.

4. Begin recording.

5. Run a 'swallow' on the model.

6. End recording once swallow has concluded.

3.5 Experiments with Human Participants

3.5.1 Ethical Approval

Ethical approval was granted by the University of Kent Faculty of Sciences Research Ethics Advisory Group to proceed with participant involvement.

3.5.2 Participant Recruitment

A request for participants (see Appendix A) was sent out to staff and students at the University of Kent to participate in a study that would involve them drinking 30ml liquid boluses of three different consistencies while data from neck-mounted sensors were captured.

A meal voucher up to the value of £5 per participant was offered as incentive to participate. The voucher was given to participants regardless of whether they completed the experiment.

Respondents were screened using a questionnaire (also in Appendix A) and excluded if they disclosed that they were less than 18 years of age, that they had undergone surgery to the throat, or that they suffer swallowing problems, on the grounds that the experiment was intended to gather data only from healthy adults with normal physiology.

Selected respondents were contacted to arrange individual sessions lasting 30 minutes each. At this point, a pseudonymous identifier (PID) was assigned to the participant; see section 3.7 for details of the pseudonymization scheme, as well as data protection practices.

Written informed consent was obtained from the participants; they were provided with a participant information sheet to read prior to agreement

Twenty-three (23) participants, twelve (12) male and eleven (11) female, aged 19 to 65 years, were recruited. In the case of one (1) of the participants (female), sensor data was not captured due to technical problems. Three (3) additional respondents were offered sessions, but either withdrew from the study, or failed to attend their session, and were therefore not included in the study.

3.5.3 Materials

The following materials were used for data capture from human participants:

Laptop A laptop computer was used to record data. The laptop was unplugged from the mains (i.e. battery powered) during the procedure, for electrical safety reasons.

Data Capture Software A bespoke suite of software was developed in preparation for participant involvement to visualise sensor data in real-time, and to record it to disk.

Sensor A LSM9DS0 inertial motion unit (IMU) which is composed of an accelerometer (tri-axis) and a gyrometer (tri-axis) was used as the sensor in all experiments. The sensor was covered in electrical insulation to protect the participants from risk of receiving an electrical shock from the equipment.

Sensor Control Board A microcontroller board was constructed to configure and synchronise multiple sensors, and to format the data from the sensors and transmit it to the laptop.

Calliper A calliper was used to take measurements of the participants' throats, to a precision of 0.01 mm.

Bolus Three consistencies of liquid were used as boluses in experiments: water, orange juice, and banana smoothie.

Single-Use Vinyl Gloves To protect participants from risk of infection, gloves were worn while measurements were taken of the participant's throat (see below), and while the sensors were attached to the participant's throat. Vinyl gloves were used, as latex presents a risk of allergic reaction in some members of the population.

3.5.4 Experimental Procedure

During the study:

1. The participant was seated at a table and briefed with an explanation of the study and the experimental procedure. The participant was encouraged to ask questions and engage with the study.

2. Written informed consent was obtained from the participant. All data captured from this point onwards is identified using the pseudonymous PID number to protect the identity of the participant.

3. Measurements of the participant's throat were taken, according to the procedure described in 3.5.5.

4. Two sensors were placed on the participant's throat, one immediately above the participant's laryngeal prominence, and one bisecting the participant's laryngeal prominence and thyroid gland.

5. Sensor data was recorded, according to the method described in 3.5.6, while the participant consecutively swallowed the water, juice and smoothie boluses.

3.5.5 Anatomical Data Capture Procedure

1. Measure excursion of LP using callipers.

2. Measure distance from LP to cricoid cartilage using callipers.

3. Measure distance from LP at rest to lower jaw using callipers.

3.5.6 Sensor Data Capture Procedure

1. Position sensor(s) in the appropriate position. The X axis of the sensor is aligned to the vertical axis (SI) of the throat; the Y axis is aligned to the coronal axis (ML); the Z axis is aligned to the saggital axis (AP).

2. Enter name of subject into data capture software.

3. Enter bolus type into data capture software.

4. Begin recording.

5. Administer bolus.

6. End recording once swallow has concluded.

A word about sensor orientation: in the simulation model and in chapter 5, a two-dimensional view is taken of the throat, as there is, ordinarily, very little side-to-side motion of the larynx in healthy subjects. The Z and X axes of accelerometry

correspond to the x' and y' axes, respectively, while only the Y axis of gyrometry is used as the sole gyrometry axis of interest. In chapter 4, section 4.4.2, analysis of the raw sensor data from all six axes justifies this approach by demonstrating that the activity in the other axes is negligible: the Y axis accelerometer trace is flat; the X and Z axes gyrometer traces are attenuated copies of the Y axis gyrometer trace.

3.6 Data Capture System

The architecture of the system used to capture sensor data in experiments described in sections 3.4 and 3.5 is illustrated in figure 3.8.

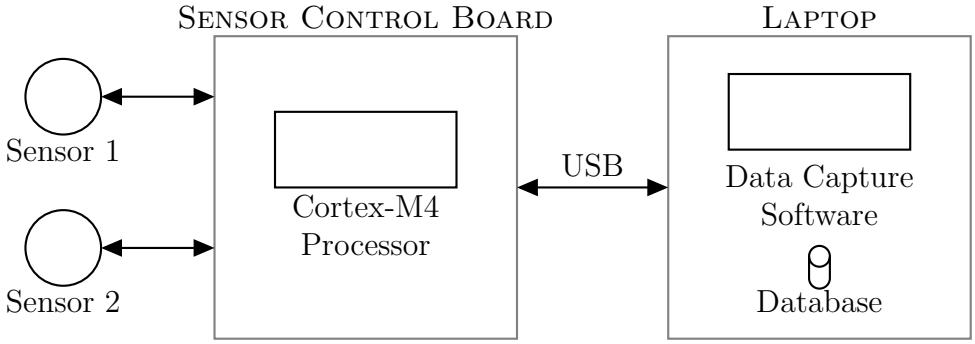

Figure 3.8: *Block diagram of the data capture system.*

The sensors are configured and synchronised by the sensor control board, which also captures the data from the sensors and transmits it to the laptop, which displays the data and stores it.

3.6.1 Data Capture Software

The software suite for capturing sensor data was written using the Processing programming language. See appendix C for a full listing of the source code.

The software presents a graphical user interface requesting the input of the participant ID, as shown in figure 3.9, followed by a live visualisation of the sensor

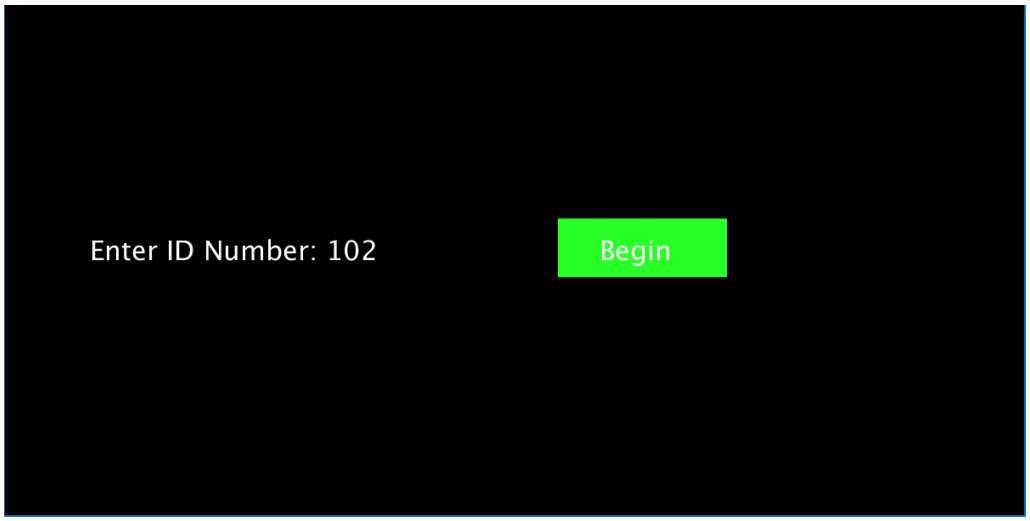

Figure 3.9: *The data capture software participant ID entry screen.*

data, shown in figure 3.10, allowing the researcher to quickly assess whether the hardware is working, and the sensors positioned appropriately. The researcher enters the context of the session, e.g. the bolus type and any special circumstances, and presses the green 'play' button, which sets the software to begin recording data. The location of the recording is displayed for convenience (see figure 3.11). Once the participant has completely swallowed the bolus, the researcher presses the red 'stop' button, to end the recording.

Recordings were stored in comma-separated-values format, stored in a data structure that grouped the recordings under the participant ID. Later, the data was imported into a *.mat* file for processing and analysis using MATLAB.

User Interface The software initially presents the researcher with the means to enter the participant ID. Once this is entered, the sensor data is visualised in real-time. A name is given to each recording, which is then stored using comma-separated values.

Figure 3.10: *The data capture software displaying live sensor data. The recording name is entered here. The green button commences the recording.*

3.6.2 Sensor Choice and Mounting

The LSM9DS0 (ST Microelectronics [76]) inertial motion unit was chosen to use as the sensor for work documented in this thesis, as it performs well in the following criteria:

Accelerometer The LSM9DS0 incorporates a three-dimensional accelerometer

Gyrometer The LSM9DS0 incorporates a three-dimensional gyrometer

Size The LSM9DS0 has an extremely small footprint, and is commercially available incorporated into a self-contained module as small as 16mm-by-16mm-by-0.8mm

Interface The LSM9DS0 incorporates an ADC and interfaces using an I2C bus; this adds robustness against electromagnetic interference, and limits the number of wires necessary to connect the sensor to the sensor control board to four wires - ground, 3.3V supply, data and clock

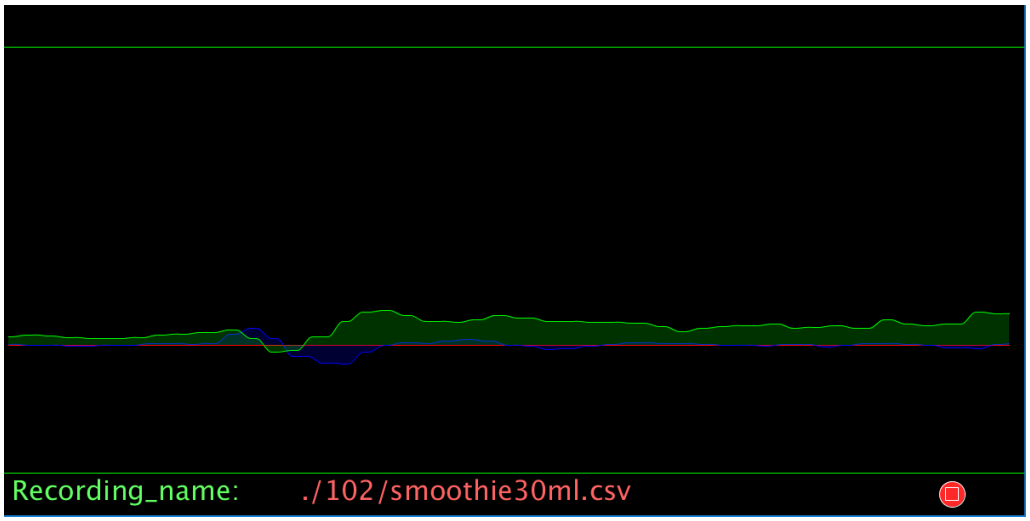

Figure 3.11: *The data capture software during recording. The filename for the recording is shown at the bottom of the screen. The red button ends the recording.*

The sensor was electrically insulated using insulation tape, and mounted on both the mechanical model, and participants, using double sided tape.

Special care had to be taken in connecting the sensor to the sensor control board, so that the connecting wires did not influence the motion of the sensor to too great an extent.

Prior to the experiment, the sensor's accelerometer was calibrated by placing the device in three orientations, in turn, on a level table, and, for each, recording the difference from zero for the two horizontal axes and the difference from $1G$ of the vertical axis. The offset from zero of each axis was subsequently subtracted from the sensor's output in software, and the scaling of each axis corrected using the offset from $1G$.

Prior to each session, the sensor's gyrometer was zeroed by placing the device flat on a level table, and the difference from zero of each gyrometer axis recorded, and subsequently subtracted from the output in software.

3.7 Data Protection

3.7.1 Pseudonymisation

For the purpose of the study, which has as its aim to explore the effects of inter-personal differences in physiology, it is important that separate pieces of data relating to each participant are associated with each other.

To protect participants from being identified, and to prevent data that has been recorded in the course of the study being used in ways that the participant has not explicitly given their consent for, it is important that none of the data from the study can be traced back to any participants, except by the researcher, and only for the purpose of destroying the data under instruction from the participant.

To prevent the researcher from introducing undocumented information into their analysis of data, for example their impressions of a given participant, or an event that occurred during the data capture process, and thus risking the analysis being biased towards the researcher's preconceptions, it is important that *at the point of analysis*, the researcher does not associate participant data with the individual.

To meet the above requirements for the study, the data was pseudonymised under the following scheme:

1. A unique random number of between 0 and 99 (inclusive) was generated for each participant, and used as the participant identification number PID. The randomness is important to prevent the researcher guessing the participant from the order of data capture sessions.

2. Recorded data was stored against the PID.

3. The only document which links the participant with data captured in the course of the study is the participant information sheet.

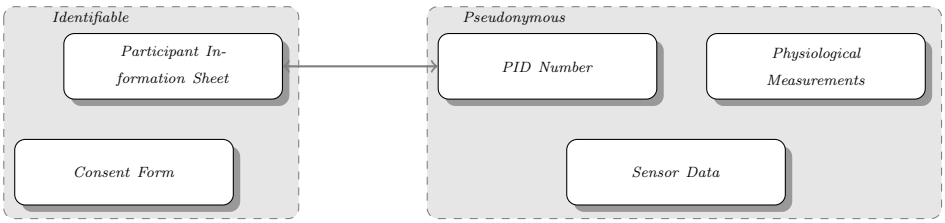

Figure 3.12: *A diagrammatic representation of the pseudonymization scheme, showing how study data (to be published) was separated from personal identifiable information (to be kept secure), but still associated with an individual (pseudonymous).*

Figure 3.12 shows how this scheme is effective in separating information which must be protected from information which may be published.

3.7.2 Encryption

Digital copies of identifiable information was stored in an encrypted archive, protected by AES-256 encryption algorithm, using 7-Zip archiving software, which must also be used, with the chosen password, to access the data.

3.7.3 Physical Security

Physical copies of identifiable information was stored double-locked; i.e. in a locked cupboard, which resides in a room within the School of Digital Arts that has restricted access, and is kept locked.

Physical copies of identifiable information were digitised and shredded once they were no longer needed for the study, to reduce the risk of a security breach.

3.8 Data Processing

To make the sensor data more comprehensible, and to bring out its implications for physiological instrumentation, several processes were applied to the data. The

techniques used in these processes can be categorised as either *pre-processing* or *post-processing*, where the former does not alter the data, but only converts it from one form to another, and the latter is designed to isolate, or alternatively eliminate, a feature from the data.

It is important to separate processes applied to the data in this way, so that artefacts introduced by post-processing techniques are not seized upon as great discoveries. Any feature which is revealed by post-processing, must also be identifiable in pre-processed or raw data to be valid.

Pre-Processing Techniques

1. Calculation of sensor tilt, derived from accelerometer and gyrometer data
2. Transposition of Accelerometer data from the sensor axes (x' and y',) to the reference axes (x and y)

Post-Processing Techniques

1. Segmentation of data
2. Removal of the effects of head tilt from the data

The methodology for each process is explained in detail in this section.

3.8.1 Calculating Sensor Tilt

Sensor tilt is calculated using a fusion of accelerometry and gyrometry data. A simple time-integration of gyrometry (equation 3.12) data produces tilt, however any error in the sample period will cause a scaling error, and even the smallest inaccuracy in calibration of the gyrometer will cause an accumulating error (referred to as drift). The aggregate of these errors is referred to as $e_{\theta.\gamma}$.

$$\theta_\gamma = \int \phi.dt + \theta_0 \tag{3.12}$$

In equation 3.12, θ_γ is the tilt calculated from gyrometer data alone, ϕ is the measured rotational velocity of the sensor, i.e. the gyrometer output, and θ_0 is the initial tilt of the sensor.

The initial tilt, θ_0, can not be known from gyrometer data alone, and is initially assumed to be 0; later calculations using accelerometer data will correct this (see below).

If it is assumed that the sensor is suspended in space, freely rotating, with no external forces acting upon it – other than the earth's gravitational field – the tilt of the sensor can be calculated as the angle of the gravitational force vector, using equation 3.13:

$$\theta_\alpha = \tan^{-1}\left(\frac{-\alpha_y}{\alpha_x}\right) \tag{3.13}$$

As we are using the accelerometer to measure the force exerted upon the sensor by the larynx during deglutation, it is obvious that these assumptions do not apply and this technique will also introduce an error, however unlike the integration method, the error is not accumulative.

Given that when the error is zero, the absolute acceleration is $1G$, the error can be estimated by equation 3.14:

$$e_{\theta.\alpha} \approxeq 1G - \sqrt{\alpha_x^2 + \alpha_y^2} \tag{3.14}$$

When $e_{\theta.\alpha}$ is close to zero, θ_α can be used as an acceptable estimate of θ. Moments where the above conditions are satisfied are used to correct $e_{\theta.\gamma}$, following the equations in 3.15:

$$\theta_{\gamma.i} - \theta_{\alpha.i} = e_{\theta.\gamma.i} + \theta_0 \left[e_{\theta.\alpha} \approx 0\right] \tag{3.15a}$$

$$\theta_m = \frac{\theta_{\alpha.2} - \theta_{\alpha.1}}{\delta t} \tag{3.15b}$$

$$\theta_0 = \theta_{\alpha.1} \tag{3.15c}$$

$$\theta = \theta_\gamma + \theta_m t + \theta_0 \tag{3.15d}$$

This data fusion technique functions, in summary, by using θ_α (which is stable, but noisy) to correct the systematic error in θ_γ.

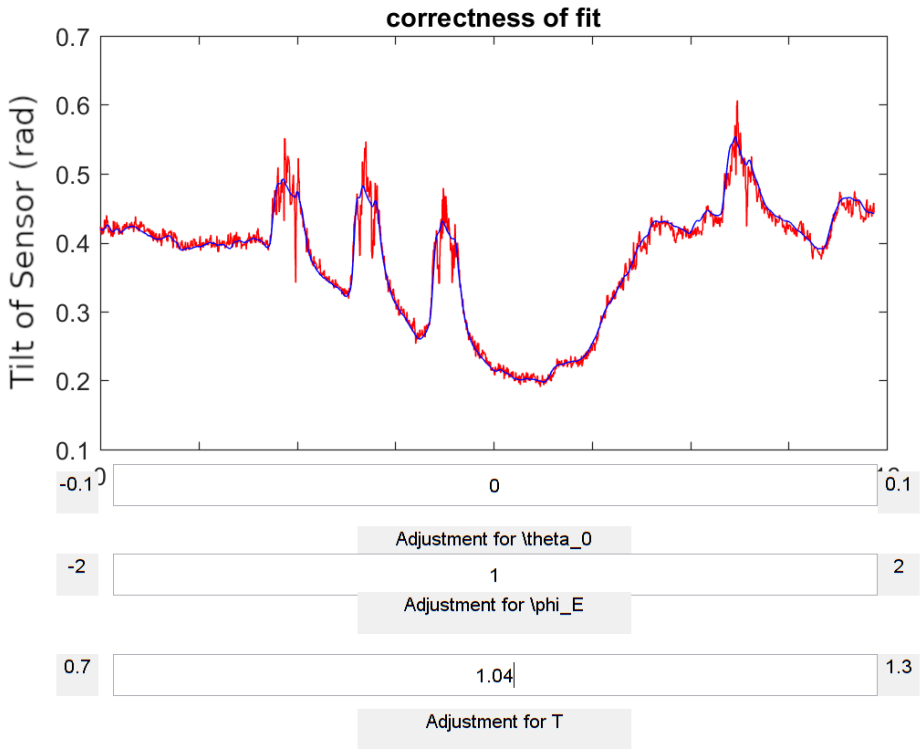

Figure 3.13: *A MATLAB tool to use θ_α (red), which is contaminated by high frequency noise originating from laryngeal motion, to correct systematic errors in θ_γ (blue), showing sliders which set manual correction factors for (top to bottom) initial tilt, drift, and sample period.*

A tool was created using MATLAB, shown in figure 3.13 and listed in appendix C, to perform this fusion operation on the sensor data.

3.8.2 Transposition of Data to Axes of Reference

To reverse the effects of sensor rotation on accelerometry data, the tilt of the sensor must first be calculated by fusion of accelerometry and gyrometry data (see section 3.8.1). Using accelerometry data alone, a tilt (θ_α) can be calculated using equation 3.16.

$$\theta_\alpha = \arctan\left(\frac{y'}{x'}\right) \tag{3.16}$$

Once the tilt is known, then a rotation matrix is used, as shown in equation 3.17, to transpose the acceleration signals from the sensor's relative axes (x',y') to the absolute reference axes (x,y).

$$\begin{bmatrix} x \\ y \end{bmatrix} = \begin{bmatrix} x' \\ y' \end{bmatrix} \cdot \begin{bmatrix} \cos\theta & \sin\theta \\ -\sin\theta & \cos\theta \end{bmatrix} \tag{3.17}$$

The final step in pre-processing the accelerometer data, is to separate the AP and SI accelerations, i.e. due to laryngeal motion, from the gravitational acceleration vector, calculated from the tilt, using equation 3.18.

$$\begin{bmatrix} AP \\ SI \end{bmatrix} = \begin{bmatrix} x \\ y \end{bmatrix} - G \begin{bmatrix} \sin\theta \\ \cos\theta \end{bmatrix} \tag{3.18}$$

As even a small error in calibration of the accelerometer will result in a misalignment of the real and theoretical gravitational vectors, a second tool was created using MATLAB, shown in figure 3.14 and listed in appendix C, to manually make small adjustments.

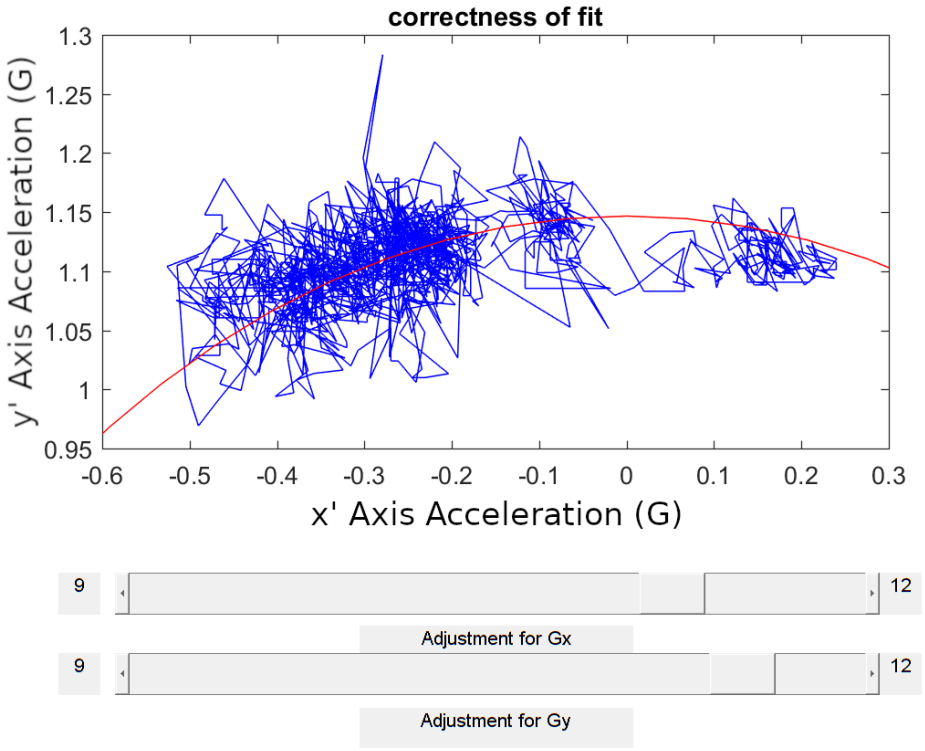

Figure 3.14: *A MATLAB tool to adjust nominal x and y values for G at a given value of θ. The red trace shows G, while the blue trace shows accelerometry data. When G is correctly calculated, the mean for any accelerometry series should rest on the red trace.*

3.8.3 Segmentation

Attempts have been made to automatically segment [62] accelerometer data. These methods are based on the assumption that a swallow will present certain features, which once detected indicate a swallow. There is, however, little justification presented that this will always be the case, particularly as the mechanisms that govern laryngeal accelerometry were reported by some of the same authors [41] to be poorly understood. In addition, dysphagic swallows may present unusual traces, or a complete absence of features whatsoever (in the case of the subject not elevating their larynx in response to the passage of a bolus through their pharynx.)

For the purpose of this work, segmentation was done by hand, guided by times-

tamps encoded during the data capture marking start and end of ingestion, to ensure that anomalous signals are segmented in the same way as those that present the expected pattern.

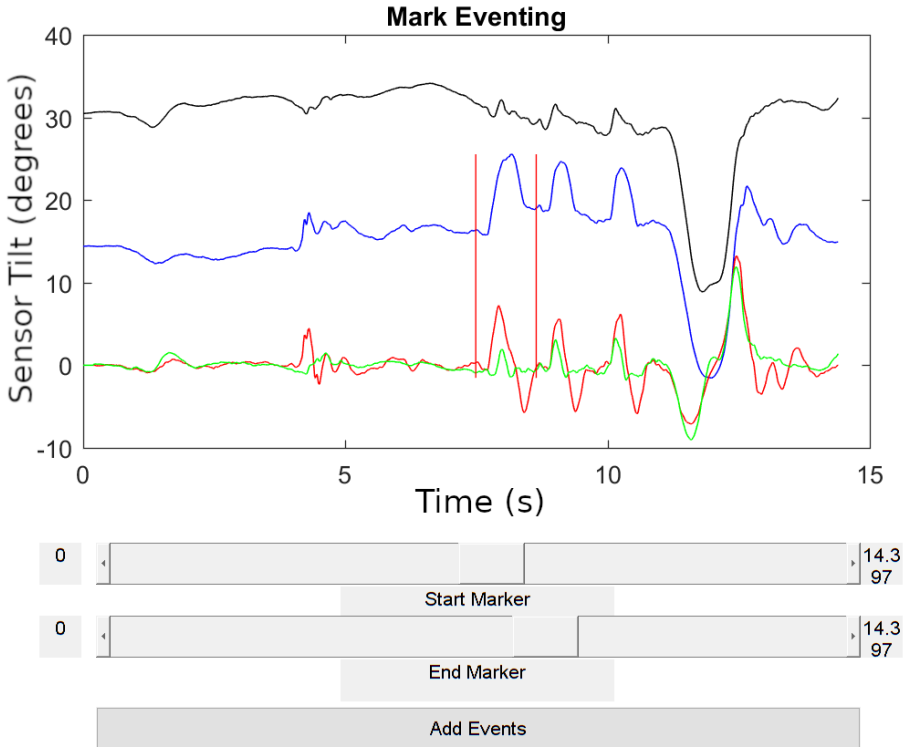

Figure 3.15: *A MATLAB tool for marking the start and end of swallowing segments. The blue and black traces show sensor tilt, while the red and green traces show the difference of the sensor tilt and a 0.2 s time-shift of the same, which can help to identify laryngeal elevation. the blue and red traces are from the top sensor (placed immediately above the laryngeal prominence), while the black and green traces are from the bottom sensor (placed between the laryngeal prominence and the thyroid gland).*

A MATLAB tool, shown in figure 3.15, was created to aid this process.

3.8.4 Removing Head Tilt

Figure 3.16 shows the typical pattern of sensor tilt as a subject mimes drinking from a cup. As the subject's head is tilted backwards, so is the sensor.

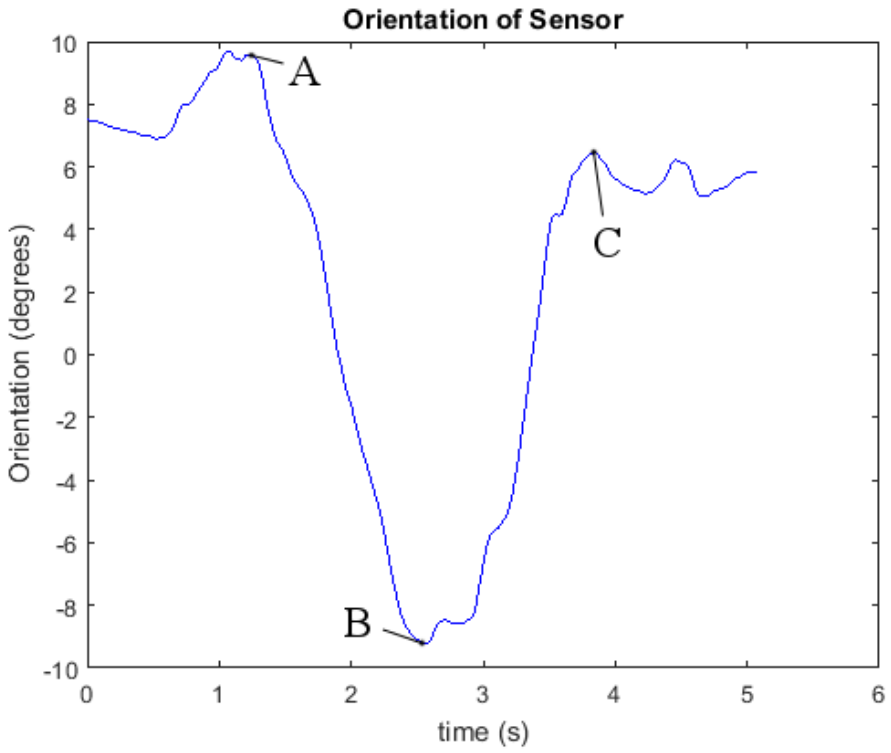

Figure 3.16: *Tilt (orientation) of the sensor as the subject mimes drinking from a cup. The sensor rotates backwards from point A to B following the subject placing the cup against their lips, and then forwards again from B to C, at which point the subject moves the cup away from their lips again.*

As this is behaviour that was not experimentally controlled, and which varies greatly between individuals, a method was designed to neutralise the effect that head tilt has on sensor tilt for the purpose of measuring sensor tilt *due to laryngeal elevation.*

Firstly, we establish that we are interested in controlling for only the head-derived tilt that occurs for the period immediately before laryngeal elevation begins, until immediately after the larynx returns to rest position.

Secondly, we observe that the head tilt is characterised by mostly steady gradients.

From this, once the data is segmented, we can calculate a baseline gradient which

incorporates head tilt using equation 3.19:

$$\theta_h = \left(\frac{\theta_2 - \theta_1}{t_2 - t_1}\right) t + \theta_1 \tag{3.19}$$

This baseline is subtracted from the segmented trace (see figure 3.17).

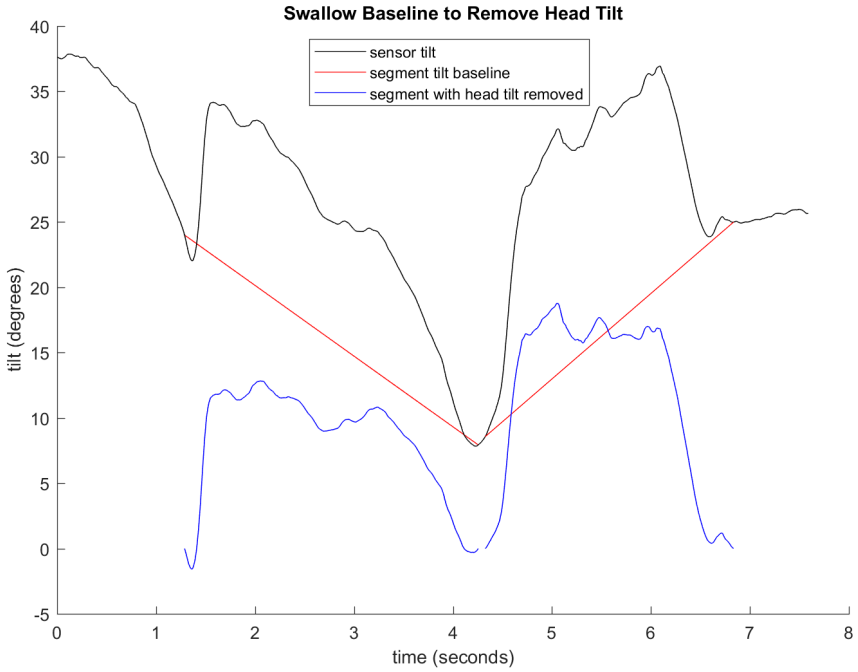

Figure 3.17: *The baseline of each swallow (post-segmentation) is calculated (red), and subtracted from the sensor tilt (black) to produce the segment tilt, minus the effects of head tilt.*

For our immediate purposes, of characterising the sensor output during swallowing for a range of anatomical variables, this produces adequate data. For practical instrument design, an automatic means of eliminating the effect of head tilt on the sensor must be developed. The use of a separate sensor to achieve this, that solely measures head tilt, is introduced in section 5.4.

3.9 Conclusion

In this chapter, we set out the methods we used to study the interaction between a throat-mounted sensor and the larynx during swallowing, including the design of our simulation and mechanical models, our experiments with human participants, and our methods of sensor data processing.

In the next chapter, we report the results from our experiments.

Chapter 4

Results

In this chapter, the results from experiments following the methods described in chapter 3 are presented.

First, all results relating to the simulation model are presented (section 4.1). Next, all results relating to the mechanical model are presented (section 4.2). Thirdly, all results relating to human participants are presented (section 4.4). Lastly, basic analysis is performed on the results (sections 4.5 and 4.6).

4.1 Simulation Model

The simulation model was used to run simulations in 435 combinations: 29 LP sizes and 15 elevation speeds; for each iteration, the accelerometer and gyrometer signals were calculated, the sensor tilt calculated, and also the AP and SI acceleration signals with gravity removed. The peak-to-peak acceleration was measured for each iteration, as was the peak tilt, and the peak gyrometer signal.

Figure 4.1 shows an example of the signals from the (simulated) sensor, for an laryngeal prominence (LP) size of 5 mm and an elevation period of 0.5 s; the peak in the blue gyrometer signal (at around 2 seconds) shows that the model predicts

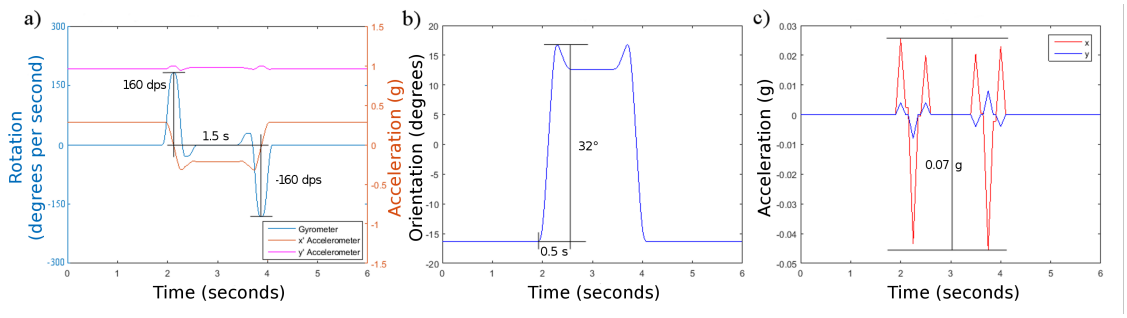

Figure 4.1: *Simulation model output signals for a laryngeal prominence of 5mm.* a) Raw accelerometer and gyrometer signals. b) Angle of the sensor over time. c) The acceleration of the sensor along the global X and Y axes.

a clear forwards tilt associated with larynx elevation (and corresponding backwards tilt upon lowering of the larynx, at around 4 seconds.) This is made clear in figure 4.1 b, which shows the orientation of the sensor, calculated from the raw data using the method described in section 3.8.1. Figure 4.1 c reports the acceleration along the global axes (x in red and y in blue); both lines, red and blue, are characterised by peaks which represent an oscillatory acceleration when the larynx is elevated (at around 2 seconds), and a second when it is lowered (at around 4 seconds).

The maximum sensor displacement in the x (anterior) direction is equal to the size of the LP, since the sensor must move this far in the anterior direction to permit the LP to pass from below the sensor to above it. As the sensor completes a full cycle of displacement (i.e. forwards past the LP, and then back towards the cricoid cartilage once the LP has passed) in the time taken for the larynx to be elevated, we hypothesise that the acceleration is proportionate to displacement, and proportionate to the speed of elevation squared. Similarly, we hypothesise that the rotational angular velocity increases in proportion to the LP size, and in proportion to the speed of elevation, and that the maximum tilt increases in proportion to the LP size only.

From the results of our simulations, as shown in figure 4.2, the simulation model

output matches these expectations. Figure 4.2a shows a linear increase in acceleration with respect to LP size, shown as straight lines from bottom left towards top right, and a super-linear increase in acceleration with respect to speed of elevation, shown as curved lines from bottom right towards top left. Figure 4.2b shows a linear increase in maximum tilt with respect to LP size, shown as straight lines from bottom left to top right, and no relationship between speed of elevation and maximum sensor tilt, shown by the rectangular shape of the surface. Figure 4.2c shows an almost-linear increase of maximum rotational velocity of the sensor with respect to LP size, shown as almost-straight lines from bottom left towards top right, and a linear increase of maximum rotational velocity with respect to speed of elevation, shown as straight lines from bottom right towards top left.

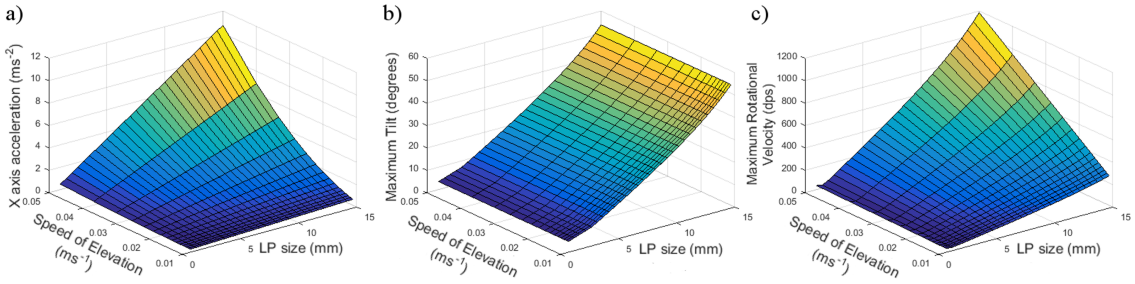

Figure 4.2: *Influence of laryngeal prominence size and speed of elevation on sensor characteristics.* a) Peak-to-peak X axis acceleration increases linearly with laryngeal prominence size and quadratically with speed of elevation. b) Maximum sensor tilt increases linearly with laryngeal prominence size, and is unaffected by speed of elevation. c) Peak angular velocity increases linearly with both laryngeal prominence size and speed of elevation.

4.2 Mechanical Model

Data was recorded from the mechanical model during eight (8) sessions – two (2) for each combination of larynx shape size (3 mm and 15 mm LP) and elevation period (0.5 s and 1 s). In each session, a series of 'swallows' were recorded. Two recordings

for each combination was sufficient, as the signals were highly consistent (see figure 4.3 for an example of three consecutive swallows).

4.2.1 Raw Mechanical Model Data

The raw data from the sensor placed on the mechanical model is presented here.

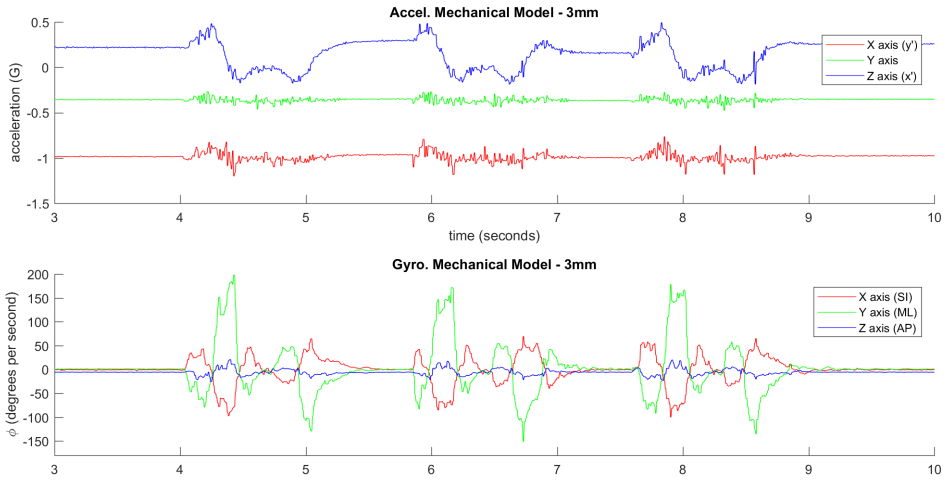

Figure 4.3: *Data from mechanical model with 3 mm laryngeal prominence larynx shape. The top graph shows the three axes of the accelerometer; the bottom graph shows the three axes of the gyrometer. Three successive swallows are shown, starting at 4 s, 5.8 s and 7 s, each moving to maximum elevation in 0.5 s.*

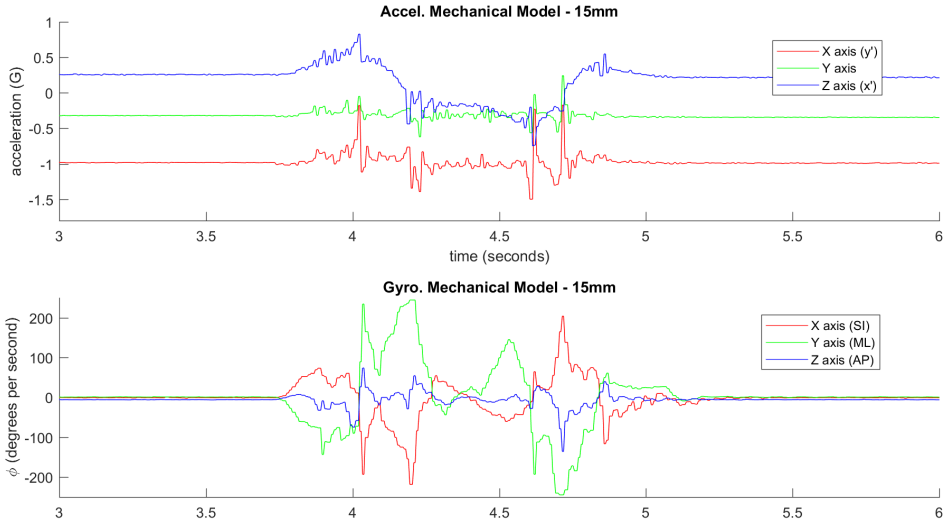

Figure 4.4: *Data from mechanical model with 15 mm laryngeal prominence larynx shape and an elevation period of 0.5 s.*

Three successive swallows using a 3 mm LP larynx shape are shown in figure 4.3 and a swallow using a 15 mm LP larynx shape size is shown in figure 4.4. Swallows across sessions were highly repeatable; the same patterns in the accelerometry and gyrometry data were visible each time.

The positive peaks in the Y axis gyrometer signals (the green gyrometer trace in figures 4.3 and 4.4) indicate a forwards rotation of the sensor; negative peaks indicate a backwards rotation. The forwards rotation can be seen to coincide with the start of the accelerometry activity for each swallow, and the backwards rotation with the end of the accelerometry activity.

4.2.2 Pre-Processed Mechanical Model Data

Figure 4.5 shows the tilt of the sensor over time, as calculated using equation 3.15 in section 3.8.1.

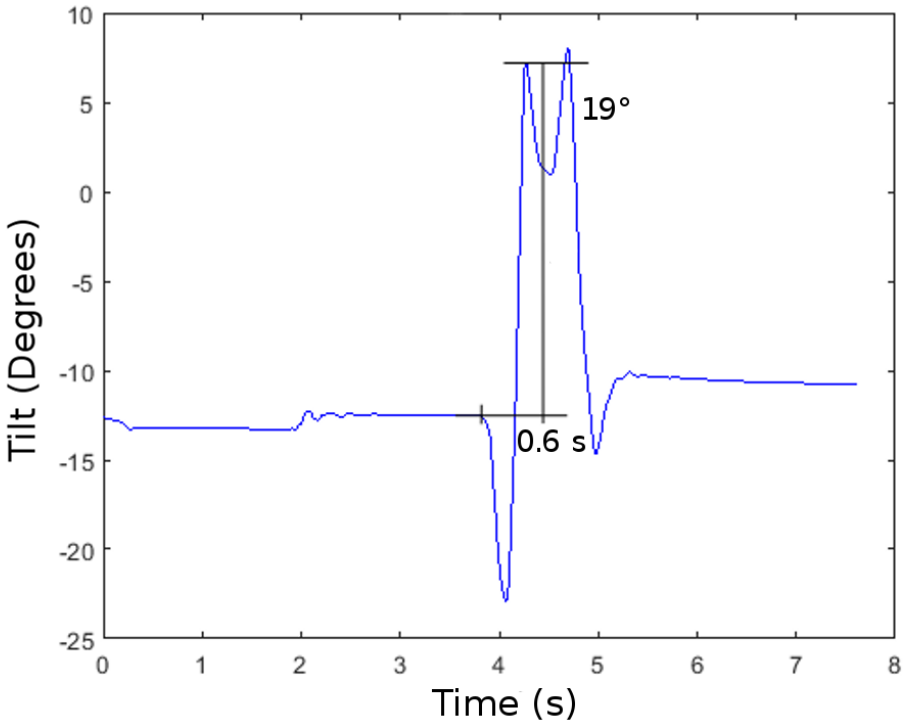

Figure 4.5: *Sensor orientation (tilt) on mechanical model, calculated using a fusion of gyrometer and accelerometer data.*

The trace shows a negative peak of -9°, indicating a backwards tilt, followed by a positive peak of 19°, indicating a larger forwards tilt, then a local negative peak, indicating a small backwards tilt, then another positive peak, a smaller negative peak, and then a return to the starting tilt angle. In the placement of the sensor on the model, there was a small gap between the LP and the sensor. The initial negative peak on the trace corresponded to the point that the LP touched the lowest point on the sensor.

The peak-to-peak tilt using the 3 mm larynx shape was 28°, and the peak-to-peak tilt using the 15 mm larynx shape was 46°.

Figure 4.6 shows the acceleration of the sensor transposed to the reference axes

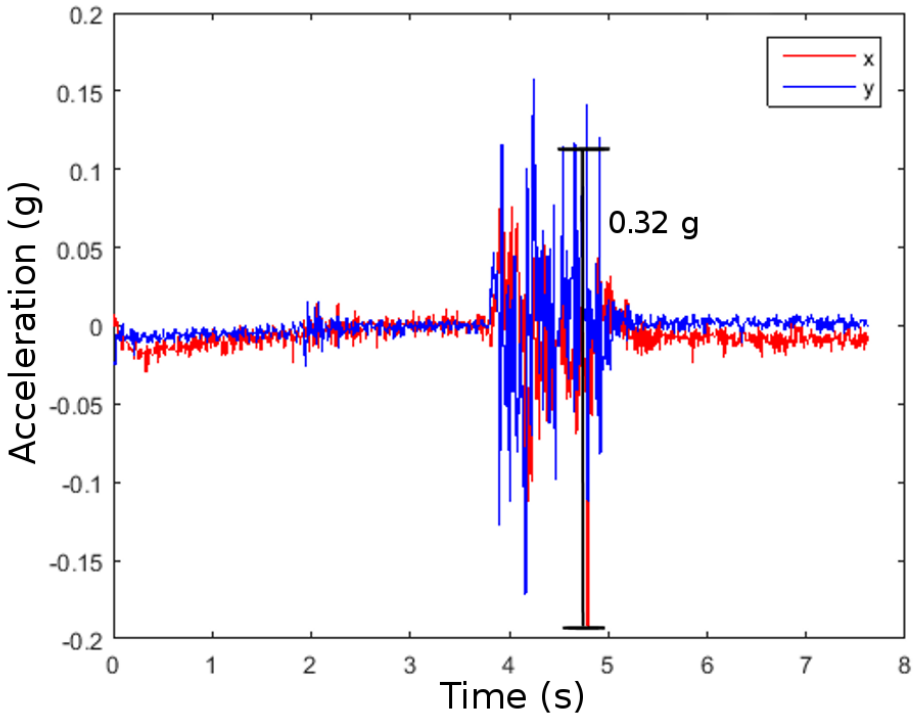

Figure 4.6: *Sensor acceleration on mechanical model, transposed to reference axes.*

using equations 3.17 and 3.18 in section 3.8.2.

4.3 Validation of Simulation Model

Our description of the relationship between laryngeal motion and throat-mounted sensor is the basis of the simulation model. To have confidence in this description, it must be shown to be predictive of real-world experiments. For this, we examine the results from experiments with the mechanical model, and compare them to the simulation model results.

Comparing the simulation model traces shown in figure 4.1 with the mechanical model traces shown in figures 4.3, 4.5 and 4.6, the similarities in the shape of the traces is unmistakable, and the key to the shape of the simulation model traces is

the pattern of sensor tilt as the larynx is elevated.

The simulation model results indicate that the tilt of the sensor is a function of the laryngeal elevation and the laryngeal prominence size. In particular, the maximum tilt increases linearly with an increase in LP size. Figure 4.7 shows how the sensor tilt calculated for the simulation model compares to the sensor tilt recorded on the mechanical model.

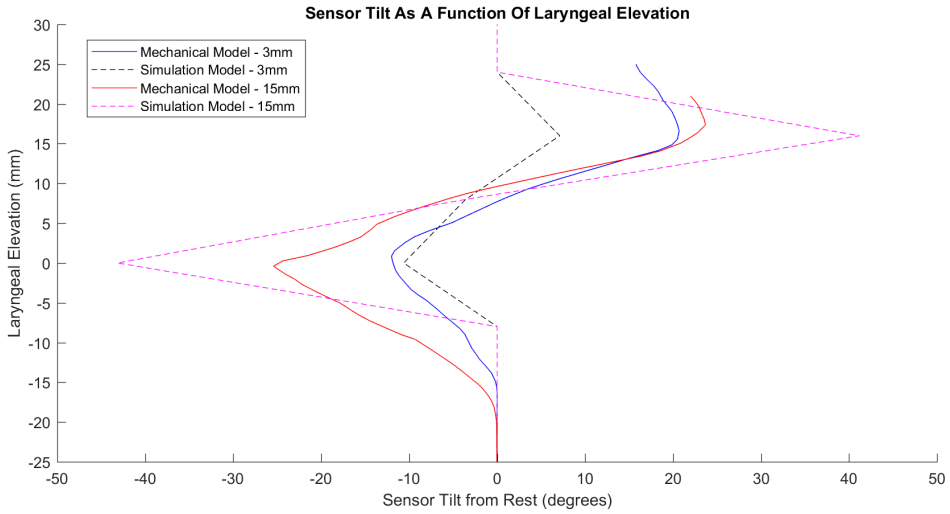

Figure 4.7: *Comparison of sensor tilt over laryngeal elevation between the mechanical model (3 mm laryngeal prominence, blue trace, 15 mm laryngeal prominence, red trace) and the simulation model (3 mm laryngeal prominence, black dashed trace, 15mm laryngeal prominence, magenta dashed trace)*

It can be seen that there is agreement in the general shape of the traces. There is a negative tilt up until the point that the lower edge of the sensor is resting on the LP (defined as 0 mm elevation.) There is also a reasonably linear increase in tilt in the forward direction until the upper edge of the sensor is resting on the LP (at 16 mm elevation), and that the tilt then decreases towards resting position.

We must address the differences between the mechanical model traces and the simulation model traces: the negative peak in the tilt, for the 15 mm LP, differs in amplitude between the simulation model and mechanical model trace; the posi-

tive peaks of both LP sizes differs in amplitude between the simulation model and mechanical model trace; the sensor tilt begins to be effected by laryngeal elevation at a lower elevation in the mechanical model than in the simulation model; the mechanical model traces apparently trend towards returning to rest tilt at a higher elevation than in the simulation model, however the data for this is incomplete, due to limitations of the mechanical model's range of elevation (50 mm total range).

Differences in the detail of the simulation model and the mechanical model are to be expected, as the simulation model represents a simplification of the physical situation, and does not take all details of the shape that the skin forms in response to laryngeal elevation into account. The question is whether the principles of the model are accurate.

For our simulation model, it can be seen that while the precise values of the tilt differ, the pattern of increasing LP size correlating with greater tilt peaks and greater peak-to-peak acceleration does agree. In addition, the pattern of linear tilt between 0 and 16 mm elevation is present for both the mechanical model and the simulation model. It is reasonable, therefore, to infer that the physical principles that the simulation model is built on are, as far as they go, a plausible account of the relationship between the laryngeal motion and the sensor output.

4.4 Human Participants

Twenty-three (23) respondents participated in the experimental procedure described in section 3.5.

The measurements taken of the participants' throats is presented in table 4.1, together with the participant's age and sex.

Table 4.1: Participant Measurements

Participant ID	Age	Sex	LP Size	LP to Thyroid Length	LP to Chin Distance
P1	43	M	8.23	35.39	19.32
P2	36	M	7.42	31	14.9
P3	55	F	2.58	28.5	27.22
P4	35	M	13.61	54.38	23.84
P5	34	F	2.95	28.56	18
P6	29	F	1.04	27	11.15
P7	23	F	1.2	28.4	20.29
P8	37	M	5.62	35.49	20.67
P9	61	M	10.58	40.17	18.41
P10	35	M	11.51	56.73	25.61
P11	21	F	2.91	26.58	13.63
P12	25	M	7.99	35	18.13
P13	26	F	2.19	29.67	13.23
P14	29	M	5.96	44.73	19.65
P15	29	M	9.88	35.61	40.04
P16	50	F	1.22	24.2	18.11
P17	40	F	1.13	37.57	15.88
P18	25	F	2.65	28.26	15.92
P19	48	M	9.54	36.03	40.51
P20	24	M	4.95	33.27	15.18
P21	35	F	1.95	29.32	14.9
P22	57	M	11.64	45.15	33.06
P23	42	F	1.27	34.78	24.54

All measurements are in mm

4.4.1 General Observations of Human Participants

The participants all reported that they were comfortable swallowing the three liquids in the quantity provided, and all picked up the cup in their dominant hand, before moving the cup to their lips and tilting the liquid into their mouth in a continuous motion.

There were differences observed in the gross swallowing behaviour of the participants from this point onwards, however: in some cases, the bolus was ingested in multiple, discrete, small sips, with a corresponding plurality of swallows, and in others, the entire bolus was swallowed in one motion ('downed') with their larynx

held in an elevated position for the duration of the swallow; in some cases, their head was held level, while in other cases, they tilted their head quite far backwards.

Bolus viscosity played a role in the participants' swallowing behaviour: the water bolus produced the most variation between participants, with the greatest head-tilt, and fastest swallowing; the smoothie produced the most carefully controlled swallowing all the participants took multiple small sips. In the data (see section 4.4.2), this behaviour produced an easily recognizable, repeated pattern from the sensor. The 'downed', continuous swallow observed in some participants with the thin liquids (water and juice), this produced a markedly different pattern from the sensor (see section 4.4.2).

4.4.2 Raw Data from Participants

Data was captured successfully with twenty-two (22) participants. A minimum of five (5) swallows were captured for each of the participants (and a minimum of one (1) for each bolus type,) capturing a total of two-hundred-and-one (201) swallows.

An example of data from a swallow using a water bolus is shown in figure 4.8. The swallow starting at 3.5 seconds can be seen to last for twice as long as the swallow starting at 7 seconds. The baseline of each accelerometry axis can be seen to be fairly flat, as there was little head movement. There is a slight upward tilt on the blue trace (and downwards on the red trace,) which is indicative of a small, but steady, lifting of the chin for the duration of the swallow. The peaks in the green gyrometer trace indicate rotation of the sensor, similar to that seen in the mechanical model data.

An example of data from a swallow using a juice bolus is shown in figure 4.9. The swallow starting at 2.5 seconds can be seen to last for nearly three times as long as the swallow starting at 8.5 seconds. This is an example of downing behaviour. A

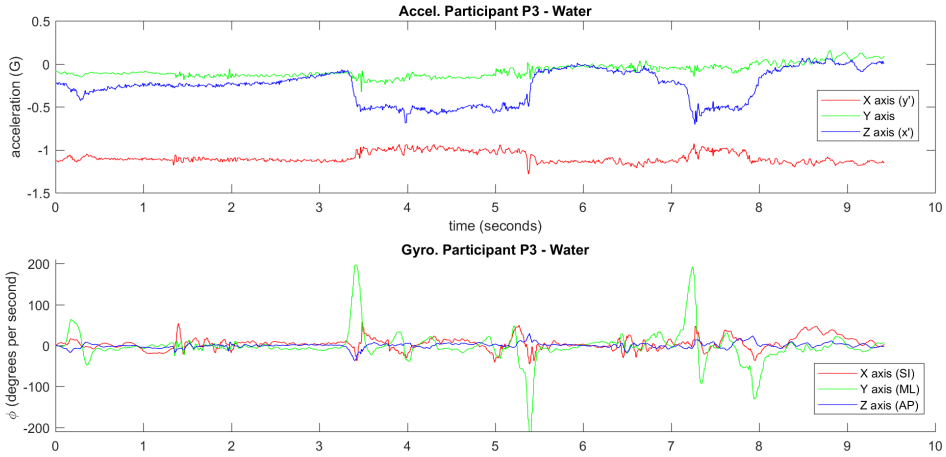

Figure 4.8: *Data from P3 swallowing a water bolus. The bottom graph shows the three axes of the gyrometer. One long swallow is visible from 3.5 s, and one short swallow is seen from 7 s.*

positive peak in the green gyrometer trace at $3s$ and negative peak at $6s$ indicates that the sensor rotated quickly forwards (peaking at 182 degrees per second) at the start of the swallow, and quickly backwards (peaking at -148 degrees per second) at the end of the swallow.

An example of data from a swallow using a smoothie bolus is shown in figure 4.10. There are three swallows visible here, each lasting roughly a second. Gyrometer peaks corresponding to the start and end of swallows can be seen here also.

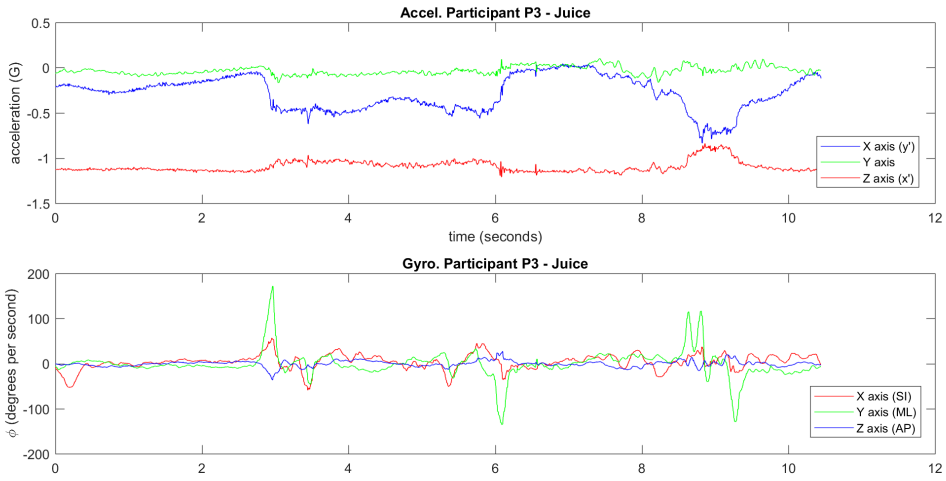

Figure 4.9: *Data from P3 swallowing a juice bolus. The top graph shows the three axes of the accelerometer; the bottom graph shows the three axes of the gyrometer. One long swallow is visible from 2.5 s, and one short swallow is seen from 8.5 s.*

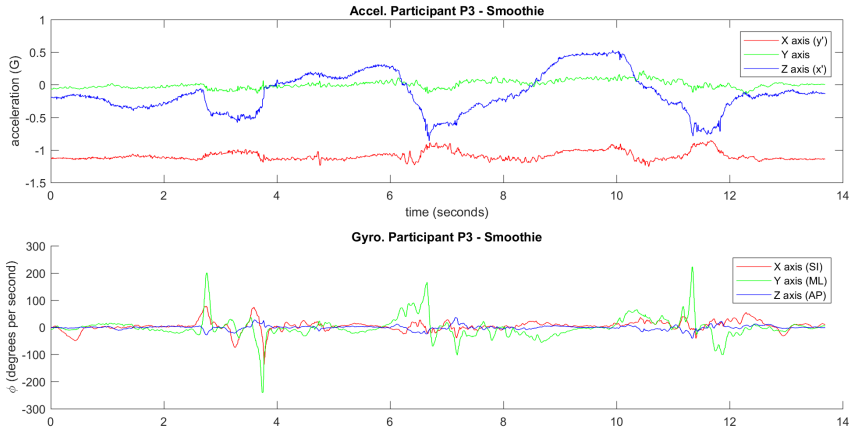

Figure 4.10: *Data from P3 swallowing a smoothie bolus. The top graph shows the three axes of the accelerometer; the bottom graph shows the three axes of the gyrometer. Three swallows are visible, starting at 2.5 s, 6 s and 11 s. The head is tilted backwards between 6 s and 9 s.*

The time taken to swallow the bolus can be seen to increase with the thickness of the bolus, from under 10 seconds (for water), to nearly 11 seconds (juice), to 14

seconds (smoothie).

The Y axis of the accelerometer (nominally aligned to the medial-lateral axis of the participant) can be seen to output close to 0 G throughout all three swallowing sessions; this is typical of all recordings of swallowing sessions.

The Z axis of the gyrometer (nominally aligned to the anterior-posterior axis of the participant) can be seen to output close to 0 degrees per second throughout all three swallowing sessions; this is typical of all recordings of swallowing sessions.

The X axis of the gyrometer (nominally aligned to the superior-inferior axis of the participant) can be seen to produce a small signal that roughly shadows the Y axis (medial-lateral); the amplitude of the X axis is small in comparison to the Y axis in all recording of swallowing sessions.

4.4.3 Processed Data from Participants

The participant data was processed, using the tools and techniques described in section 3.8. The sensor tilt was calculated from the data, the accelerometer data was transposed from relative to reference axes, individual swallows were segmented out, and the effects of head tilt were removed from the segmented swallows.

4.4.3.1 Tilt Calculated from Participant Data

Figure 4.11 shows the tilt calculated from the data from participant P21, selected as a representative trace of the data-set.

The behaviour exhibited by this participant in this recording was to briefly tilt their head forward as they brought the cup to their lips, swallowed twice as they ingested the bolus, then tilted their head back to drain the cup before swallowing twice to clear the residue from their throat.

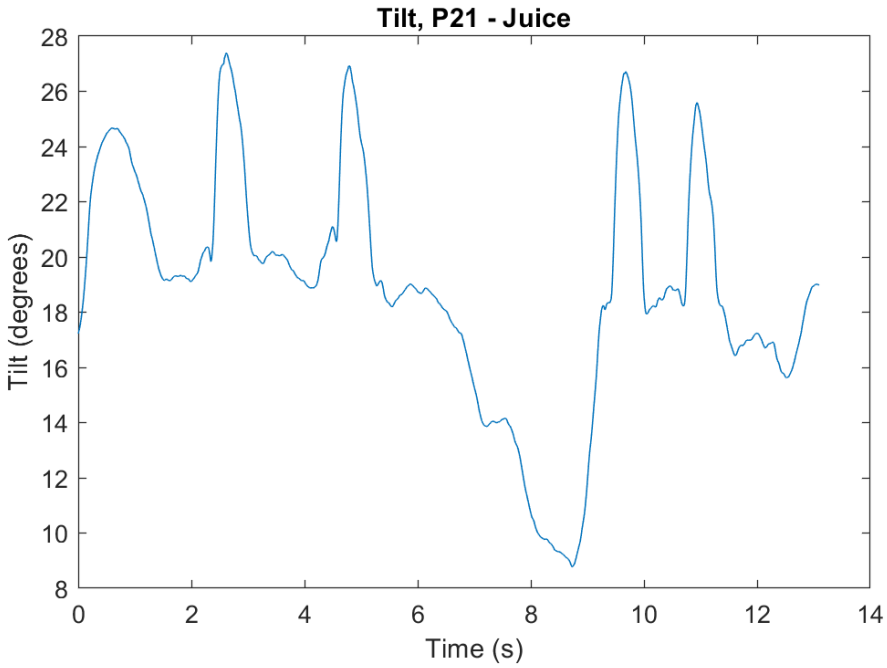

Figure 4.11: *Sensor tilt for participant P21 consuming 30ml of juice. Swallows starting at 2.1 s, 4.4 s, 9.2 s and 10.6 s. Significant head movement from 0 to 1.8 s, and from 6 to 9.2 s.*

4.4.3.2 Transposition of Participant Data

Figure 4.12 shows the result of transposing the accelerometer data of the same data-set as discussed above, in section 4.4.3.1.

The effect of the transposition is to mostly eliminate the low-frequency signal visible in the raw data, leaving low-amplitude broad-spectrum noise (i.e. general 'fuzziness' in the trace) and sharp 'spikes' that correspond with the swallows visible in figure 4.11.

The spikes are visible on both axes, and the amplitude of the spikes is proportional to the subject's LP size.

Interestingly, the transposed accelerometry data is not contaminated by head movement, however it is important to note that the transposition operation depends on the sensor tilt being calculated. Transposed accelerometry data is an addition to

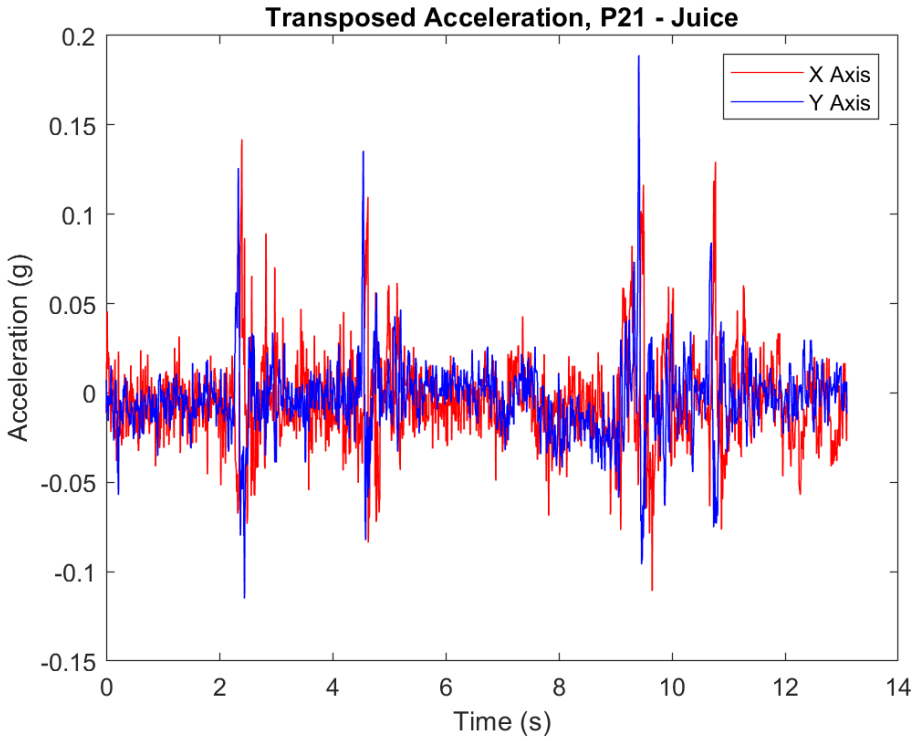

Figure 4.12: *Acceleration graph for participant P21 consuming 30ml of juice, transposed to x and y axes.*

sensor tilt, not an alternative.

4.4.3.3 Variation of Swallowing Data

The swallows recorded from some participants were extremely consistent in nature (see figure 4.13,) while other participants displayed variability in duration of swallows (see figure 4.14,) and in maximum tilt (see figure 4.15.)

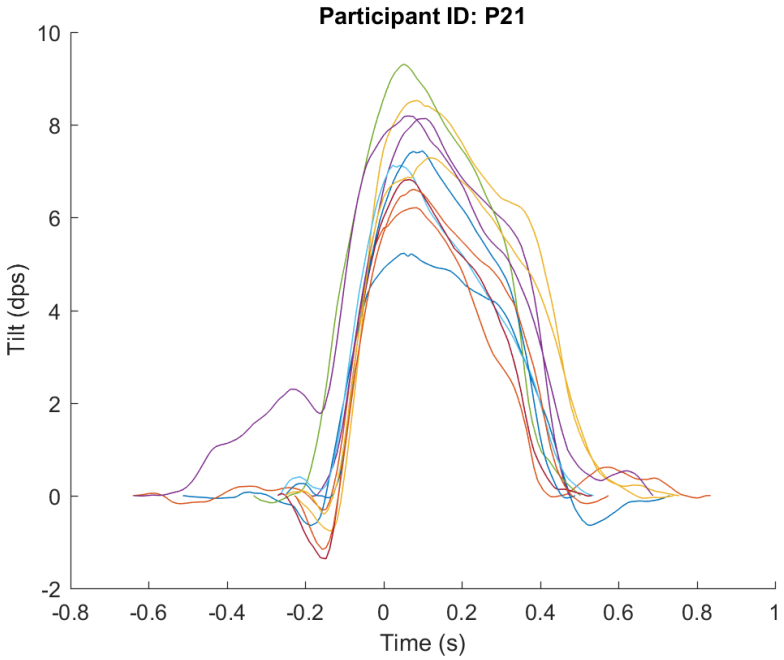

Figure 4.13: *Segmented swallows from participant P21. Colours are to distinguish successive traces. There can be seen to be very little variation in the tilt pattern between swallows.*

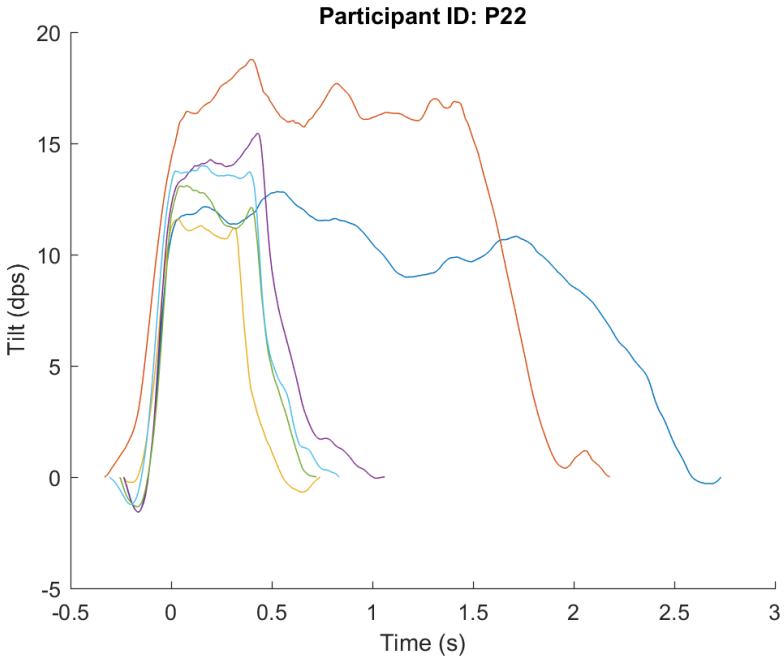

Figure 4.14: *Segmented swallows from participant P22. Colours are to distinguish successive traces. There can be seen to be significant variation in the duration of the swallows.*

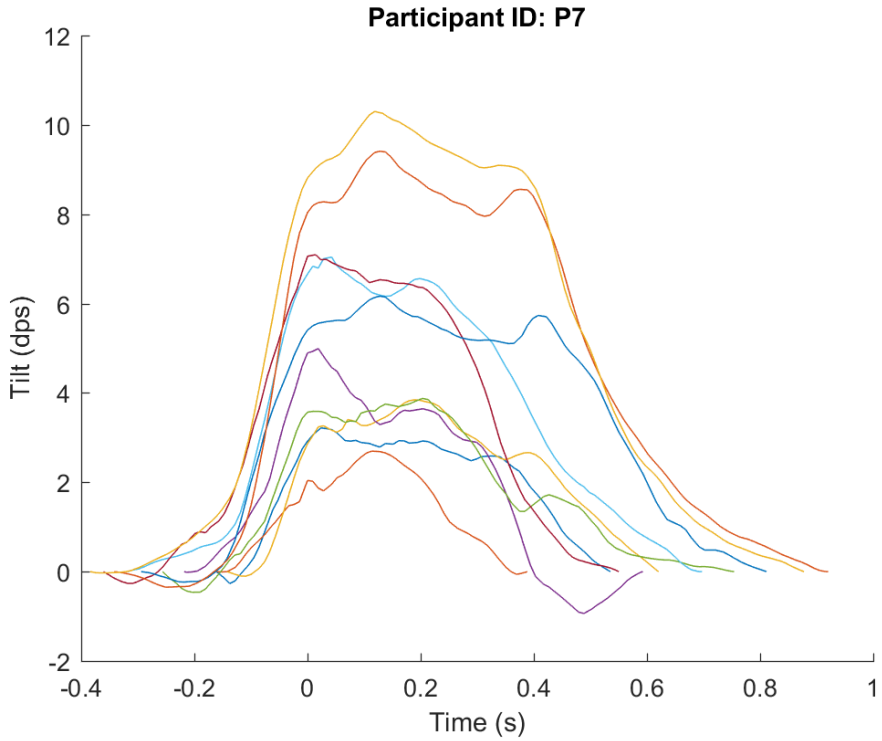

Figure 4.15: *Segmented swallows from participant P7. Colours are to distinguish successive traces. There can be seen to be significant variation in the maximum tilt across swallows.*

Figure 4.16 shows the duration of each swallow for each participant, from the time the larynx begins to elevate (measured as the beginning of the sharp forward tilt of the sensor,) to the time it returns to rest (measured as the end of the sharp backward tilt of the sensor.)

The mean duration of a swallow was $0.64s$, with a standard deviation of $0.14s$. Outliers tended to be a multiple of the typical duration for that participant, suggesting that when the larynx is held at maximum elevation, this is a kind of repeated behaviour at a neurological level.

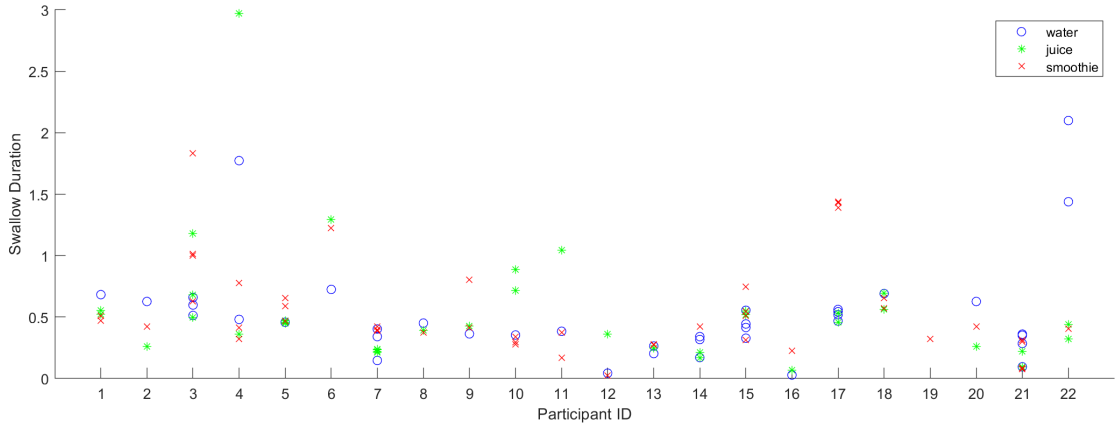

Figure 4.16: *The time from the sharp forward rotation of the sensor, to the sharp backwards rotation of the sensor for each swallow, grouped by participant. Water is shown as blue circles; juice is shown as green stars; smoothie is shown as red x's.*

s

Figure 4.17 shows the time from resting sensor tilt to maximum sensor tilt for each swallow.

The mean time to maximum sensor tilt was $0.3s$, with a standard deviation of $0.17s$.

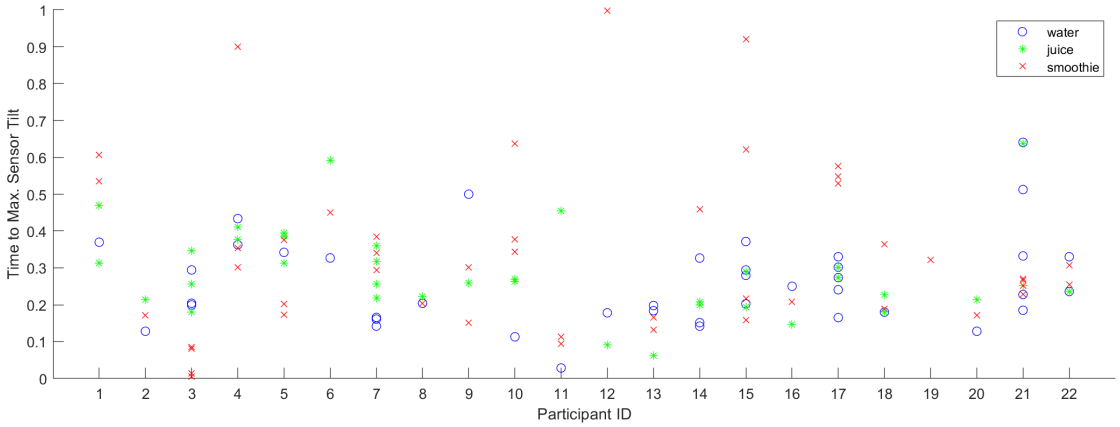

Figure 4.17: *The time from resting sensor tilt to maximum sensor tilt for each swallow, grouped by participant. Water is shown as blue circles; juice is shown as green stars; smoothie is shown as red x's.*

4.5 Statistical Analysis of Participant Data

In the simulation model results, we saw that the size of the accelerometer peak-to-peak, gyrometer peak and maximum tilt all increase linearly with laryngeal prominence size; in this section we present analysis which shows this to be the case with the results from experiments with the human participants also. Regression analysis was performed with the gyrometer peak, maximum tilt, and accelerometer peak-to-peak as outcome variables, and the LP size as the predictor variable.

The maximum accelerometer peak-to-peak, maximum sensor tilt, and maximum gyrometer peak were measured from all traces of participants drinking the smoothie bolus (used here because, as stated in section 4.4.1, participants exhibited the most consistent and comparable behaviour with the smoothie bolus.)

Figure 4.18 reports the gyrometer peak plotted against the LP size of different human participants. Figure 4.18 shows a general trend that as the LP increases

in size, the gyrometer peak increases as well (also as described by the simulation model). The application of least squares regression analysis (dashed blue line in Fig 4.18) reports a slope of 8.9 dps/mm, which is significantly different from zero ($p = .00013$), with $R^2 = .53$; this means that gyrometer peak is influenced by LP size.

According to the simulation model, speed of elevation directly influences the gyrometer peak. In our experiment, we did not control for speed of elevation. It is reasonable to infer that speed of elevation is a primary source of the scattering of the data in figure 4.18.

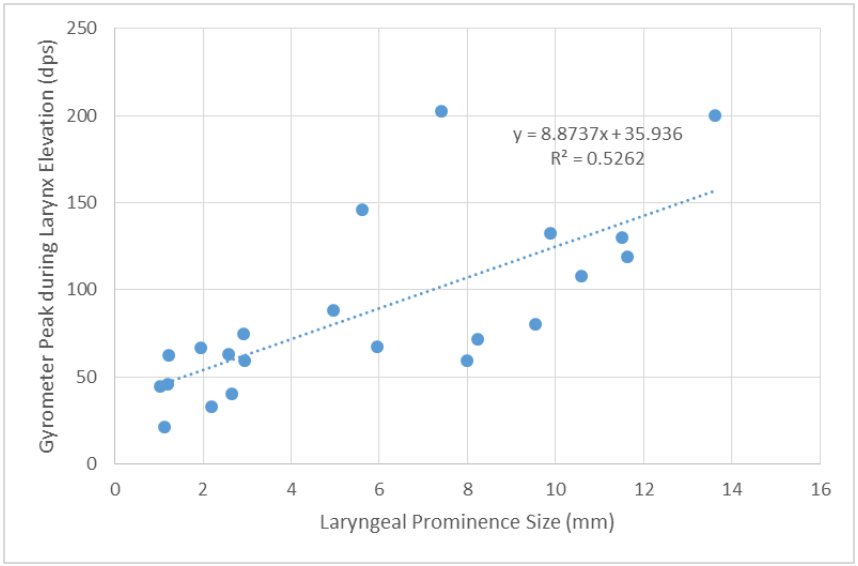

Figure 4.18: Laryngeal prominence size vs. gyrometer peak observed during larynx elevation (smoothie bolus only)

Fig 4.19 shows the maximum tilt of the sensor in response to swallowing, plotted against the LP size of the participants. Fig 4.19 shows a general trend that as LP size increases, the maximum tilt also increases. Applying least squares regression analysis to this data (dotted blue line in Fig 4.19) reports a slope of 1.2 degrees/mm, which is significantly different from zero ($p = .000046$), with $R^2 = .53$; this means maximum sensor tilt is influenced by LP size.

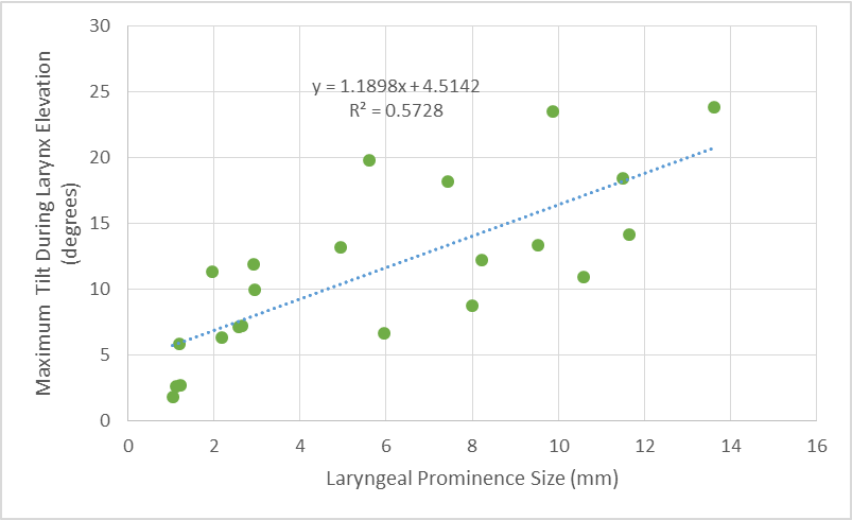

Figure 4.19: Laryngeal prominence size vs. maximum sensor tilt observed during larynx elevation (smoothie bolus only)

Figure 4.20 shows the acceleration peak-to-peak in response to swallowing, plotted against the LP size of the participants. Figure 4.20 shows a general trend that as LP size increases, the acceleration peak also increases. Applying least squares regression analysis to this data (dotted blue line in figure 4.20) reports a slope of 0.07 ms-2/mm, which is significantly different from zero ($p = .035$), with $R^2 = .2$; this means that the accelerometer peak-to-peak is influenced by LP size, albeit less than the previous two quantities. According to our simulation model, speed of elevation has a strong influence on accelerometer peak-to-peak. In our experiment, we did not control for speed of elevation, which we believe to be a primary source of the scattering of the data in figure 4.20.

4.6 Review of Proposed Mechanisms

In section 3.2 we proposed some basic mechanisms underlying laryngeal accelerometry. Here we show that the results from our experiments support the proposed mechanisms.

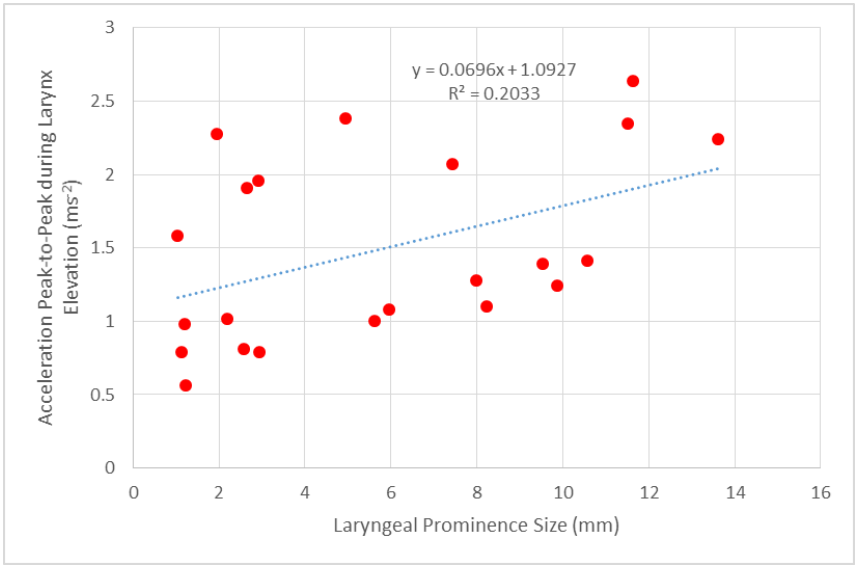

Figure 4.20: Laryngeal prominence size vs. acceleration peak-to-peak observed during larynx elevation (smoothie bolus only)

In the results above, a high-amplitude, low-frequency signal is visible on the accelerometer trace, which coincides with sensor tilt. In addition, it was demonstrated in section 3.8.4 that head tilt produces a particularly large low-frequency signal.

The existence of consistent gyrometer activity at the point of deglutation demonstrates that sensor rotation is a fundamental component of the accelerometry signal documented in the literature. In our results we have consistently observed a gyrometry peak in response to laryngeal elevation, both in the case of the mechanical model and with human participants. Also supporting this view is the consistent observation (during a swallow) of an accelerometry signal of 0.5G which can be attributed to sensor rotation alone – this is far in excess of the remaining accelerometer signals, which we attribute to sensor displacement.

With the removal of the effects of sensor tilt from the accelerometer (through the transposition of the accelerometry signals to the x and y reference axes,) a dependable pattern in the accelerometry signal at the points of elevation and de-elevation of the larynx can be seen along both axes. This indicates that there is

acceleration of the sensor along both axes.

There is insufficient information to determine which features and aspects of the accelerometry signals are caused by laryngeal elevation and which by laryngeal excursion, however the combined influence of the two axes of laryngeal displacement on the sensor is clear.

4.7 Conclusion

In this chapter, the results from our experiments were reported, as well as our initial analysis of the data, providing direction for the next stage of the project.

In the next chapter, we draw out the specifications for an instrument useful for screening and assessment of dysphagia through further analysis of our results, and present a prototype instrument based on these specifications.

Chapter 5

Further Analysis and Instrument Design

This chapter builds upon the findings in chapter 4, with the aim of elucidating information useful to the development of instrumentation for assessment of dysphagia based on the sensors described in chapter 3. Where chapter 4 is exploratory in its approach, broadening our understanding of sensor data, this chapter is targeted, deepening our knowledge of the particular effects relevant to the measurement of laryngeal elevation.

We begin by analysing the anatomical measurements of participants in section 5.1, to determine which factors are important to consider in the design of dysphagia instrumentation. Next, section 5.2 evaluates the various strands of processed data for clinical usefulness. Section 5.3 sets out a specification for instrumentation that is likely to be of clinical use based on the earlier analysis. The chapter closes in section 5.4 with a description of a prototype instrument, based on the specifications laid out in section 5.3.

5.1 Participant Anatomical Measurements

The mechanics of swallowing physiology described in chapter 3 predict that LP size influences the amplitude of both accelerometry and gyrometry data. In chapter 4, this effect was seen in participant data. For a potential instrument to mitigate this effect, the LP size of the subject must be measured. This may not be practical in all applications, for example in the case of a screening procedure which requires as few and as simple actions as possible. In such cases, it is useful to identify predictors of LP size, which may be used to estimate LP size.

The ages of our participants were well distributed between 21 and 61 years of age, and reasonably gender balanced, as can be seen in figure 5.1. Male laryngeal prominence (LP) size was evenly distributed between 5.65 and 13.61 millimetres, while female LP size was evenly distributed between 1.04 and 2.91 millimetres.

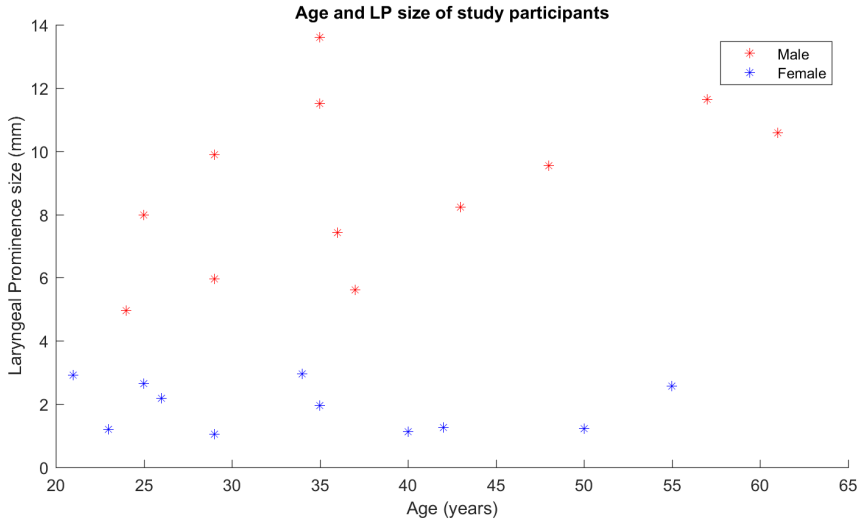

Figure 5.1: *The distribution of participant age and laryngeal prominence size. Male participants are shown in red, while female participants are shown in blue.*

This section presents analysis which establishes the level of correlation between the three anatomical variables, and whether the age and sex of the subject is predictive of the LP size, concluding with an assessment of the importance on these

factors in consideration of instrument design.

Our sample size is small, but the literature does not give the popular distribution of the measurements we are interested in, and their correlations between one another.

5.1.1 Correlation between LP Size, LP to Chin, and LP to Thyroid Gland

First, we examine the correlation between the three anatomical measurements. The Pearson's correlation coefficient between LP size and LP to chin distance is $\rho = 0.5906$ ($p = 0.0038$), between LP size and LP to thyroid length is $\rho = 0.8031$ ($p < 0.0001$), and between LP to thyroid length and LP to chin distance is low ($\rho < 0.4$) and not statistically significant.

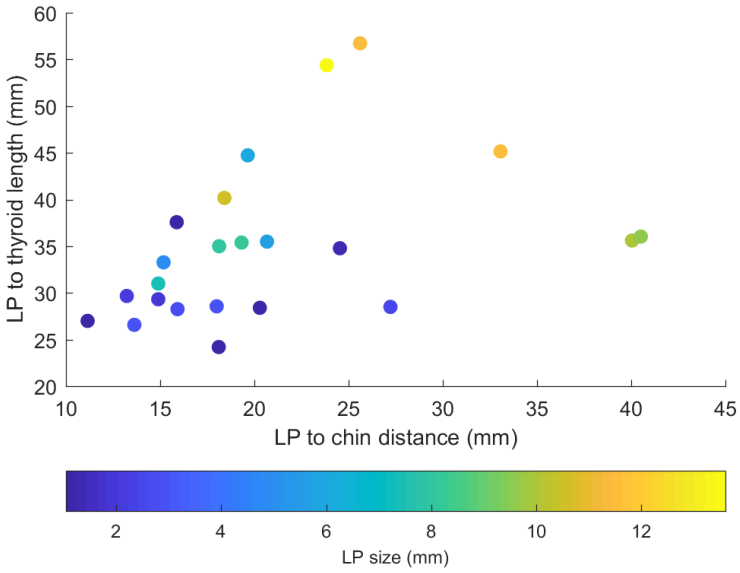

Figure 5.2: Laryngeal prominence to chin distance plotted against laryngeal prominence to thyroid gland length, with laryngeal prominence size heatmapped.

From this, we can determine that there is a strong positive relationship between the size of the laryngeal prominence and the length of the larynx body, a moderate

positive relationship between the LP size and the distance from the LP at rest to the chin, and no real relationship between the length of the larynx and the distance from LP at rest to the chin. This can be observed in figure 5.2, where the LP size can be seen to increase (i.e. the dots move from blue to yellow) along the vertical axis (LP to thyroid length), but not along the horizontal axis (LP to chin distance).

A subject with a larger LP size is highly likely to have a longer larynx, but only somewhat likely to have a larynx lower from their jaw-line. The length of a subject's larynx cannot be deduced from a measurement taken of the distance between their LP and their chin, nor vice versa.

5.1.2 LP Size dependence on Age Groups

To evaluate the effect of age on LP size, one-way anaylysis of variance (ANOVA) (see table 5.1) was performed, regarding age (grouped by decade) as the independent variable and LP size as the dependent variable. Figure 5.3 visualizes the spread of LP size for each age group.

Table 5.1: One-way analysis of variance: LP Size from Age Groups

Source	Sum Sq.	d.f.	Mean Sq.	F	P
Between Age Groups	56.578	4	14.1444	0.82	0.5272
Within Age Groups	309.202	18	17.1779		
Total	365.78	22			

The low F-number ($F < 1$) and high p-number ($p > 0.5$) in the analysis shown in table 5.1 demonstrate that the LP sizes of different age groups is not significantly different. It would be impossible to predict a subject's LP size based on their age, or to infer their likely age group from knowledge of their LP size.

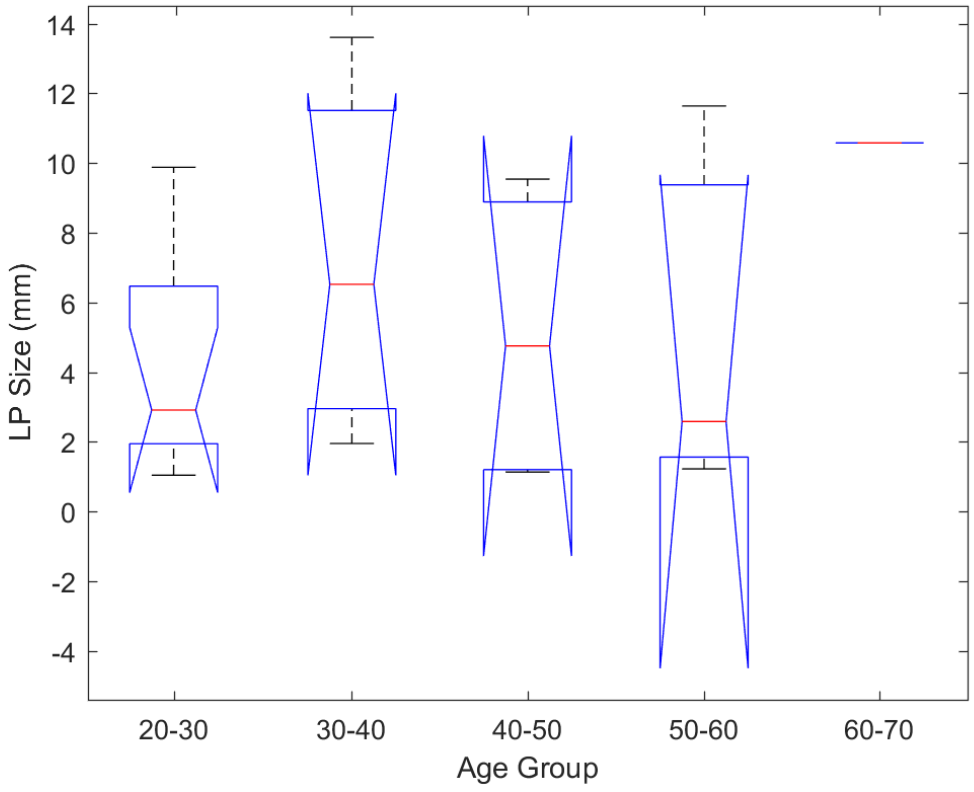

Figure 5.3: *Visualization of distribution of laryngeal prominence size for each age group, where participants were grouped into age groups by decade. Significant overlap between groups suggests that age does not predict laryngeal prominence size. In this box-whisker plot, the horizontal red lines represent the mean for each group; the black horizontal lines at the end of the 'whiskers' represent the maximum and minimum values of each group; the horizontal blue lines at the top and bottom of the 'boxes' represent the* 75^{th} *and* 25^{th} *percentile, and the corners of the diagonal section of the box, called the 'notches', represent the* 95 *percent upper and lower confidence limit of the true mean value for each group.*

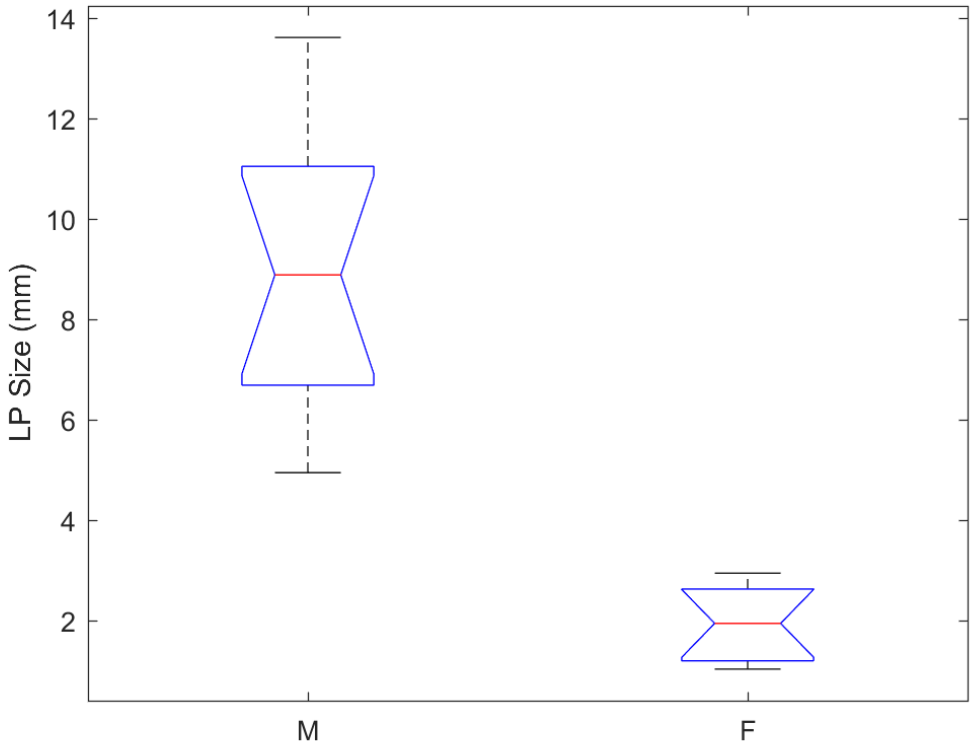

Figure 5.4: *Visualization of distribution of laryngeal prominence size for male and female groups. The total absence of overlap between the two groups suggests that sex predicts laryngeal prominence size.*

5.1.3 LP Size dependence on Sex

To evaluate the effect of sex on LP size, one-way ANOVA (see table 5.2) was performed, treating sex (male and female) as the independent variable and LP size as the dependent variable. Figure 5.4 visualizes the spread of LP size for participants grouped into male and female categories. The high F-number ($F > 10$) and low

Table 5.2: One-way analysis of variance: LP Size from Sex

Source	Sum Sq.	d.f.	Mean Sq.	F	P
Between Sexes	280.7	1	280.7	69.28	4.3345×10^{-8}
Within Sexes	85.079	21	4.051		
Total	365.78	22			

p-number ($p < 0.001$) in the analysis shown in table 5.2 demonstrate that the LP size of male and female subjects is significantly different. Female subjects may be predicted to have an LP size of 2 ± 1mm; male subjects may be predicted to have an LP size of 9 ± 5mm.

5.1.4 Summary of Anatomical Measurement Analysis

In summary, there is no significant trend correlating age with LP size; there is, however, a clear, statistically significant separation in LP size between male and female participants: i.e. there were no female participants with a LP size greater than 3mm, and also no male participants with an LP size measured smaller than 5mm.

It is important to note that children were excluded from the data capture; The literature shows that the male/female distinction would be smaller for younger children, and that the LP size would increase with age up to the mid-teens [46], [47].

5.2 Comparison of Tilt and Acceleration as Indicators of LP Elevation

Using the processing techniques developed in section 3.8, and applied to our raw participant data in section 4.4.3, we have access to a rich feature-set. Both the transposed accelerometer data and the sensor tilt can be used to identify when the larynx has been elevated.

Where the usefulness of the two classes of data differ, is that the sensor tilt has been shown in this work to be a function of LP size and elevation, whereas the transposed accelerometry data is a function of LP size alone. In the literature, there is a suggestion that accelerometer peaks are proportional to peak laryngeal

elevation, however this refers to un-transposed accelerometer signals, which contain rotation as a major component. The transposed accelerometer data has proved to have a natural independence from head-movement.

The suggestion is that transposed accelerometry data is most useful for *detecting* laryngeal elevation, and sensor tilt is most useful for *measuring* laryngeal elevation.

5.3 Instrument Specifications

From the analysis in this chapter and the results from chapter 4, we can begin to design an instrument which measures laryngeal elevation. In this section we set out the requirements for such an instrument.

5.3.1 Pre-requisite measurements

It can be seen from our findings in section 4.4.3.1 that sensor tilt is a clear indicator of laryngeal activity, and can be used to infer moment-by-moment laryngeal elevation. *A priori*, the subject's LP size must be known for this calculation to be made, so there must be the means to input the subject's LP size into the instrument.

For screening procedures, it may be sufficient for the instrument to have a simple means of switching between a male and female setting, so that the difference in LP size can be adjusted for based on the mean prominence size for each sex.

5.3.2 Elimination of head tilt

The calculation of laryngeal elevation relies on the principle that the sensor tilt is a function of the SI position of the LP. As tilting of the head also causes tilting of the sensor, a way of rejecting the effect of head tilt on the sensor must be a requirement for the instrument.

To suggest a plausible method for isolating larynx-induced sensor tilt from other tilt sources: the inclusion of a second sensor in the instrument, that moves with the subject, but not with the larynx, could be used as a reference to ground the tilt.

5.3.3 Positioning of sensor

The instrument must have a reliable method of positioning it to ensure that the sensor rests against the skin medially on the anterior of the throat, immediately above the resting position of the LP. One possible method for achieving this could be to use the chin as a guide, however the fact that there is significant variability in the distance between the LP and the chin ($11mm$ to $41mm$) presents a significant challenge in designing such a guide. It may be necessary to require the clinician operating the instrument to locate the LP to properly position the instrument.

5.3.4 Sampling and calculation rate

From our results, in the typical swallow the larynx reaches peak elevation in roughly $0.1s$. To ensure that the peak elevation is not missed in-between samples, the calculation speed should ensure that there are at least 10 output data-points in that period, i.e. an output of 100Hz.

5.3.5 Form factor

The instrument should be as portable as possible, and as comfortable to wear as possible. The instrument must have a clear, efficient and practical sterilization procedure.

5.3.6 Electrical Safety

The requirements of IEC 60601 must be considered in the design (see section 2.8 for further details on how this impacts portable electrical medical equipment.)

5.3.7 Medical Device Classification

Under the Medical Device Directive (see section 2.8), a device built to these specifications would be considered a Class Im medical device, as it is in contact with unbroken skin only, and take measurements in recognised units.[1]

5.4 Prototype Instrument for Dysphagia

In section 4.3, it was demonstrated that the relationship between the subject's laryngeal elevation and the sensor's tilt is approximately linear over the larynx's typical range (given the careful positioning of the sensor.) The main limitation in using the sensor tilt for inferring laryngeal elevation is that the tilt is also influenced by the inclination of subject's head and neck. This effect was mitigated in our prototype instrument by the use of a second, reference sensor, from which the tilt of the subject's neck is calculated and subtracted from the tilt of the sensor placed over the LP; figure 5.5 illustrates this basic principle.

Also shown by figure 5.5 is the method we used to detect that the instrument is in contact with the throat: capacitive sensors detect the presence of skin and enable the output of the instrument – this helps to ensure that only valid measurements are taken.

[1]Rule 10 of device classification states that active medical devices are Class IIa "if they are intended to allow direct diagnosis or monitoring of vital physiological processes". Laryngeal elevation is not considered a vital process; if it were, then a device built to these specifications would be Class IIa.

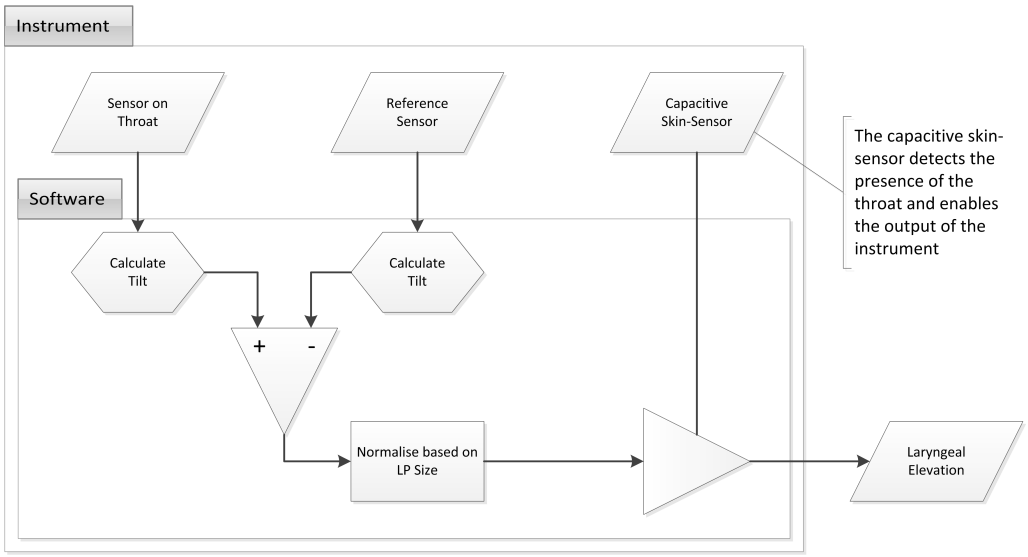

Figure 5.5: *The basic process by which the prototype instrument calculates laryngeal elevation from IMU sensor data.*

Using this design, a prototype device was constructed from:

- A 3D-printed hard plastic body for the instrument, shaped to fit comfortably on the throat while leaving a cavity for the sensor and other electronics
- A velcro neck strap
- A natural latex rubber membrane shaped to cover the hard instrument body and suspend a sensor over the larynx
- A USB-powered microcontroller development board, with a ARM Cortex-M0+ processor
- Copper tape, used to form the electrodes for capacitive sensors

None of these materials are particularly expensive, difficult to acquire, or difficult to work with; with the exception of the 3D-printed body, the prototype was constructed entirely by hand.

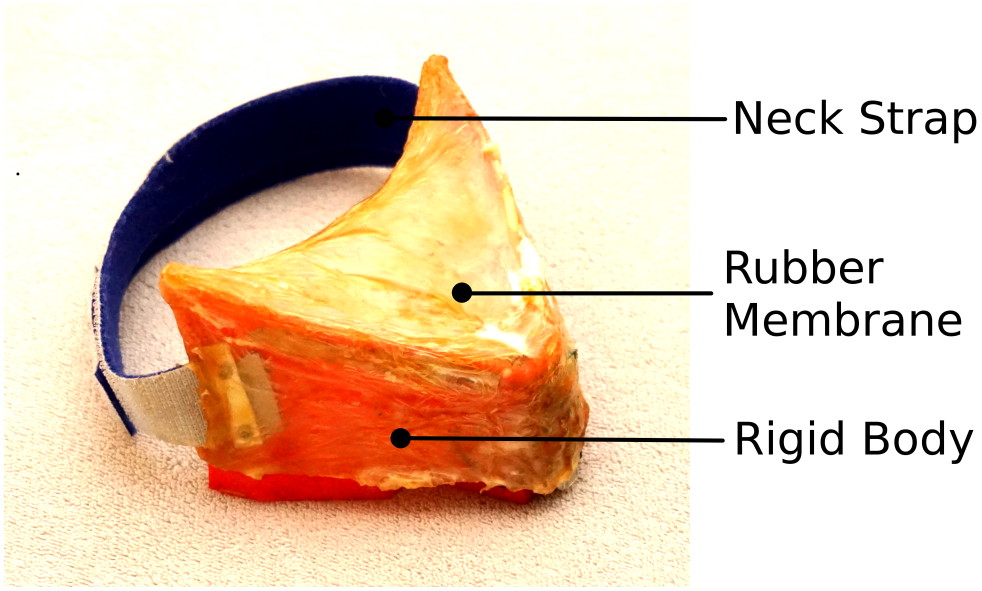

Figure 5.6: *The prototype instrument, viewed from the top.*

The constructed prototype is shown in figures 5.6 and 5.7, where the IMU sensor and capacitive skin sensor can be seen suspended by the rubber membrane, which is held in position by the hard plastic instrument body, upon which the reference IMU sensor is also mounted. The microcontroller development board is mounted on the front of the instrument (i.e. the side furthest from the throat and capacitive sensors) and can be seen as a dark shape under the rubber membrane in figure 5.6.

5.4.1 Testing

As the purpose of the prototype instrument is to show that it is possible to create an inexpensive, portable, simple-to-use instrument that quantitatively measures laryngeal elevation during swallowing, these attributes are the criteria that the prototype was evaluated against. Low-expense and portability were factored into the design of the instrument. Ease of use was evaluated based on the consistency of results when the device was hurriedly positioned on the throat, and compared to when it was carefully positioned. To evaluate whether the instrument quantitatively mea-

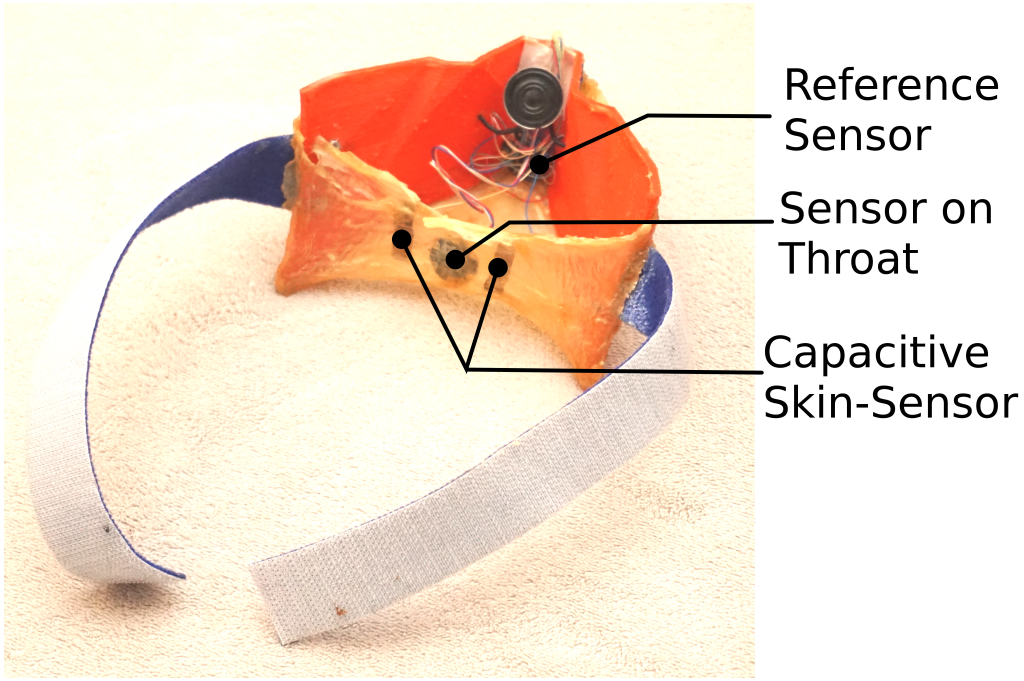

Figure 5.7: *The prototype instrument, viewed from the bottom.*

sures the elevation of the larynx, the output was compared to the sensor tilt graphs from the data capture (as presented in section 4.4.3.1.) The expectation is that the pattern of swallows should closely resemble the tilt graph, with the exception that head tilt should be strongly attenuated or rejected altogether.

5.4.1.1 Testing procedure

Data was captured from the instrument mounted on the researcher's throat, in three successive exercises:

1 Swallowing 30 ml bolus of water while keeping head level

2 Swallowing 30 ml bolus of water while tilting head backwards

3 No bolus or swallowing, head nodded up and down in exaggerated movements

Each excercise was repeated 5 times, with the instrument removed and replaced between each repetition.

Figure 5.8: *The prototype instrument, in position on the throat.*

5.4.2 Prototype Test Results

The prototype instrument outputs three streams of data: the throat-mounted sensor, the reference sensor, and the calculated laryngeal elevation.

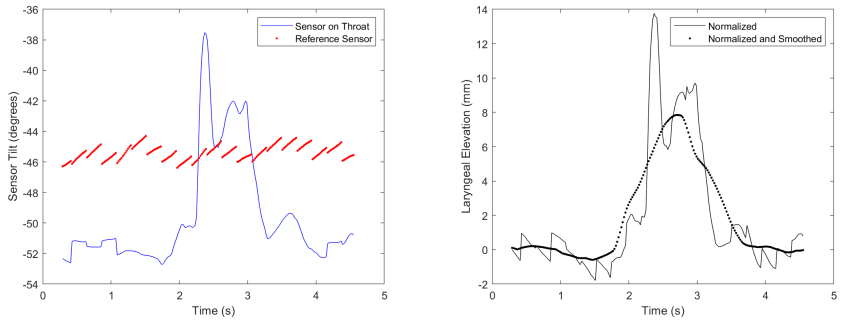

Figure 5.9: *Data from the prototype instrument. Left – throat sensor tilt (blue solid line) and reference sensor tilt (red dotted line). Right – Laryngeal elevation calculated by the instrument (black solid line) and smoothed laryngeal elevation (black dotted line). Data recorded while subject drank from a glass of water, keeping head level.*

In all of the recordings where a bolus was swallowed, the throat-mounted sensor tilt was recognisable as following the same forward tilt, plateau, backwards tilt pattern that can be seen in the participant data.

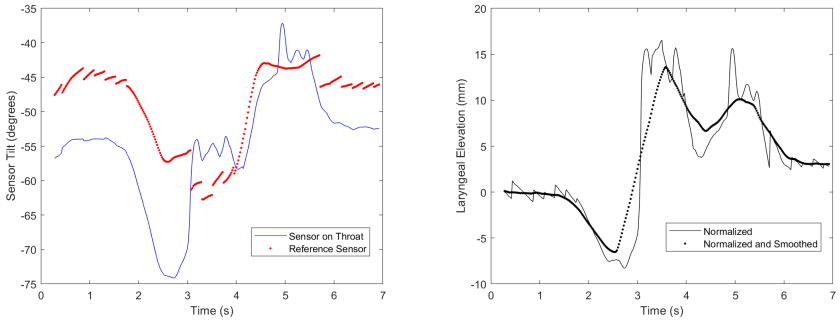

Figure 5.10: *Data from the prototype instrument. Left – throat sensor tilt (blue solid line) and reference sensor tilt (red dotted line). Right – Laryngeal elevation calculated by the instrument (black solid line) and smoothed laryngeal elevation (black dotted line). Data recorded while subject drank from a glass of water and tilted head backwards to assist swallowing. Two swallows are visible.*

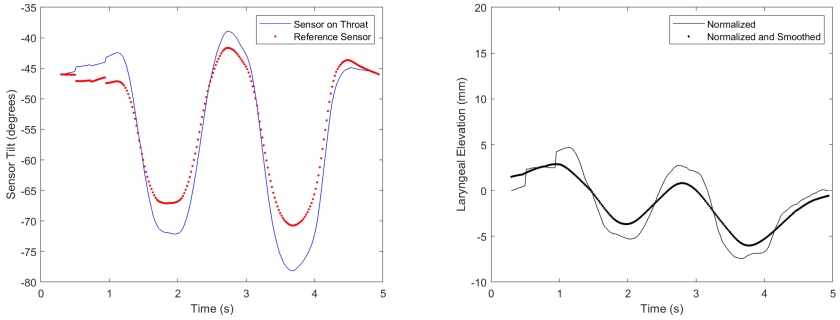

Figure 5.11: *Data from the prototype instrument. Left – throat sensor tilt (blue solid line) and reference sensor tilt (red dotted line). Right – Laryngeal elevation calculated by the instrument (black solid line) and smoothed laryngeal elevation (black dotted line). Data recorded while subject nodded head up and down.*

In the recordings where there was no head movement (see figure 5.9 for a representative sample), the reference sensor (red dotted trace) had negligible effect on the laryngeal elevation calculation (black solid trace). This demonstrates that our reference sensor is insensitive to laryngeal motion, as intended.

In the recordings where there was head movement (see figure 5.10 for a representative sample), the reference sensor can be seen to track the low-frequency shape of the throat-mounted sensor, which, when the former is subtracted from the latter, attenuates the head-movement component to a large extent. The laryngeal eleva-

tion trace still exhibits some of the head movement, however in comparison with the throat-mounted sensor trace, the swallows are far more pronounced.

In figures 5.9, 5.10, and 5.11, the instrument output (right-hand graphs) is given in millimetres of laryngeal elevation, calculated from the sensor tilt (left-hand graphs) using the LP size of the subject, according to the fomula given by equation 5.1, where l is the length of the sensor, θ is the calculated tilt of a sensor, θ_0 is the difference in tilt between the two sensors at zero elevation, and $4.5 + 1.19\,(\text{LP size})$ is taken from the regression analysis visualized in figure 4.19 in chapter 4.

$$\text{elevation} = l\left(\frac{\theta_{\text{throat}} - \theta_{\text{reference}} - \theta_0}{4.5 + 1.19\,(\text{LP size})}\right) \tag{5.1}$$

The top line of the equation shows how the tilt is offset to have a baseline of $0mm$ elevation; the bottom line shows how the tilt is normalised according to the subject's LP size; the output is then multiplied by the length of the sensor, l, to convert to millimetres — $16mm$ is the length of the sensor used in the prototype instrument, which means that this is the maximum elevation that can be measured in a linear fashion by the instrument.

The 'stepping' effect visible along the red dotted trace in figures 5.9 to 5.11 is due to a periodic drift-correction being applied to the sensor data when there is little movement in the reference sensor (and the accelerometer-calculated tilt error defined in section 3.8.1, $e_{\theta.\alpha}$, is therefore small.) The magnitude of drift for each sensor depends on the success of a simple calibration routine, which is run prior to the recording session. A more sophisticated calibration process could conceivably eliminate this effect.

In the recordings where there was head movement only (no swallowing; see figure 5.11 for a representative sample), the nodding of the head can be seen on the

laryngeal elevation trace, however the amplitude is quite low in comparison to the swallows (5 mm, compared to 15 mm), despite the peak-to-peak amplitude in the throat-mounted sensor trace being greater (40 degrees, compared to 15 degrees). This demonstrates that head movement is greatly attenuated, however it is not eliminated.

This attenuation is essential to the viability of the instrument, however. In figure 5.10, there are two distinct swallows, but from the throat-mounted sensor tilt alone (the blue solid trace), it would be impossible to measure the peak elevation of each swallow – indeed the peak tilt of the first swallow is at the same angle as the resting tilt after the second. In the corrected output (the black solid trace), the peak elevation for both swallows can be seen to be equivalent.

A 10-point running mean was applied to the instrument output (black dotted trace in figures 5.9 to 5.11) to evaluate whether some smoothing improves the fidelity of the output; from the limited data available, this appears to eliminate the noise from the drift-correction, at the cost of a reduction in the accuracy of measuring rapid changes in laryngeal elevation.

5.5 Conclusion

In this chapter, we have looked at the variation in subject's anatomical measurements, and established that sex, but not age, is a predictor of laryngeal prominence size, and that there is an 80% correlation between greater LP size and longer larynx length. We have set out the specifications for an instrument capable of measuring laryngeal elevation over time, and constructed a prototype to those specifications. The results from testing the prototype support the view that our instrumentation technique is effective in measuring laryngeal elevation in real-time.

In the next and final chapter, we conclude the thesis by reviewing our findings in the context of literature and current clinical practice, summarising of the outcomes of our work, and making recommendations for the direction of future work.

Chapter 6

Discussion

6.1 Dysphagia

Dysphagia is a complex health condition which manifests in many ways, has many possible causes, and the prognosis of which depends heavily on the general health of the subject. As with many types of disease, early diagnosis of dysphagia greatly improves the subject's chances of a good outcome.

Two physiological functions of the pharyngeal stage of deglutation, essential for safe swallowing, are protection of the airway, and propulsion of the bolus onward through the UES. Pharyngeal dysphagia generally originates from a frustration of either of these two functions – failure to protect the airway may result in aspiration, while failure to progress the bolus may result in choking, as the protected airway cannot be reopened until the bolus has been cleared. As both of these functions rely, in part, on the elevation and excursion of the larynx, practical quantitative measurement of laryngeal movement would be of high clinical value in the screening and diagnosis of dysphagia. At present, there is no standard means of quantitatively measuring laryngeal movement.

6.2 Instrumentation Techniques

Both sEMG and accelerometry / gyrometry present non-invasive means of measuring laryngeal physiology, however neither technique has been developed to the point where it is widely used in clinical practice.

The gold standards in modern clinical practice are VFSS and FEES, which together may provide a comprehensive view of a subject's swallowing apparatus, but as they are both invasive, both may be unsuitable for use with some potentially dysphagic subjects, and VFSS in particular can be be too restrictive for use with frail patients. The use and interpretation of VFSS and FEES both require high levels of training. In addition, neither VFSS nor FEES provide quantitative measurement of laryngeal function.

VFSS is expensive, gives the subject a relatively high dose of ionising radiation, and requires the subject to be transported to the radiology clinic and to conform posture to the requirements of the imaging machine. These factors render this technique inadvisable for young subjects and unsuitable for frail subjects. There must be a clear need for videofluoroscopy, not addressable by other technologies, before proceeding with VFSS; it is not suitable for routine dysphagia screening.

FEES is portable, but invasive and more limited in scope.

Both VFSS and FEES require expert interpretation, which limit their usefulness in screening further.

There is a clear need for a non-invasive dysphagia screening technique which uses advanced instrumentation to produce a quantitative measure of dysphagia risk, so as to remove the barriers to the widespread routine screening for dysphagia.

Accelerometry provides the potential for a low-cost, non-invasive instrumentation technique, but has historically had poor theoretical support for its use.

6.3 Processing of Data

6.3.1 De-noising

We have seen in the literature that it is common practice to pass data through de-noising filters as part of the data-capture for laryngeal accelerometry, however it is premature to design a de-noising filter prior to understanding the components of the signal well enough to be sure of what is and isn't noise.

As the understanding of the nature of the laryngeal accelerometry signal is a primary subject of this work, to apply any filter to the data runs the risk of removing relevant data, which will ultimately prevent a well-grounded understanding of the causal link between physiology and sensor data from being developed.

In principle, filtering should be targeted; i.e. a known noise source can be filtered out; unknown noise sources cannot be, as it is impossible to distinguish novel noise from novel signal features. Characterising sources of noise is therefore an important secondary subject of this work.

Through comparison of the sensor signals from human participant swallows with *i)* signals from participant head movement and *ii)* signals from mechanical model swallows, head movement signals could be characterised. A strategy was developed to remove the effects of head tilt from the swallowing signals *without* using a crude frequency-based filter, which would inevitably distort the swallowing signal, removing the possibility of accurate reconstruction of sensor motion, and therefore of inferring physiological motion.

6.3.2 Feature Extraction

In contrast to the literature, where there is a preponderance of abstract mathematical features, often further derived from abstract transformations of the data, we

have set our focus on features that have a direct physiological explanation, using transformations that have concrete meaning.

Looking at the two accelerometer axes and one gyrometer axis that relate to activity on the sagittal (median) plane of the throat, we can calculate the tilt of the sensor, and using that, we can discriminate between accelerometer output originating from tilt and accelerometer output originating from an impulse, and further decompose the latter into AP axis acceleration and SI axis acceleration.

We extracted the following features for the purpose of analysis:

- Peak-to-peak acceleration
- Maximum gyrometer peak
- Maximum sensor tilt
- Time to maximum sensor tilt
- Swallow duration

6.4 Instrumentation for Classification of Swallowing Behaviour

We have seen in literature (see chapter 2) that a number of studies have looked into constructing classifiers to discriminate dysphagic from healthy patients based on accelerometry signals. It does not seem wise to the author to attempt to build a classifier, which is likely to be regarded as a *de facto* diagnosis system, based on raw, or even processed, sensor data alone, for several reasons.

Firstly, the significance of any given feature in the data depends entirely on both the set-up of the sensor, and on the nature of the subject.

Secondly, to draw a clinically influential conclusion from data requires an exceptionally sound theoretical basis, and manufacturers of medical instruments are required by law to demonstrate that their design measures what it claims to measure, and to a sufficient (and stated) degree of accuracy [104].

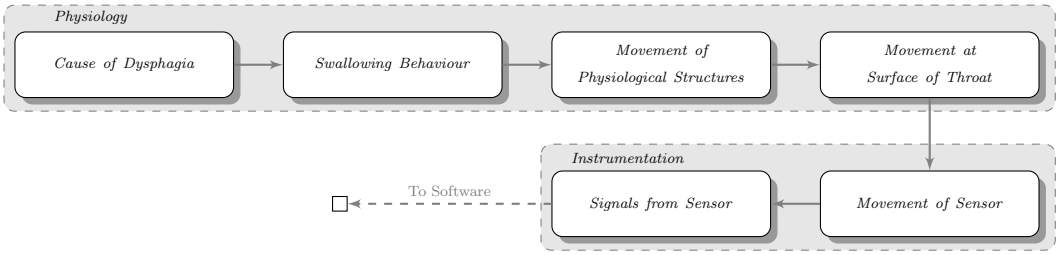

Figure 6.1: *The flow of causality from the physiological source of dysphagia to signals from throat-mounted sensors*

If we examine the causality of the system (see figure 6.1), it is clear that the signals are abstract by several stages from the state of the subject's swallowing (healthy or dysphagic). For clinically useful instrumentation, it is essential that the inferences that we make should be well founded for each stage from effect to cause. In the case of laryngeal accelerometry, the first inference that we should be able to make with confidence should be measurement of laryngeal motion based on the sensor data. The accuracy of this inference can be independently verified using simple means, such a model throat, e.g. as described in section 3.3.10. With this relationship firmly established, it becomes possible to focus research efforts on characterising and categorising swallowing behaviour based on the measured laryngeal motion. In addition, the purpose and use of such an instrument can be more easily understood by clinicians, which fosters trust in the instrument and encourages clinicians to consider its use in their practice.

Thirdly, there is a serious risk that classifiers designed and tested using data from only one accelerometry system, are valid only when applied to data from the

same system. This creates an inherent systemic fragility in an instrument based on such a classifier: any change to the physical part of the instrument, particularly the sensor, amplifier or hardware filter, whether due to damage, wear-and-tear, or due to substitution of parts in the manufacturing process, risks invalidating the intangible part of the instrument, i.e. the classification software.

Critically, it is not clear how the accuracy of an instrument which returns a diagnosis from sensor data in a single step can be verified. The design of such an instrument could be verified using type testing, but the conformity of an individual instrument to type could not be.

In this body of work, we have sought to establish the causality of specific accelerometry and gyrometry features from known physiological events, and also developed a means of testing the accuracy of a measuring device which reports on said features.

6.5 Development of Instrumentation

To demonstrate that a viable instrument for quantitatively measuring laryngeal elevation during swallowing can be portable, easy to use, and made inexpensively, a proof-of-concept prototype was constructed to the specifications that were evolved from our models and analysis of data collected from human participants. The initial results from the prototype instrument are positive, and do demonstrate that the approach used is valid. In particular, the instrument calculates sensor tilt in real time, and from this calculates laryngeal elevation. Our research identified that head-tilt is a major noise source for using this method; our instrument mitigates the effect of heat-tilt by using a second sensor to greatly attenuate the head-tilt component of the throat-mounted sensor's tilt.

The instrumentation technique that we developed depends on just a few elements:

- Two Inertial Measurement Unit-type sensors, which each incorporate
  - At least two dimensions of accelerometer
  - At least one dimension of gyromter, that measures rotational velocity around the axis perpendicular to the two accelerometer axes
- The first sensor must be positioned medially, immediately superior to the LP
- The second sensor must be positioned such that it is sensitive to head and neck gross movement, but not sensitive to laryngeal motion
- A processor with sufficient computational power to perform the necessary calculations in real-time — this can be done on a desktop computer, but for a truly portable system, a suitable microcontroller should be selected
- There must be some means of outputting the laryngeal elevation to the clinician to a level of detail suitable to the type of assessment that the instrument is being used for (i.e. screening of full assessment)

Our prototype instrument uses these elements to implement our technique in a portable and comfortable form-factor.

6.6 Potential for Clinical Use

In chapter 2, we established that detection of silent aspiration, or alternatively the evaluation of the risk thereof, is of high importance for early intervention in a significant proportion of dysphagia patients. We established in chapter 1 that the gold standards, VFSS and FEES, have drawbacks that hinder their routine

use in early stages of dysphagia assessment. The absence of laryngeal elevation during deglutation, weak elevation, and delayed elevation are all strong indicators of insufficient protection of the vocal folds.

We have shown that the combination of single-axis gyrometry with dual-axis accelerometry of the larynx is effective in detecting and quantifying laryngeal motion in healthy subjects. From literature, we know that it is possible to discriminate healthy swallows from dysphagic swallows using accelerometry alone, but without a clear understanding of the mechanisms which cause particular features of the accelerometry signal to correlate with the dysphagic swallow, however, it is difficult to know the limitations of the technique or to inspire the confidence in the technique necessary for clinical adoption.

By demonstrating how it is possible to measure laryngeal elevation over time using a combination of accelerometry and gyrometry signals, we have taken an important step in addressing this limitation of laryngeal accelerometry – the separation of *measurement* from *clinical interpretation* into two steps makes evaluation of the instrumentation technique simpler and adds transparency to the clinical decision-making process; it is far more comprehensible for a screening test to indicate dysphagia risk due to a physiological indicator such as weak elevation, than an abstract indicator such as the number of acceleration zero-crossings (as used by Lee [81]).

In terms of practicality, an accelerometry and gyrometry-based system can be made into a small form-factor, can be battery-powered and therefore highly portable. Wireless communication may be used to configure the instrument and display its output. Application of the sensors on the throat is straightforward and non-invasive, which makes it an attractive candidate for use in screening procedures.

Aside from laryngeal motion, accelerometers have been used for recording sound from the throat, including swallowing sounds and coughing. Swallowing sounds

alone have been shown to be ineffective for evaluation of aspiration risk, but there is also evidence that swallowing sounds have clinical value as one contributing factor of a larger assessment process. While not assessed in this thesis, the author sees no reason that prevents swallowing sounds for being detected using the same sensor that is used for measuring laryngeal motion, in effect producing a multi-modal system using no additional hardware.

Multi-modal systems were shown in literature to be more sensitive and specific in discriminating dysphagic subjects from healthy subjects than systems that take data from only one source. Accelerometry and gyrometry of the larynx may be readily combined with other non-invasive instrumentation techniques, for instance sEMG. Electronic instrumentation techniques may also be combined with other tests, such as the water swallow test, or elements of the Sydney Swallow Questionnaire, to form a more effective screening test that is still simple to administer.

6.6.1 Clinical Applications

The motivation for the body of work presented in this thesis is to develop quantitative instrumentation for the screening and assessment of dysphagia, which addresses the draw-backs of the current gold standards of dysphagia assessment.

The distinction between instrumentation for screening and for assessment lies in the simplicity of the procedure, and the complexity of the data. For assessment, the clinician is interested in building as complete a picture of the patient's swallowing as possible. The appropriateness of an instrument in an assessment setting will be determined by the trade-off between cost and convenience on one hand, and quality of relevant information gathered on the other. For screening, it is far more important that the procedure can be carried out quickly, and by non-specialist clinicians. The information that a screening instrument outputs must be concise and relevant to

calculating their personal risk of dysphagia.

In the design of our instrument, there is scope for flexibility in how the data is presented to the clinician. With the input of the patient's laryngeal prominence size, it is possible to output a trace of laryngeal elevation over time. For application to a screening procedure, it would be more appropriate to develop a routine in the instrument's software that seeks to detect elevation of a minimum speed or height, and plays a tone if a threshold is reached: this would provide the means for an easily and quickly administered pass/fail screening test.

6.7 Summary of Outcomes

In this thesis, we have presented our results and contributions, which are summarised here:

- A simulation model was developed, which describes the interaction between the larynx and a throat-mounted sensor.
- A mechanical model was constructed, which allows the mechanics of laryngeal elevation to be studied in the absence of other physiological processes.
- Methods and MATLAB tools for processing IMU data, in order to calculate sensor tilt over time and transpose accelerometer data to subject-centric axes were developed.
- Our models predicted that sensor tilt can be combined with knowledge of LP size to measure laryngeal elevation.
- Sensor data captured during experiments with human participants showed sensor tilt patterns which conformed to our models' predictions, with peaks that corresponded with laryngeal elevation.

- The magnitude of the maximum sensor tilt was shown to correlate linearly with the LP size of the subject.

- The accelerometer signal during swallowing was shown be predominantly due to sensor tilt; the remaining accelerometer peak once tilt had been discounted by use of our transposition technique was shown to coincide with the elevation of the larynx.

- In experiments with healthy participants, head tilt was identified as the main impediment for using sensor tilt as a practical indicator of laryngeal elevation. A method of compensating for head tilt using a second sensor was proposed.

- From the outcomes listed above, an instrumentation technique for measuring laryngeal elevation in real-time was developed, which incorporates our proposal for compensating for head tilt.

- A prototype instrument was built, providing proof of concept to support our instrumentation technique. Our prototype also meets our key criteria for clinical usefulness as a dysphagia screening instrument: it is portable, inexpensive, non-invasive and provides quantitative measurement of swallowing behaviour.

6.8 Limitations

The work presented in this thesis has the following limitations:

1. The simulation model describes the sensor response to laryngeal elevation only. In reality, the larynx also moves in an anterior direction, and rotates in a forward direction, during normal swallowing. In addition, the sensor detects vibrations from the vocal chords and breathing; these two physiological pro-

cesses were purposefully excluded from the simulation model's definition, in order to study the process of swallowing in isolation.

2. Our experiments involved healthy participants only.

3. The instrumentation techniques developed in this thesis measure laryngeal elevation, which is one aspect of swallowing behaviour. There are other aspects of swallowing behaviour which are crucial to safe swallowing, for example bolus preparation and closure of the vocal chords, which would need to be addressed in an assessment for dysphagia.

6.9 Recommended Directions for Future Work

Based on the limitations listed in section 6.8, we propose the following directions for future research and development:

Further Simulation Model Development Our simulation model provides the means to test instrumentation techniques in a virtual environment, outputting test swallowing sensor data for any combinations of anatomical measurements, laryngeal elevation behaviour, sensor position and sensor configuration. Extension of the model could include the effects of speech and breathing, and head and jaw movement. Further experiments carried out with the simulation model could include an exploration of the applicability of instrumentation techniques to paediatric subjects, and exploration of alternative sensor positions on the throat.

Further Instrumentation Development Our prototype instrument provides proof of concept for our proposed techniques. It is not, however, market-ready. A further stage in development is necessary to produce a device which meets the essen-

tial requirements of the MDD. A clinical evaluation with patients under assessment for dysphagia should then be carried out, in order to determine:

1. The sensitivity in detecting laryngeal dysphagia
2. The specificity in detecting laryngeal dysphagia
3. The sensitivity in detecting silent dysphagia

The third point is crucial, as detecting silent dysphagia is the precise outcome that the state of art under-performs in, a fact which the development of our technique is intended to address.

There is also work to be done in developing a practical method of positioning the sensor reliably, and in measuring LP size, needed for calculating laryngeal elevation from sensor tilt.

In addition to the above, there is scope for work to be done on optimising and extending the algorithms used to process the sensor data. Our prototype calculates tilt in real-time, but does not transpose accelerometer data from the sensor-centric axes (x' and y') to subject-centric axes (x and y). This would provide a far richer set of information to infer swallowing behaviour from.

Multi-Modal Instrumentation A significant advantage presented by electronic detection of laryngeal elevation, is the co-ordination of this with instrumentation of other parts of the swallowing apparatus. In particular, measurement of the time between the bolus entering the oro-pharynx to the start of laryngeal elevation may provide an indication of the efficacy of the swallowing reflex. It is similarly worth exploring the clinical usefulness of measuring the time taken to process the bolus in the mouth prior to entering the pharynx, as a potential indication of oral dysphagia.

6.10 Conclusion

In this thesis, we have addressed some of the limitations in the literature, and shown that inertial measurement units can form the basis of instrumentation useful in the assessment of dysphagia. We have conducted an objective examination of the state of art and identified that there is a need for low-cost, portable, non-invasive, and quantitative instrumentation for dysphagia, and made significant progress towards making such an instrument a reality.

This work has provided some clarity in the causality of accelerometer signals during swallowing, and in the process has proven the usefulness of an integrated gyrometer in measuring laryngeal elevation.

A large quantity of data from a throat mounted IMU has been collected and analysed. The involvement of participants of both sexes and a wide range of ages in the collection of this data has ensured that we may have confidence in the applicability of our findings to the general population. We have shown that the difference between male and female larynges has a significant effect on sensor data, and we have developed methods of controlling for laryngeal prominence size. We have also shown that age (21 to 65) does not play a significant factor in the anatomical structure of the throat, although the literature suggests that swallowing behaviour may change in geriatric subjects.

Based on our findings, we have developed a prototype instrument, which has demonstrated the potential of using the relative tilt of a pair of IMUs to measure laryngeal elevation, to proof-of-concept level.

It is the author's hope that this body of work may see further development, so that the methods used in this thesis may introduced into clinical practice, and in doing so, promote the early detection of dysphagia in at-risk populations.

References

[1] P. Enderby, C. Pickstone, A. John, K. Fryer, A. Cantrell, and D. Papaioannou, "Resource manual for commissioning and planning services for slcn," *London: Royal College of Speech and Language Therapists*, 2009.

[2] S. K. Daniels, J. A. Anderson, and P. C. Willson, "Valid items for screening dysphagia risk in patients with stroke," *Stroke*, vol. 43, no. 3, pp. 892–897, 2012.

[3] D. G. Smithard, P. A. O'Neill, R. E. England, C. L. Park, R. Wyatt, D. F. Martin, and J. Morris, "The natural history of dysphagia following a stroke," *Dysphagia*, vol. 12, no. 4, pp. 188–193, 1997, ISSN: 0179051X. DOI: 10.1007/PL00009535.

[4] G. J. Bours, R. Speyer, J. Lemmens, M. Limburg, and R. De Wit, "Bedside screening tests vs. videofluoroscopy or fibreoptic endoscopic evaluation of swallowing to detect dysphagia in patients with neurological disorders: Systematic review," *Journal of advanced nursing*, vol. 65, no. 3, pp. 477–493, 2009.

[5] M. Nagaya, T. Kachi, T. Yamada, and Y. Sumi, "Videofluorographic observations on swallowing in patients with dysphagia due to neurodegenerative diseases," 2004.

[6] I. S. W. Party *et al.*, *National clinical guideline for stroke*, 2012.

[7] D. Ramsey, D. Smithard, and L. Kalra, "Silent aspiration: What do we know?" *Dysphagia*, vol. 20, no. 3, pp. 218–225, 2005, ISSN: 0179051X. DOI: 10.1007/s00455-005-0018-9.

[8] C. H. Smith, J. A. Logemann, L. A. Colangelo, A. W. Rademaker, and B. R. Pauloski, "Incidence and patient characteristics associated with silent aspiration in the acute care setting," *Dysphagia*, vol. 14, no. 1, pp. 1–7, 1999.

[9] K. Corbin-Lewis and J. M. Liss, *Clinical Anatomy & Physiology of the Swallow Mechanism*, Second Edi. Stamford: Cengage Learning, 2015, p. 336, ISBN: 1435493001.

[10] R. Drake, A. W. Vogl, and A. W. Mitchell, *Gray's Anatomy for Students E-Book*. Elsevier Health Sciences, 2009.

[11] C. Ertekin, "Neurogenic dysphagia in brainstem disorders and emg evaluation," 2017.

[12] W. Culbertson and D. Tanner, *The Anatomy And Physiology of Speech and Swallowing*, 1st Editio. Kendall Hunt, 2011, p. 310, ISBN: 1465277420.

[13] L. W. Baijens, P. Clavé, P. Cras, O. Ekberg, A. Forster, G. F. Kolb, J.-C. Leners, S. Masiero, J. Mateos-Nozal, O. Ortega, *et al.*, "European society for swallowing disorders–european union geriatric medicine society white paper: Oropharyngeal dysphagia as a geriatric syndrome," *Clinical interventions in aging*, vol. 11, p. 1403, 2016.

[14] O. Ekberg and M. J. Feinberg, "Altered swallowing function in elderly patients without dysphagia: Radiologic findings in 56 cases.," *AJR. American journal of roentgenology*, vol. 156, no. 6, pp. 1181–1184, 1991.

[15] P. Leslie, M. J. Drinnan, G. A. Ford, and J. A. Wilson, "Swallow respiratory patterns and aging: Presbyphagia or dysphagia?" *The Journals of Gerontology Series A: Biological Sciences and Medical Sciences*, vol. 60, no. 3, pp. 391–395, 2005.

[16] M. Rugiu, "Role of videofluoroscopy in evaluation of neurologic dysphagia," *Acta Otorhinolaryngologica Italica*, vol. 27, no. 6, p. 306, 2007.

[17] B. R. Pauloski, A. W. Rademaker, J. A. Logemann, C. L. Lazarus, L. Newman, A. Hamner, E. MacCracken, J. Gaziano, and L. Stachowiak, "Swallow function and perception of dysphagia in patients with head and neck cancer," *Head & neck*, vol. 24, no. 6, pp. 555–565, 2002.

[18] M. B. Kronenberger and A. D. Meyers, "Dysphagia following head and neck cancer surgery," *Dysphagia*, vol. 9, no. 4, pp. 236–244, 1994.

[19] Y. Wakasugi, H. Tohara, F. Hattori, Y. Motohashi, A. Nakane, S. Goto, Y. Ouchi, S. Mikushi, S. Takeuchi, and H. Uematsu, "Screening test for silent aspiration at the bedside," *Dysphagia*, vol. 23, no. 4, pp. 364–370, 2008.

[20] J. A. Hinchey, T. Shephard, K. Furie, D. Smith, D. Wang, S. Tonn, *et al.*, "Formal dysphagia screening protocols prevent pneumonia," *Stroke*, vol. 36, no. 9, pp. 1972–1976, 2005.

[21] D. Mant and G. Fowler, "Mass screening: Theory and ethics.," *BMJ: British Medical Journal*, vol. 300, no. 6729, p. 916, 1990.

[22] J. C. O'horo, N. Rogus-Pulia, L. Garcia-Arguello, J. Robbins, and N. Safdar, "Bedside diagnosis of dysphagia: A systematic review," *Journal of hospital medicine*, vol. 10, no. 4, pp. 256–265, 2015.

[23] S. Reilly and L. Carr, "Foreign body ingestion in children with severe developmental disabilities: A case study," *Dysphagia*, vol. 16, no. 1, pp. 68–73, 2001.

[24] B. Rogers, J. Arvedson, G. Buck, P. Smart, and M. Msall, "Characteristics of dysphagia in children with cerebral palsy," *Dysphagia*, vol. 9, no. 1, pp. 69–73, 1994.

[25] L. Perry and C. P. Love, "Screening for dysphagia and aspiration in acute stroke: A systematic review," *Dysphagia*, vol. 16, no. 1, pp. 7–18, 2001.

[26] C. Borr, M. Hielscher-Fastabend, and A. Lücking, "Reliability and validity of cervical auscultation," *Dysphagia*, vol. 22, no. 3, pp. 225–234, 2007.

[27] M. Henderson, "Quantitative and portable instrumentation for dysphagia," in *Elementary particle theory*, Proceedings of the Graduate Forum on Advanced Instrumentation and Measurement Technology, Beijing: School of Science and Opto-electronics Engineering, Beihang University, 2014.

[28] M. Henderson, D. Smithard, S. W. Kelly, and G. Marcelli, "The use of gyrometry to correctly interpret accelerometry in dysphagia," 2015.

[29] ——, "Quantitative and portable instrumentation for dysphagia," 2014.

[30] F. B. de Sauvages, *NOSOLOGIA METHODICA SISTENS MORBORUM CLASSES: Juxta Sydenhami mentem & Botanicorum ordinem. TOMUS SECUNDUS*. sumptibus Fratrum de Tournes, 1768, vol. 2.

[31] R. T. Smith, "Practical hints in medicine (psychological)," *Postgraduate medical journal*, vol. 3, no. 32, p. 142, 1928.

[32] A. A. Campbell, "Cancer of the larynx: With observations on 103 cases," *Canadian Medical Association journal*, vol. 49, no. 6, p. 509, 1943.

[33] H. R. Viets, "Diagnosis of myasthenia gravis in patients with dysphagia," *Journal of the American Medical Association*, vol. 134, no. 12, pp. 987–992, 1947.

[34] P. A. Thorpe, "Dysphagia in a woman of 78 cured by tonsillectomy," *British medical journal*, vol. 1, no. 4453, p. 723, 1946.

[35] P. Kramer, M. Atkinson, S. M. Wyman, and F. J. Ingelfinger, "The dynamics of swallowing. ii. neuromuscular dysphagia of pharynx," *Journal of Clinical Investigation*, vol. 36, no. 4, p. 589, 1957.

[36] W. J. Logan and J. F. Bosma, "Oral and pharyngeal dysphagia in infancy," *Pediatric Clinics of North America*, vol. 14, no. 1, pp. 47–61, 1967.

[37] H. B. Kelly, *Dysphagia in adults (non-malignant) the role of spasm in œsophageal disease*, 1960.

[38] H. D. Adams, "Dysphagia causes and treatment," *Postgraduate medicine*, vol. 38, no. 3, pp. 200–209, 1965.

[39] M.-L. Huckabee, K. Lamvik, and R. Jones, "Pharyngeal mis-sequencing in dysphagia: Characteristics, rehabilitative response, and etiological speculation," *Journal of the neurological sciences*, vol. 343, no. 1, pp. 153–158, 2014.

[40] W. Hill and C. Hope, "Two cases of carcinoma of the œsophagus; lower thoracic with superadded pharyngeal dysphagia;? paretic or spasmodic," *Proceedings of the Royal Society of Medicine*, vol. 5, no. Laryngol Sect, p. 25, 1912.

[41] D. C. B. Zoratto, T. Chau, and C. M. Steele, "Hyolaryngeal excursion as the physiological source of swallowing accelerometry signals.," *Physiological measurement*, vol. 31, no. 6, pp. 843–855, 2010, ISSN: 1361-6579. DOI: 10.

1088/0967-3334/31/6/008. [Online]. Available: http://www.ncbi.nlm.nih.gov/pubmed/20479519.

[42] I. J. Cook, W. J. Dodds, R. O. Dantas, M. K. Kern, B. T. Massey, R. Shaker, and W. J. Hogan, "Timing of videofluoroscopic, manometric events, and bolus transit during the oral and pharyngeal phases of swallowing," *Dysphagia*, vol. 4, no. 1, pp. 8–15, 1989.

[43] R. O. Dantas, M. K. Kern, B. T. Massey, W. J. Dodds, P. J. Kahrilas, J. G. Brasseur, I. J. Cook, and I. M. Lang, "Effect of swallowed bolus variables on oral and pharyngeal phases of swallowing," *The American journal of physiology*, vol. 258, no. 5 Pt 1, G675–G681, 1990, ISSN: 0002-9513.

[44] D. A. Mendell and J. A. Logemann, "Temporal sequence of swallow events during the oropharyngeal swallow," *Journal of Speech, Language, and Hearing Research*, vol. 50, no. 5, pp. 1256–1271, 2007.

[45] E. Zahnd, F. Movahedi, J. L. Coyle, E. Sejdić, and P. G. Menon, "Correlating tri-accelerometer swallowing vibrations and hyoid bone movement in patients with dysphagia," in *ASME 2016 International Mechanical Engineering Congress and Exposition*, American Society of Mechanical Engineers, 2016, V003T04A083–V003T04A083.

[46] K. J. C., "A morphological study of the human prepubertal and pubertal larynx," *American Journal of Anatomy*, vol. 151, no. 1, pp. 11–19, 1978. DOI: 10.1002/aja.1001510103. eprint: https://onlinelibrary.wiley.com/doi/pdf/10.1002/aja.1001510103. [Online]. Available: https://onlinelibrary.wiley.com/doi/abs/10.1002/aja.1001510103.

[47] R. S. Litman, E. E. Weissend, D. Shibata, and P.-L. Westesson, "Developmental changes of laryngeal dimensions in unparalyzed, sedated children,"

Anesthesiology: The Journal of the American Society of Anesthesiologists, vol. 98, no. 1, pp. 41–45, 2003.

[48] C. M. Steele, "The blind scientists and the elephant of swallowing: A review of instrumental perspectives on swallowing physiology," *Journal of Texture Studies*, vol. 46, no. 3, pp. 122–137, 2015.

[49] B. Jones, Ed., *Normal and Abnormal Swallowing: Imaging in Diagnosis and Therapy*, 2nd ed. New York: Springer-Verlag, 2003, ISBN: 978-1-4419-2904-4.

[50] M. L. Skolnick and E. R. Cohn, *Videofluoroscopic Studies of Speech in Patients with Cleft Palate*. New York: Springer-Verlag, 1989, p. 186, ISBN: 978-1-4613-8876-0. DOI: 10.1007/978-1-4613-8874-6.

[51] B. Fattori, P. Giusti, V. Mancini, M. Grosso, M. Barillari, L. Bastiani, S. Molinaro, and A. Nacci, "Comparison between videofluoroscopy, fiberoptic endoscopy and scintigraphy for diagnosis of oro-pharyngeal dysphagia," *Acta Otorhinolaryngologica Italica*, vol. 36, no. 5, p. 395, 2016.

[52] N. Rao, S. Brady, G. Chaudhuri, J. Donzelli, and M. Wesling, "Gold-standard? analysis of the videofluoroscopic and fiberoptic endoscopic swallow examinations," *J Appl Res*, vol. 3, pp. 89–96, 2003.

[53] K. L. DePippo, M. A. Holas, and M. J. Reding, "The burke dysphagia screening test: Validation of its use in patients with stroke," *Archives of physical medicine and rehabilitation*, vol. 75, no. 12, pp. 1284–1286, 1994.

[54] M. Celeste, K. Azadeh, E. Sejdić, G. Berall, and T. Chau, "Quantitative classification of pediatric swallowing through accelerometry," *Journal of neuroengineering and rehabilitation*, vol. 9, no. 1, p. 34, 2012.

[55] A. M. Kelly, M. J. Drinnan, and P. Leslie, "Assessing Penetration and Aspiration: How Do Videofluoroscopy and Fiberoptic Endoscopic Evaluation of Swallowing Compare?" *The Laryngoscope*, vol. 117, pp. 1723–1727, 2007.

[56] P. M. Zenner, D. S. Losinski, and R. H. Mills, "Using cervical auscultation in the clinical dysphagia examination in long-term care," *Dysphagia*, vol. 10, no. 1, pp. 27–31, 1995.

[57] S. Hamlet, D. G. Penney, and J. Formolo, "Stethoscope acoustics and cervical auscultation of swallowing," *Dysphagia*, vol. 9, no. 1, pp. 63–68, 1994.

[58] J. L. Ferrucci, L. D. Mangilli, F. C. Sassi, S. C. O. Limongi, and C. R. F. d. Andrade, "Swallowing sounds in speech therapy practice: A critical analysis of the literature," *Einstein (São Paulo)*, vol. 11, no. 4, pp. 535–539, 2013.

[59] O. Bretan and M. Henry, "Laryngeal mobility and dysphagia.," *Arquivos de gastroenterologia*, vol. 34, no. 3, pp. 134–138, 1997.

[60] P. Konrad, "The abc of emg," *A practical introduction to kinesiological electromyography*, vol. 1, pp. 30–35, 2005.

[61] J. Lee, S. Blain, M. Casas, D. Kenny, G. Berall, and T. Chau, "A radial basis classifier for the automatic detection of aspiration in children with dysphagia," *Journal of NeuroEngineering and Rehabilitation*, vol. 3, no. 1, p. 14, 2006.

[62] E. Sejdić, C. M. Steele, and T. Chau, "Segmentation of dual-axis swallowing accelerometry signals in healthy subjects with analysis of anthropometric effects on duration of swallowing activities," *IEEE Transactions on Biomedical Engineering*, vol. 56, no. 4, pp. 1090–1097, 2009, ISSN: 00189294. DOI: 10.1109/TBME.2008.2010504.

[63] N. Reddy, E. Canilang, J. Casterline, M. Rane, A. Joshi, R. Thomas, and R. Candadai, "Noninvasive acceleration measurements to characterize the pharyngeal phase of swallowing," *Journal of biomedical engineering*, vol. 13, no. 5, pp. 379–383, 1991.

[64] F. Movahedi, A. Kurosu, J. L. Coyle, S. Perera, and E. Sejdić, "A comparison between swallowing sounds and vibrations in patients with dysphagia," *Computer Methods and Programs in Biomedicine*, vol. 144, pp. 179–187, 2017.

[65] E. Zahnd, F. Movahedi, J. L. Coyle, E. Sejdić, and P. G. Menon, "Correlating tri-accelerometer swallowing vibrations and hyoid bone movement in patients with dysphagia," in *ASME 2016 International Mechanical Engineering Congress and Exposition*, American Society of Mechanical Engineers, 2016, V003T04A083–V003T04A083.

[66] D. M. Suiter, S. B. Leder, and D. E. Karas, "The 3-ounce (90-cc) water swallow challenge: A screening test for children with suspected oropharyngeal dysphagia," *Otolaryngology-Head and Neck Surgery*, vol. 140, no. 2, pp. 187–190, 2009.

[67] D. M. Suiter and S. B. Leder, "Clinical utility of the 3-ounce water swallow test," *Dysphagia*, vol. 23, no. 3, pp. 244–250, 2008.

[68] K. L. DePippo, M. A. Holas, and M. J. Reding, "Validation of the 3-oz water swallow test for aspiration following stroke," *Archives of neurology*, vol. 49, no. 12, pp. 1259–1261, 1992.

[69] *Sydney swallow questionnaire (ssq)*, Available from (http://www.stgeorgeswallowcenter.
Accessed: 2017-10-19.

[70] R. C. Dwivedi, S. S. Rose, J. W. Roe, A. S. Khan, C. Pepper, C. M. Nutting, P. M. Clarke, C. J. Kerawala, P. H. Rhys-Evans, K. J. Harrington, *et al.*,

"Validation of the sydney swallow questionnaire (ssq) in a cohort of head and neck cancer patients," *Oral oncology*, vol. 46, no. 4, e10–e14, 2010.

[71] N. Audag, C. Goubau, M. Toussaint, and G. Reychler, "Screening and evaluation tools of dysphagia in children with neuromuscular diseases: A systematic review," *Developmental Medicine & Child Neurology*, 2016.

[72] S. Prasad, "Accelerometer Theory & Design," in *Design simulation and fabrication of micromachined acceleration sensor*, Jawaharlal Nehru Technological University, 2011, ch. 2, pp. 11–56.

[73] *1293-1998 (r2008) - ieee standard specification format guide and test procedure for linear, single-axis, non-gyroscopic accelerometers*, 2008.

[74] *1431-2004 - ieee standard specification format guide and test procedure for coriolis vibratory gyros*, 2004.

[75] A. Trusov, *Overview of mems gyroscopes: History, principles of operations, types of measurements*, `http://www.alexandertrusov.com/uploads/pdf/2011-UCI-trusov-whitepaper-gyros.pdf`, Accessed: 17/04/2017, May 2011.

[76] *Inemo inertial module: 3d accelerometer, 3d gyroscope, 3d magnetometer*, LSM9DS0, Rev. 2, ST-Microelectronics, Aug. 2013.

[77] H. Firmin, S. Reilly, and A. Fourcin, *Non-Invasive Monitoring of Reflexive Swallowing*, 1997. [Online]. Available: `http://www.laryngograph.com/pdfdocs/paper5.pdf`.

[78] N. P. Reddy, A. Katakam, V. Gupta, R. Unnikrishnan, J. Narayanan, and E. P. Canilang, "Measurements of acceleration during videofluorographic evaluation of dysphagic patients," *Medical Engineering and Physics*, vol. 22,

no. 6, pp. 405–412, 2000, ISSN: 13504533. DOI: 10.1016/S1350-4533(00)00047-3.

[79] V. Gupta, N. P. Reddy, and E. P. Canilang, "Emg for sensing pharyngeal swallow," pp. 1221–1222, ISSN: 05891019.

[80] N. P. Reddy, D. L. Simcox, V. Gupta, G. E. Motta, J. Coppenger, A. Das, and O. Buch, "Biofeedback therepy using accelerometry for treating dysphagic patients with poor laryngeal elevation: case studies," *Journal of Rehabilitation Research and Development*, vol. 37, no. 3, pp. 361–372, 2000.

[81] J. Lee, C. M. Steele, and T. Chau, "Classification of healthy and abnormal swallows based on accelerometry and nasal airflow signals," *Artificial Intelligence in Medicine*, vol. 52, no. 1, pp. 17–25, 2011, ISSN: 09333657. DOI: 10.1016/j.artmed.2011.03.002. [Online]. Available: http://dx.doi.org/10.1016/j.artmed.2011.03.002.

[82] E. Sejdic, C. M. Steele, and T. Chau, "Classification of penetration-aspiration versus healthy swallows using dual-axis swallowing accelerometry signals in dysphagic subjects," *IEEE Transactions on Biomedical Engineering*, vol. 60, no. 7, pp. 1859–1866, 2013, ISSN: 00189294. DOI: 10.1109/TBME.2013.2243730.

[83] C. M. Steele, E. Sejdić, and T. Chau, "Noninvasive detection of thin-liquid aspiration using dual-axis swallowing accelerometry," *Dysphagia*, vol. 28, no. 1, 2013, ISSN: 0179051X. DOI: 10.1007/s00455-012-9418-9.

[84] C. S. S. Greco, L. G. M. Q. Nunes, and P. L. Melo, "Instrumentation for bedside analysis of swallowing disorders," *2010 Annual International Conference of the IEEE Engineering in Medicine and Biology Society, EMBC'10*, pp. 923–926, 2010, ISSN: 1557-170X. DOI: 10.1109/IEMBS.2010.5627509.

[85] S. Suryanarayanan, N. P. Reddy, and E. P. Canilang, "A fuzzy logic diagnosis system for classification of pharyngeal dysphagia," *International Journal of Bio-Medical Computing*, vol. 38, no. 3, pp. 207–215, 1995, ISSN: 00207101. DOI: 10.1016/S0020-7101(05)80002-9.

[86] J. Lee, C. Steele, and T. Chau, "Time and time–frequency characterization of dual-axis swallowing accelerometry signals," *Physiological measurement*, vol. 29, no. 9, p. 1105, 2008.

[87] S. Damouras, E. Sejdic, C. M. Steele, and T. Chau, "An online swallow detection algorithm based on the quadratic variation of dual-axis accelerometry," *IEEE Transactions on Signal Processing*, vol. 58, no. 6, pp. 3352–3359, 2010.

[88] J. Lee, E. Sejdić, C. M. Steele, and T. Chau, "Effects of liquid stimuli on dual-axis swallowing accelerometry signals in a healthy population.," *Biomedical engineering online*, vol. 9, p. 7, 2010, ISSN: 1475-925X. DOI: 10.1186/1475-925X-9-7.

[89] E. Sejdić, C. M. Steele, and T. Chau, "A procedure for denoising dual-axis swallowing accelerometry signals," *Physiological measurement*, vol. 31, no. 1, N1, 2009.

[90] F. Hanna, S. M. Molfenter, R. E. Cliffe, T. Chau, and C. M. Steele, "Anthropometric and demographic correlates of dual-axis swallowing accelerometry signal characteristics: A canonical correlation analysis," *Dysphagia*, vol. 25, no. 2, pp. 94–103, 2010.

[91] E. Sejdić, V. Komisar, C. M. Steele, and T. Chau, "Baseline characteristics of dual-axis cervical accelerometry signals," *Annals of Biomedical Engineering*, vol. 38, no. 3, pp. 1048–1059, 2010.

[92] E. Sejdić, C. M. Steele, and T. Chau, "A method for removal of low frequency components associated with head movements from dual-axis swallowing accelerometry signals," *PLoS One*, vol. 7, no. 3, e33464, 2012.

[93] L.-A. Farkas, L. Entrekin, N. Milstead, K. Mosman, K. Berggren, and J. Sampson, "Application of digital accelerometry for swallow imaging (dasi) for dysphagia evaluation and treatment in a series of myotonic dystrophy type 1 (dm1) patients (p05. 189)," *Neurology*, vol. 78, no. 1 Supplement, P05–189, 2012.

[94] J. M. Dudik, I. Jestrović, B. Luan, J. L. Coyle, and E. Sejdić, "Characteristics of dry chin-tuck swallowing vibrations and sounds," *IEEE Transactions on Biomedical Engineering*, vol. 62, no. 10, pp. 2456–2464, 2015.

[95] F. Movahedi, A. Kurosu, J. L. Coyle, S. Perera, and E. Sejdić, "Anatomical directional dissimilarities in tri-axial swallowing accelerometry signals," *IEEE Transactions on Neural Systems and Rehabilitation Engineering*, vol. 25, no. 5, pp. 447–458, 2017.

[96] E. Sejdić, J. M. Dudik, A. Kurosu, I. Jestrović, and J. L. Coyle, "Understanding differences between healthy swallows and penetration-aspiration swallows via compressive sensing of tri-axial swallowing accelerometry signals," in *Proceedings of SPIE*, NIH Public Access, vol. 9190, 2014, p. 91090M.

[97] M. S. Nikjoo, C. M. Steele, E. Sejdić, and T. Chau, "Automatic discrimination between safe and unsafe swallowing using a reputation-based classifier," *Biomedical engineering online*, vol. 10, no. 1, p. 100, 2011.

[98] M. Celeste, K. Azadeh, E. Sejdić, G. Berall, and T. Chau, "Quantitative classification of pediatric swallowing through accelerometry," *Journal of neuroengineering and rehabilitation*, vol. 9, no. 1, p. 34, 2012.

[99] U. Imtiaz, K. Yamamura, W. Kong, S. Sessa, Z. Lin, L. Bartolomeo, H. Ishii, M. Zecca, Y. Yamada, and A. Takanishi, "Application of wireless inertial measurement units and emg sensors for studying deglutation-preliminary results," in *Engineering in Medicine and Biology Society (EMBC), 2014 36th Annual International Conference of the IEEE*, IEEE, 2014, pp. 5381–5384.

[100] N. Casiddu and C. Porfirione, "Design for dysphagia: A new hardware-and-software mobile system to monitor patients' swallowing," *The Design Journal*, vol. 20, no. sup1, S2078–S2089, 2017.

[101] S. Afkari *et al.*, "Measuring frequency of spontaneous swallowing," *Australas Phys Eng Sci Med*, vol. 30, no. 30, pp. 313–317, 2007.

[102] E. Sazonov, S. Schuckers, P. Lopez-Meyer, O. Makeyev, N. Sazonova, E. L. Melanson, and M. Neuman, "Non-invasive monitoring of chewing and swallowing for objective quantification of ingestive behavior," *Physiological measurement*, vol. 29, no. 5, p. 525, 2008.

[103] The European Parliment and The Council of European Union, *Regulation (eu) 2017/745 of the european parliment and the council of european union of 5 april 2017 on medical devices*, `http://eur-lex.europa.eu/legal-content/EN/TXT/PDF/?uri=CELEX:32017R0745&from=EN`, 2017.

[104] Council of European Union, *Council directive 93/42/eec of 14 june 1993 concerning medical devices*, `http://eur-lex.europa.eu/LexUriServ/LexUriServ.do?uri=CELEX:31993L0042:EN:HTML`, 1993.

[105] I. E. Commission *et al.*, "Iec 60601-1 medical electrical equipment general requirement for safety standard. 2nd amendment," *CE/IEC*, vol. 60601, no. 1, 1995.

[106] J. Backes, *A practical guide to IEC 60601-1*. Rigel Medical, United Kingdom, 2007.

[107] A. Kelly, "Modern inertial and satellite navigation systems," CARNEGIE-MELLON UNIV PITTSBURGH PA ROBOTICS INST, Tech. Rep., 1994.

[108] B. Amirlak, *Skin anatomy*, `https://emedicine.medscape.com/article/1294744-overview`, Accessed: 2017-12-02.

Appendix A

Participant Documents

The following documents are included here, in order:

- Appeal for Participants – an advertisement for the study
- Participation Application Form – a form for potential participants to register their interest, and provide enough information for the researcher to evaluate the applicant against inclusion and exclusion criteria.
- Participant Information Sheet – An explanation of the purpose of the study, as well as the study procedure, designed to give the participant sufficient information to provide informed consent.
- Participant Consent Form – A form designed to capture the participant's written consent to be a part of the study.

Advertising - Participant Appeal Letters

Study: The effect of inter-personal variation on accelerometer and gyrometer signals during swallowing

You are invited to take part in a short PhD study involving non-invasive electronic measurement of swallowing. This study intends to investigate how variations of throat anatomy from person to person affects signals from sensors placed on the throat during swallows.
We are looking for University students and staff members over the age of 18 in Canterbury.
Refreshments in the form of tea or coffee with cake or sandwiches will be provided to participants.
You will be required to attend a session during which measurements will be taken of your throat, sensors will be placed on your throat, and you will be asked to swallow a few items, such as water, yogurt and a biscuit while the sensors record the movement of your larynx. The session is estimated to take no more than 15 minutes.
The sensors are small and unobtrusive, non-invasive, and should cause no discomfort.
After the session is complete you will also be asked to fill out a short questionnaire, which should not take more than 2 minutes.
If you would like to know more and are interested in taking part and receiving tea/coffee and cake/sandwich for your time, please contact me at mh550@kent.ac.uk .

Thanks,
Martin Henderson

Application for Study Participation

Study: *The effect of inter-personal variation on accelerometer and gyrometer signals during swallowing*

Thank-you for your interest in the study.

The purpose of this form is to provide us with information relevant to the study and to choose appropriate candidates for participation. The information you provide is confidential and will be treated with the utmost care and sensitivity.

Please complete the following:-

Name: Click here to enter text.

Email: Click here to enter text.

Age: Click here to enter text.

Sex: Click here to enter text.

Is there any type of food or drink that you cannot take due to swallowing difficulties? **Yes** ☐ **No** ☐

On average, do you have trouble eating or drinking (e.g. choking or coughing) more than once a week? **Yes** ☐ **No** ☐

Is there any type of food or drink that you do not take for health or religious reasons? **Yes** ☐ **No** ☐

Details (if yes): Click here to enter text.

Have you ever had surgery on your throat? **Yes** ☐ **No** ☐

Details (if yes): Click here to enter text.

To be completed by researcher; applicant please leave blank:-

Participant ID: Click here to enter text.

Notes:

Click here to enter text.

PARTICIPANT INFORMATION SHEET

Study of the effect that inter-personal variation in throat anatomy has on accelerometer and gyrometer signals during swallowing

Introduction

Swallowing difficulties (dysphagia) is a common side-effect of various health conditions, diseases and disabilities. Aside from further deterioration of the sufferer's health, dysphagia can have a profound impact on their quality of life, as shared meals are central to human social behaviour.

To diagnose and monitor dysphagia, a new generation of sensors is needed to detect potential swallowing problems.

Research into neck-mounted inertial sensors, such as accelerometers and gyrometers, shows that they can detect and describe the characteristics of very small movements in the throat, but it is currently unknown how the normal variations in physiology from person to person influences the sensors

Study Purpose

This study is intended to capture accelerometer and gyrometer signals, while swallowing, from a range of people, so that the interpretation of the sensors can be improved to account for person-to-person variations in physiology.

Study Procedure

The study will last for approximately 15 minutes; participation is voluntary.

Firstly, measurements will be taken of the participant's throat.

Secondly, sensors will be placed on the participant's throat, which will remain in place while the participant drinks liquids of different viscosities, and a dry food item.

The participant will be informed of the contents of each item, and may refuse any of them without giving a reason.

The data produced by the sensor will be recorded; this data in non-identifying and contains no sensitive information.

The sensors are then removed, concluding the study. The participant will then be asked to fill in a post-study, feedback questionnaire.

Data Protection

All personal information is stored securely.

If the participant wishes any collected information to be excluded from the study, they may request for it to be destroyed at any point.

CONSENT FORM

Title of project: The effect of inter-personal variation on accelerometer and gyrometer signals during swallowing

Name of investigator: Martin Henderson

Participant Identification Number for this project:

Please initial box

1. I confirm I have read and understand the information sheet dated 12.08.15 (version 1.1) for the above study. I have had the opportunity to consider the information, ask questions and have had these answered satisfactorily. ☐

2. I understand that my participation is voluntary and that I am free to withdraw at any time without giving any reason. *(Contact the lead researcher on 07748259884, if not present).* ☐

3. I understand that my responses will be anonymised before analysis. I give permission for members of the research team to have access to my anonymised responses. ☐

4. I agree to take part in the above research project. ☐

Name of participant	Date	Signature
Name of person taking consent *(if different from lead researcher)* *To be signed and dated in presence of the participant*	Date	Signature
Lead researcher	Date	Signature

Copies:

When completed: 1 for participant; 1 for researcher site file; 1 (original) to be kept in main file

Appendix B

Simulation Model Implementation

The following documents are included here, in order:

- Larynx Simulation Model .m file — The simulation model experiment and visualisation.
- Simulate Larynx .m file — A helper file which contains calculation details.

Larynx Simulation Model.m

Table of Contents

File description

Simulation Model of the effect of larynx elevation on a dual-axis accelerometer and integrated gyrometer for varying parameters Author: Martin Henderson

Parameter Setup

Define range of LP size and Δt to simulate

```
% Range of laryngeal prominence sizes
lp_size = 0.001:0.0005:0.015;
% Range of elevation periods
delta_t = 0.2:0.05:0.9;
```

Variable Initialization

```
n = length(delta_t);
m = length(lp_size);

max_x = zeros(n,m);
max_th = zeros(n,m);
max_phi = zeros(n,m);
```

Main Simulation Routine

The range of LP size and Δt are iterated over, returning the sensor signals for the given parameters. For each iteration, the size of key features (maximum acceleration, maximum tilt and maximum rotational velocity) are extracted from the signals and stored in max_x, max_th and max_phi, respectively.

```
progress = waitbar(0, 'Calculating');

for i = 1:n
for j = 1:m

    waitbar((i/n)+(j/(m*n)));

    %Run simulation for current parameters - requires
 simulate_larynx.m
    [t,sx,sy,th,ax,ay,g,a] = simulate_larynx(delta_t(i),1,lp_size(j));
```

```
    %Calculate accelerometer peak-to-peak amplitude
    max_x(i,j) = max(a(1,:))-min(a(1,:));
    %Calculate maximum sensor tilt
    max_th(i,j)  = max(th);
    %Calculate maximum gyrometer output
    max_phi(i,j) = max(g);
    %figure;plot(t,sqrt(ax.*ax + ay.*ay));
    %axis([-inf,inf,8,12])
end
end
close(progress);
```

Visualization of Results

Surface diagrams of the simulation predictions are plotted to communicate the findings.

```
figure;surf(lp_size*1000,0.01./delta_t,max_x);xlabel('LP size
 (mm)');ylabel('Speed of Elevation (ms^{-1})');zlabel('X axis
 acceleration (ms^{-2})');
figure;surf(lp_size*1000,0.01./delta_t,max_th*(180/pi));xlabel('LP
 size (mm)');ylabel('Speed of Elevation (ms^{-1})');zlabel('Maximum
 Tilt (degrees)');
figure;surf(lp_size*1000,0.01./delta_t,max_phi*(180/pi));xlabel('LP
 size (mm)');ylabel('Speed of Elevation (ms^{-1})');zlabel('Maximum
 Rotational Velocity (dps)');
```

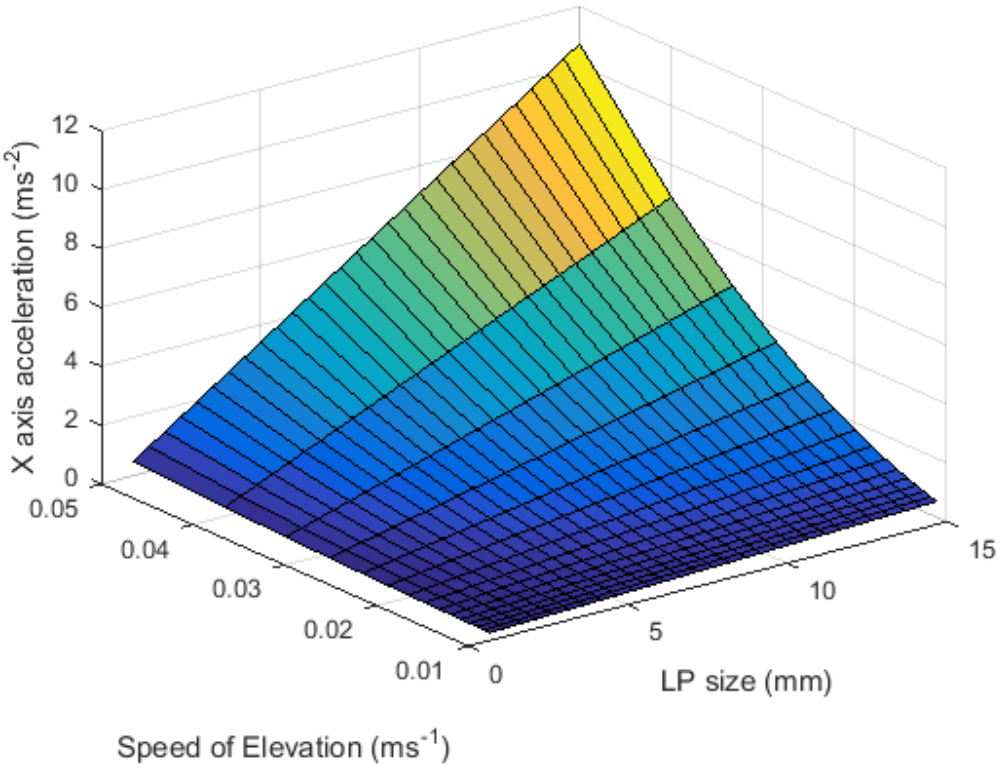

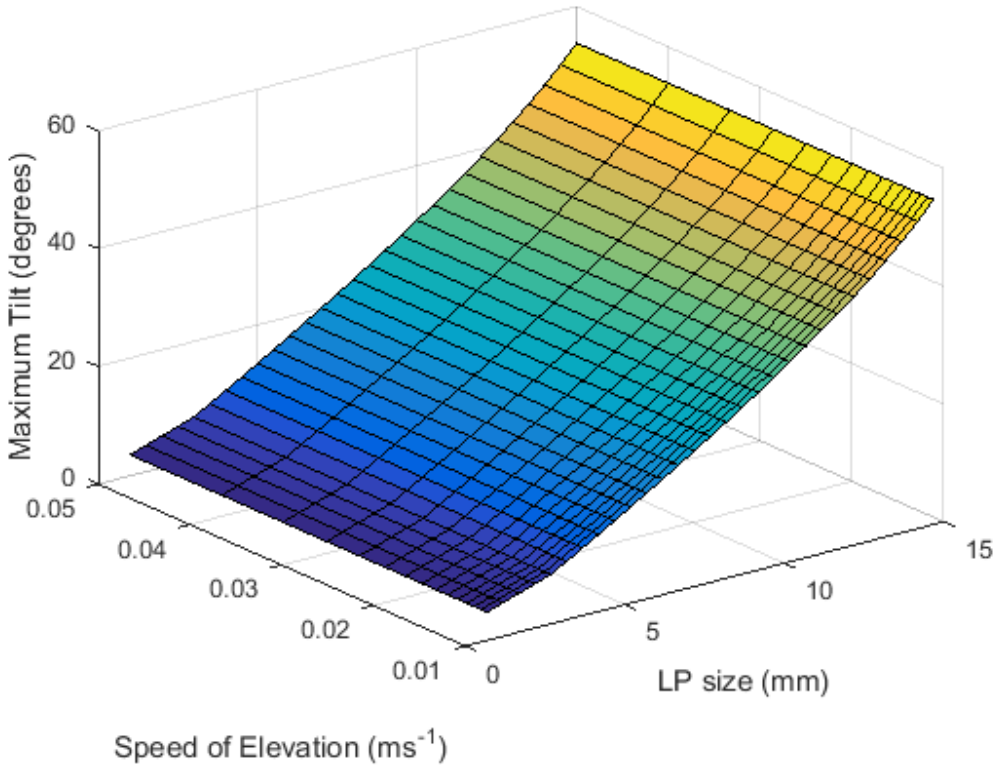
Maximum Tilt (degrees)
60
40
20
0
0.05
0.04
0.03
0.02
0.01
Speed of Elevation (ms-1)
0
5
10
15
LP size (mm)

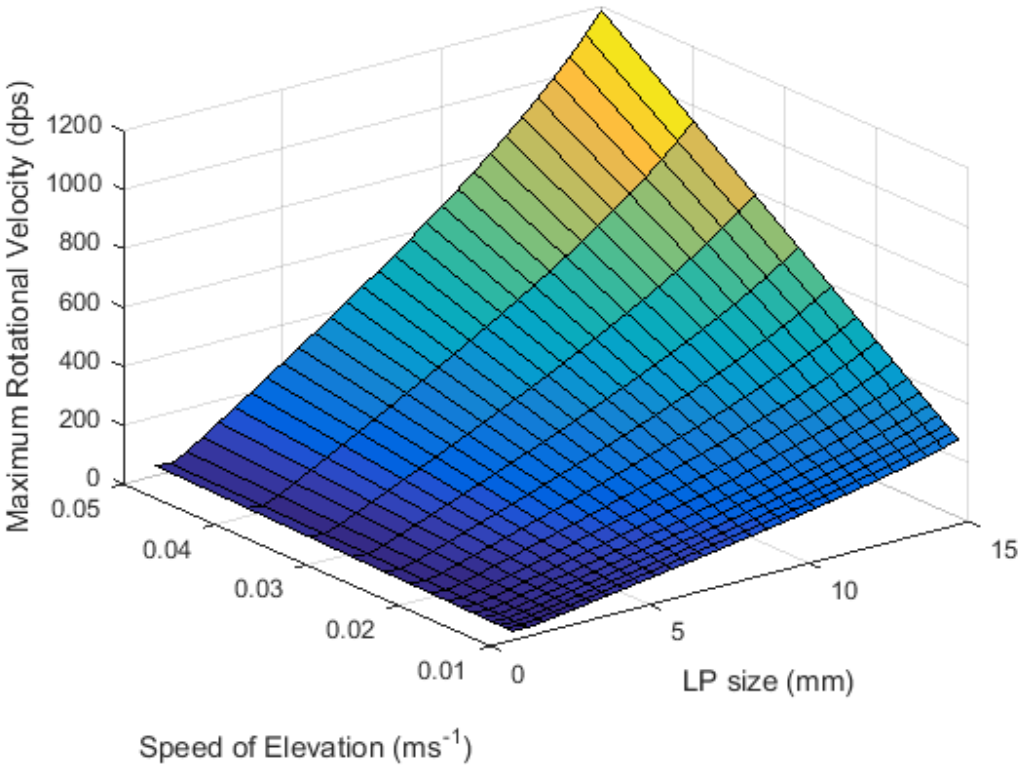
Maximum Rotational Velocity (dps)
1200
1000
800
600
400
200
0
0.05
0.04
0.03
0.02
0.01
Speed of Elevation (ms-1)
0
5
10
15
LP size (mm)

Published with MATLAB® R2015b

simulate_larynx.m

Table of Contents

Function Description

Simulate the output of a dual-axis accelerometer and integrated gyrometer for a given speed of elevation, aximum-elevation hold duration, and laryngeal prominence size.

PARAMETERS

- delta_t: period of elevation in seconds
- hold: duration of hold at maximum elevation in seconds
- laryngeal_prominence_size: in meters

RETURNS

- t: time vector in seconds
- x_pos: x axis position vector in meters
- y_pos: y axis position vector in meters
- theta: orientation of sensor in degrees
- ax: x' axis acceleration in meters per second squared
- ay: y' axis acceleration in meters per second squared
- g: rotation of sensor in degrees per second

Author: Martin Henderson

```
function [t,x_pos,y_pos,theta,ax,ay,g] = simulate_larynx(delta_t,
 hold, laryngeal_prominence_size)

dt = delta_t;
dpi = laryngeal_prominence_size;

interval = 0.001;
```

```
t = 0:interval:floor(4+hold+delta_t*2);
N = length(t);

x_pos = zeros(1,N);
y_pos = zeros(1,N);
theta = zeros(1,N);

ax = zeros(1,N);
g = zeros(1,N);
ay = zeros(1,N);

axG = zeros(1,N);
ayG = zeros(1,N);

axT = zeros(1,N);
ayT = zeros(1,N);

G = [0, 9.81];
```

Sensor angles are calculated based on LP size

As the LP size is increased, the angle of the sensor both before elevation and at maximum elevation are accentuated, as shown in the diagram below:

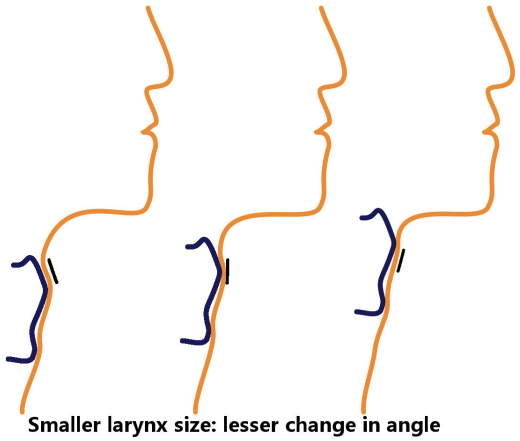

Smaller larynx size: lesser change in angle

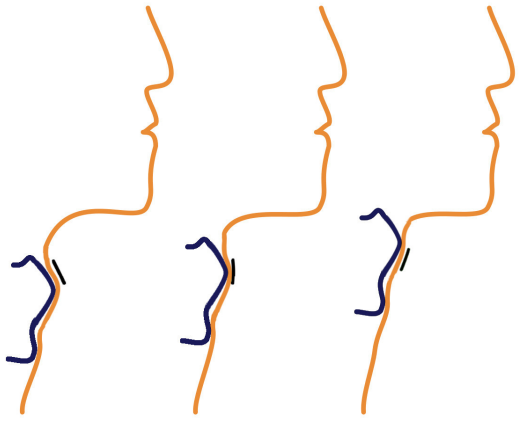

Larger larynx size: greater change in angle

The angles at these three laryngeal elevations - resting position, LP at sensor level and maximum elevation - are calculated using trigonometry, based on a sensor length of 16mm.

```
angle1 = asin((0.0015-dpi)/0.016);
angle2 = asin((dpi-0.001)/0.016);
angle3 = asin(((dpi-0.001)/2+0.001)/0.016);

theta = theta+angle1;%default angle
```

Calculate event timings based on Δt

Δt is the time taken to elevate the larynx completely.

```
elapse0 = 2;
elapse1 = dt/2;
elapse2 = dt/2;
elapse_hold = hold;
elapse3 = dt/2;
elapse4 = dt/2;
elapsen = 2;

n0=1;
n1=floor(elapse0/interval);
n2=floor((elapse0+elapse1)/interval);
n3=floor((elapse0+elapse1+elapse2)/interval);
nh=floor((elapse0+elapse1+elapse2+elapse_hold)/interval);
n4=floor((elapse0+elapse1+elapse2+elapse_hold+elapse3)/interval);
n5=floor((elapse0+elapse1+elapse2+elapse_hold+elapse3+elapse4)/
interval);
nn=floor((elapse0+elapse1+elapse2+elapse_hold
+elapse3+elapse4+elapsen)/interval);
```

Calculate sensor positions

The displacement of the sensor is 0 when the larynx is at rest and the same as the size of the LP when the LP is at the level of the sensor. We are estimating that the excursion of the crichoid cartilage is 1mm beyond the skin superior to the LP when at rest.

```
%Elevation
for k = n1:n2
    theta(k) = angle1 + (k-n1)*(angle2-angle1)/(n2-n1);
    x_pos(k) = 0 + (k-n1)*(dpi-0)/(n2-n1);
    y_pos(k) = 0 + (k-n1)*(0.001-0)/(n2-n1);
end
for k = n2:n3
    theta(k) = angle2 + (k-n2)*(angle3-angle2)/(n3-n2);
    x_pos(k) = dpi + (k-n2)*(0.001-dpi)/(n3-n2);
    y_pos(k) = 0.001 + (k-n2)*(0.000-0.001)/(n3-n2);
end
%Hold
for k = n3:nh
    theta(k) = angle3;
    x_pos(k) = 0.001;
```

```
    y_pos(k) = 0;
end
%Delevation
for k = nh:n4
    theta(k) = angle3 + (k-nh)*(angle2-angle3)/(n4-nh);
    x_pos(k) = 0.001 + (k-nh)*(dpi-0.001)/(n4-nh);
    y_pos(k) = 0.000 + (k-nh)*(-0.001-0.000)/(n4-nh);
end
for k = n4:n5
    theta(k) = angle2 + (k-n4)*(angle1-angle2)/(n5-n4);
    x_pos(k) = dpi + (k-n4)*(0.000-dpi)/(n5-n4);
    y_pos(k) = -0.001 + (k-n4)*(0.000+0.001)/(n5-n4);
end
```

Low-Pass Filter to smoothen motion

We use a low-pass filter to simulate a small inertia of the sensor, making the motion and rotation of the sensor more natural.

Without this filter, instantaneous changes in velocity produces acceleration spikes, which are unrealistic and therefore defeat the purpose of the model.

```
fn = floor(100*dt);
temp = [theta;x_pos;y_pos];
for k = 1+fn:N-fn
    temp(1,k) = mean(theta((k-fn):(k+fn)));
    temp(2,k) = mean(x_pos((k-fn):(k+fn)));
    temp(3,k) = mean(y_pos((k-fn):(k+fn)));
end
theta = temp(1,:);
x_pos = temp(2,:);
y_pos = temp(3,:);
for k = 1+fn:N-fn
    temp(1,k) = mean(theta((k-fn):(k+fn)));
    temp(2,k) = mean(x_pos((k-fn):(k+fn)));
    temp(3,k) = mean(y_pos((k-fn):(k+fn)));
end
theta = temp(1,:);
x_pos = temp(2,:);
y_pos = temp(3,:);
```

Calculate Accelerometer and Gyrometer outputs

The acceleration vector must be composed from the gravitational vector and the second time-derivative of sensor motion, then projected onto X' and Y' axes, which are determined by the instantaneous sensor angle.

The gyrometer output is simply the first time-derivative of the sensor angle.

```
a = zeros(2,length(t));
for k = 1:N-1
    g(k) = (theta(k+1) - theta(k))/interval;
```

```
    v = [(x_pos(k+1)-x_pos(k))/interval,(y_pos(k+1)-y_pos(k))/
interval];
    a(:,k) = [0,0];
    aT = a(:,k);
    if k>1
        a(:,k) = (v-[(x_pos(k)-x_pos(k-1))/interval,(y_pos(k)-
y_pos(k-1))/interval])/interval;
    end
    aT = a(:,k)'+G;
    ax(k) = a(1,k)*cos(theta(k))-a(2,k)*sin(theta(k));
    ay(k) = a(2,k)*cos(theta(k))+a(1,k)*sin(theta(k));
    axG(k) = G(1)*cos(theta(k))-G(2)*sin(theta(k));
    ayG(k) = G(2)*cos(theta(k))+G(1)*sin(theta(k));
    axT(k) = aT(1)*cos(theta(k))-aT(2)*sin(theta(k));
    ayT(k) = aT(2)*cos(theta(k))+aT(1)*sin(theta(k));
end
```

Boundary Clipping

Signals calculated from derivatives require a buffer of up to two valid values. The first value and last two values of some of the sequences are invalid, and so are excluded from the output.

```
ax = axT(2:end-2);
ay = ayT(2:end-2);
g = g(2:end-2);
axG = axG(2:end-2);
ayG = ayG(2:end-2);
axT = axT(2:end-2);
ayT = ayT(2:end-2);
t = t(2:end-2);
theta = theta(2:end-2);
x_pos = x_pos(2:end-2);
y_pos = y_pos(2:end-2);

end
```

Published with MATLAB® R2015b

Appendix C

Source Code for Data-Capture Software and Data-Processing Tools

The source code for the following software tools are included here, in order:

- Data capture software – Software for capturing sensor data, visualising it in real time, and saving it to disk; written in the Processing programming language.
- correct_for_gravity.m – A tool for removing the effects of sensor tilt from accelerometry data; written in the MATLAB programming language.
- mark_events.m – A tool for identifying and saving the start and end points of swallowing events; written in the MATLAB programming language.

Data Capture and Visualisation Software Listing

```
1  // Dysphagia sensor data capture
2  // Author: Martin Henderson
3
4  import processing.serial.*;
5
6  PrintWriter output_file;
7
8  String portName = "/dev/tty.usbmodem401851"; // Sensor Board COM ...
       port name
9  String filename = ""; // Output file location
10 String folder = "./";
11
12 Serial port;                          // The serial port
13 char[] packet = new char[14];          // incoming data
14 int serialCount = 0;                  // current packet byte position
15 int aligned = 0;
16 int interval = 0;
17
18 boolean eating = false;
19 boolean begin_swallow = false;
20 boolean end_swallow = false;
21
22 int x = 0, y = 0, z = 0, a = 0, b = 0, c = 0;
23 int mean_x = 0;
24 int mean_y = 0;
25 int mean_z = 0;
26 int mean_a = 0;
27 int mean_b = 0;
28 int mean_c = 0;
```

```
29 float x_mag = 0;
30 float y_mag = 0;
31 float z_mag = 0;
32 float a_mag = 0;
33 float b_mag = 0;
34 float c_mag = 0;
35
36 int buffer[] = {0,0,0,0,0,0,0,0,0,0,0,0,0,0,0,0,0,0,0,0,
37    0,0,0,0,0,0,0,0,0,0,0,0,0,0,0,0,0,0,0,0,0,0,0,0,0,0,
38    0,0,0,0,0,0,0,0,0,0,0,0,0,0,0,0,0,0,0,0,0,0,0,0,0,0,
39    0,0,0,0,0,0,0,0,0,0,0,0,0,0,0,0,0,0,0,0,0,0,0,0,0,0,
40    0,0,0,0,0,0,0,0,0,0,0,0,0,0,0,0,0,0,0,0,0,0,0,0,0,0,
41    0,0,0,0,0,0,0,0,0,0,0,0,0,0,0,0,0,0,0,0,0,0,0,0,0,0,
42    0,0,0,0,0,0,0,0,0,0,0,0,0,0,0,0,0,0,0,0,0,0,0,0,0,0,
43    0,0,0,0,0,0,0,0,0,0,0,0,0,0,0,0,0,0,0,0,0,0,0,0,0,0};
44
45 int mag_xyz[] = buffer;
46 int xv[] = buffer;
47 int yv[] = buffer;
48 int zv[] = buffer;
49 int av[] = buffer;
50 int bv[] = buffer;
51 int cv[] = buffer;
52
53 // Put new values into rotating buffer arrays ==============
54
55 void new_x(int nx)
56 {
57   for (int i = 0; i < 99; i++)
58   {
59     xv[i] = xv[i+1];
```

```
60      mean_x += xv[i];
61    }
62    xv[99] = nx;
63
64    mean_x /= 100;
65  }
66
67  void new_y(int ny)
68  {
69    for (int i = 0; i < 99; i++)
70    {
71      yv[i] = yv[i+1];
72      mean_y += yv[i];
73    }
74    yv[99] = ny;
75
76    mean_y /= 50;
77  }
78
79  void new_z(int nz)
80  {
81    for (int i = 0; i < 99; i++)
82    {
83      zv[i] = zv[i+1];
84      mean_z += zv[i];
85    }
86    zv[99] = nz;
87
88    mean_z /= 100;
89  }
90
```

```
91
92  void new_a(int na)
93  {
94    for (int i = 0; i < 99; i++)
95    {
96      av[i] = av[i+1];
97      mean_a += av[i];
98    }
99    av[99] = na;
100
101   mean_a /= 100;
102 }
103
104 void new_b(int nb)
105 {
106   for (int i = 0; i < 99; i++)
107   {
108     bv[i] = bv[i+1];
109     mean_b += bv[i];
110   }
111   bv[99] = nb;
112
113   mean_b /= 100;
114 }
115
116 void new_c(int nc)
117 {
118   for (int i = 0; i < 99; i++)
119   {
120     cv[i] = cv[i+1];
121     mean_c += cv[i];
```

```
122   }
123   cv[99] = nc;
124
125   mean_c /= 100;
126 }
127
128 void new_mag(int mag)
129 {
130   for (int i = 0; i < 199; i++)
131   {
132     mag_xyz[i] = mag_xyz[i+1];
133   }
134   mag_xyz[199] = mag;
135 }
136
137 boolean fileisopen=false;
138 void open_file(String fname)
139 {
140   int dup = 1;
141   while (true){
142     File f = new File(fname+dup+".csv");
143     if (!f.exists()) break;
144   print("File Exists: ");
145   println(fname+dup+".csv");
146     dup += 1;
147   }
148   print("Opening File:");
149   println(fname+dup+".csv");
150   filename = fname+".csv";
151   output_file = createWriter(filename);
152   fileisopen=true;
```

```
153 }
154
155 int countdown = 0;
156 String last_recording = "55/water.csv";
157 void close_file()
158 {
159   last_recording = filename;
160   filename = "";
161   if (!fileisopen) return;
162   output_file.flush();
163   output_file.close();
164   fileisopen=false;
165   screen = 3;
166   countdown = 50;
167 }
168
169
170
171 // Initialization =============================================
172
173 void setup() {
174     size(1200, 600);
175
176     // display serial port list for debugging/clarity
177     println(Serial.list());
178
179     frameRate(20);
180
181     // open the serial port
182     port = new Serial(this, portName, 115200);
183 }
```

```
184
185 boolean pause = false;
186
187 boolean drawing = false;
188
189
190 // Graphical display ========================================
191
192 int screen = 0;
193 String id_text = "";
194 String id = "";
195
196 int buttonX, buttonY;
197
198 void draw() {
199   switch(screen){
200   case 0:
201     background(0);
202     textSize(32);
203     if (mouseX > buttonX && mouseY > buttonY && mouseX < ...
          buttonX+200 && mouseY < buttonY+70){
204       fill(40,40,255);
205     }else{
206       fill(40,255,40);
207     }
208     stroke(0);
209     buttonX = 650;
210     buttonY = (height/2) - 50;
211     rect(buttonX, buttonY, 200, 70);
212     fill(255);
213     text("Enter ID Number: "+id_text, 100,height/2);
```

```
214       text("Begin", 700,height/2);
215       break;
216     case 1:
217     // pause function
218       if(pause)return;
219
220       drawing = true;
221       // black background
222       background(0);
223
224       // green line
225       stroke(0,255,0);
226
227       line(0, 50, displayWidth, 50);
228       line(0, 550, displayWidth, 550);
229
230       display_playpause(550,0, width, height-550);
231
232       for (int i = 0; i < 98; i++)
233       {
234         float x1 = (i*12);
235         float x2 = ((i+1)*12);
236         float x3 = ((i+2)*12);
237
238         float xs = (x1+x2) / 2;
239         float xf = (x2+x3) / 2;
240
241
242         // acceleration x
243         float y1 = 400 - (((xv[i]-mean_x)*350)/(32768));
244         float y2 = 400 - (((xv[i+1]-mean_x)*350)/(32768));
```

```
245         float y3 = 400 - (((xv[i+2]-mean_x)*350)/(32768));
246 
247         float ys = (y1+y2) / 2;
248         float yf = (y2+y3) / 2;
249         fill(255,0,0,50);
250         noStroke();
251         beginShape();
252         vertex(xf,400);
253         vertex(xs,400);
254         vertex(xs,ys);
255         bezierVertex(x2,y2,x2,y2,xf,yf);
256         vertex(xf,400);
257         endShape();
258         noFill();
259         stroke(255, 0, 0);
260         bezier(xs,ys,x2,y2,x2,y2,xf,yf);
261 
262         // acceleration z
263         y1 = 400 - (((zv[i]-mean_z)*350)/(32768));
264         y2 = 400 - (((zv[i+1]-mean_z)*350)/(32768));
265         y3 = 400 - (((zv[i+2]-mean_z)*350)/(32768));
266 
267         ys = (y1+y2) / 2;
268         yf = (y2+y3) / 2;
269         fill(0,0,255,50);
270         noStroke();
271         beginShape();
272         vertex(xf,400);
273         vertex(xs,400);
274         vertex(xs,ys);
275         bezierVertex(x2,y2,x2,y2,xf,yf);
```

```
276         vertex(xf,400);
277         endShape();
278         noFill();
279         stroke(0, 0, 255);
280         bezier(xs,ys,x2,y2,x2,y2,xf,yf);
281 
282         // gyro y
283         y1 = 400 - (((bv[i])*350)/(32768));
284         y2 = 400 - (((bv[i+1])*350)/(32768));
285         y3 = 400 - (((bv[i+2])*350)/(32768));
286 
287         ys = (y1+y2) / 2;
288         yf = (y2+y3) / 2;
289         fill(0,255,0,50);
290         noStroke();
291         beginShape();
292         vertex(xf,400);
293         vertex(xs,400);
294         vertex(xs,ys);
295         bezierVertex(x2,y2,x2,y2,xf,yf);
296         vertex(xf,400);
297         endShape();
298         noFill();
299         stroke(0, 255, 0);
300         bezier(xs,ys,x2,y2,x2,y2,xf,yf);
301 
302       }
303         drawing = false;
304       break;
305       case 3:
306       if (countdown < 1)
```

```
307     {
308       screen = 1;
309     }
310     display_recording(last_recording, 0, 0, width, height);
311     countdown -= 1;
312   }
313 }
314
315 boolean lock = false;
316 int lock_count = 0;
317
318
319 // Process serial input from COM port ============================
320 void serialEvent(Serial port) {
321
322   // expected format:
323   //  acc_x_high | acc_x_low | acc_y_high | ... | gyro_z_low | ...
        "aaaaaaaaaaaa"
324
325     interval = millis();
326     if (lock)
327     {
328       while (port.available() ≥ 24) {
329         x = (port.read() << 8) & 0xff00;
330         x |= (port.read() & 0xff);
331         //println("x: " + binary(x));
332         if ((x & 0x8000) != 0) x -= 0x10000;
333         y = (port.read() << 8) & 0xff00;
334         y |= (port.read() & 0xff);
335         if ((y & 0x8000) != 0) y -= 0x10000;
336         z = (port.read() << 8) & 0xff00;
```

```
337         z |= (port.read() & 0xff);
338         if ((z & 0x8000) != 0) z -= 0x10000;
339         a = (port.read() << 8) & 0xff00;
340         a |= (port.read() & 0xff);
341         if ((a & 0x8000) != 0) a -= 0x10000;
342         b = (port.read() << 8) & 0xff00;
343         b |= (port.read() & 0xff);
344         if ((b & 0x8000) != 0) b -= 0x10000;
345         c = (port.read() << 8) & 0xff00;
346         c |= (port.read() & 0xff);
347         if ((c & 0x8000) != 0) c -= 0x10000;
348
349         //print ("x: "); println(x);
350         //print ("y: "); println(y);
351         //print ("z: "); println(z);
352
353         // 12 a's
354         if (port.read() != 'a') lock = false;
355         if (port.read() != 'a') lock = false;
356         if (port.read() != 'a') lock = false;
357         if (port.read() != 'a') lock = false;
358         if (port.read() != 'a') lock = false;
359         if (port.read() != 'a') lock = false;
360         if (port.read() != 'a') lock = false;
361         if (port.read() != 'a') lock = false;
362         if (port.read() != 'a') lock = false;
363         if (port.read() != 'a') lock = false;
364         if (port.read() != 'a') lock = false;
365         if (port.read() != 'a') lock = false;
366
367         // if all is still well, print to file
```

```
368         float t = millis();
369         t=t/1000;
370         if (lock && /*t>2.0 &&*/ recording){
371         int marker = 0;
372           if (eating){
373             eating = false;
374             marker = 1;
375           }else if (begin_swallow){
376             begin_swallow = false;
377             marker = 2;
378           }else if (end_swallow){
379             end_swallow = false;
380             marker = 3;
381           }
382           output_file.println(""+t+','+x+','+y+','+z+'
383                               ,'+a+','+b+','+c+','+marker);
384         }
385
386         if (! drawing) // don't interrupt an update cycle
387         {
388           new_x(x);
389           new_y(y);
390           new_z(z);
391           new_a(a);
392           new_b(b);
393           new_c(c);
394         }
395       }
396     }
397     else
398     {
```

```
399
400         while (port.available() > 0)
401         {
402           int ch = port.read();
403           if (ch == 'a')
404           {
405             lock_count++;
406
407             if (lock_count == 12)
408             {
409               lock = true;
410               lock_count = 0;
411               break;
412             }
413           }
414           else lock_count = 0;
415         }
416       }
417
418   }
419
420   String filename_input = "";
421
422   void keyPressed() {
423     if (key == ESC) {
424       close_file();
425       exit();
426     }
427     else if (' ' == key)
428     {
429       pause = !pause;
```

```
430   }
431   else if (key == ENTER && screen == 0) {
432     id_selected();
433   }
434   else if (key == ENTER && screen == 1) {
435     if (!recording){
436       start_recording();
437     }else{
438       end_recording();
439     }
440   }
441   else if (key == BACKSPACE)
442   {
443     if (screen == 0){
444       id_text = id_text.substring(0,max(0,id_text.length()-1));
445     }else if (screen == 1){
446       filename_input = filename_input.substring(0
447                         ,max(0,filename_input.length()-1));
448     }
449   }else if (recording){
450     if (key == 'q' || key == 'Q'){
451       eating = true;
452     }else if(key == 'w' || key == 'W'){
453       begin_swallow = true;
454     }else if(key == 'e' || key == 'E'){
455       end_swallow = true;
456     }
457   }else if(screen == 0){
458     id_text+=key;
459   }
460   else if(screen == 1){
```

```
461     filename_input+=key;
462   }
463 }
464
465 void id_selected(){
466   screen = 1;
467   id = id_text;
468   folder="./"+id+"/";
469   print("ID:");
470   println(id);
471   print("Folder:");
472   println(folder);
473 }
474
475 int pp_x, pp_y, pp_r;
476
477 void mouseClicked(){
478   if (screen == 0 && mouseX > buttonX && mouseY > buttonY
479             && mouseX < buttonX+200 && mouseY < buttonY+70){
480     id_selected();
481   }else if (screen == 1 && overCircle(pp_x+pp_r, pp_y+pp_r, pp_r)){
482     if (!recording){
483       start_recording();
484     }else{
485       end_recording();
486     }
487   }
488 }
489
490 boolean recording = false;
491
```

```
492 void display_playpause(int t, int l, int w, int h)
493 {
494   pp_x = l + width - 2*h;
495   pp_y = t +h/5;
496   pp_r = 3*(h/10);
497   textSize(32);
498   stroke(255);
499   fill(100,255,100);
500   text("Recording_name: ", l+10, t+2*(h/3));
501   fill(255,100,100);
502   if (recording){
503     text(filename, l+350, t+2*(h/3));
504     fill(255,40,40);
505     ellipse(pp_x+pp_r,pp_y+pp_r,pp_r*2, pp_r*2);
506     fill(255,0);
507     rect(pp_x+(pp_r/2),pp_y+(pp_r/2),pp_r, pp_r);
508   }else{
509     text(filename_input, l+350, t+2*(h/3));
510     fill(40,255,40);
511     ellipse(pp_x+pp_r,pp_y+pp_r,pp_r*2,pp_r*2);
512     fill(255,0);
513     triangle(pp_x+3*(pp_r/5),pp_y+(pp_r/2),pp_x+3*(pp_r/5)
514                 ,pp_y+3*(pp_r/2),pp_x+7*(pp_r/5),pp_y+pp_r);
515   }
516 }
517
518 void start_recording(){
519   println("Opening file... "+folder+filename_input);
520   open_file(folder+filename_input);
521   recording = true;
522 }
```

```
523
524 void end_recording(){
525   recording = false;
526   filename_input = "";
527   close_file();
528 }
529
530
531 boolean overCircle(int x, int y, int radius) {
532   float disX = x - mouseX;
533   float disY = y - mouseY;
534   if(sqrt(sq(disX) + sq(disY)) < radius ) {
535     return true;
536   } else {
537     return false;
538   }
539 }
540
541 String dname = null;
542 FloatList T;
543 FloatList g1;
544 FloatList g2;
545
546 void display_recording(String recording,
547                        int t, int l, int w, int h)
548 {
549
550   if (recording != dname)
551   {
552
553   T = new FloatList();
```

```
554   g1 = new FloatList();
555   g2 = new FloatList();
556
557   dname = recording;
558
559   BufferedReader b = createReader(dname);
560   String line = null;
561   boolean flip = true;
562   while(true){
563     try{
564       line = b.readLine();
565     }catch (IOException e){
566       e.printStackTrace();
567       line = null;
568     }
569     if (line != null){
570       String words[] = split(line, ',');
571       if (flip){
572         T.append(Float.parseFloat(words[0]));
573         g1.append(Float.parseFloat(words[5]));
574         flip = false;
575       }else{
576         g2.append(Float.parseFloat(words[5]));
577         flip = true;
578       }
579     }else{
580       break;
581     }
582   }}
583   if (T.size()<2){
584     countdown = 0;
```

```
585       return;
586     }
587     float yp1 = g1.max();
588     float yn1 = g1.min();
589     float yr1 = yp1-yn1;
590 
591     float yp2 = g2.max();
592     float yn2 = g2.min();
593     float yr2 = yp2-yn2;
594 
595     float xp = T.max();
596     float xn = T.min();
597     float xr = xp-xn;
598 
599     background(0);
600 
601     for (int i = 1; i < T.size(); i++){
602       float x1 = (T.get(i-1) - xn)*w/xr;
603       float x2 = (T.get(i) - xn)*w/xr;
604       float y1 = (g1.get(i-1) - yn1)*h/(yr1*2);
605       float y2 = (g1.get(i) - yn1)*h/(yr1*2);
606       float y3 = (g2.get(i-1) - yn2)*h/(yr2*2);
607       float y4 = (g2.get(i) - yn2)*h/(yr2*2);
608       stroke(100,255,100);
609       line(l+x1,t+y1,l+x2,t+y2);
610       stroke(100,100,255);
611       line(l+x1,t+y3+h/2,l+x2,t+y4+h/2);
612     }
613 
614   }
```

Listing of MATLAB tool for removing the effects of tilt from accelerometry

```
function [ corr_x, corr_y, abs_x, abs_y, tilt ] = ...
    correct_for_gravity( x, y, g, t )
% CORRECT_FOR_GRAVITY Removes the gravity vector from ...
    accelerometer data
%   Integrates the gyrometer data, corrects for drift. and uses ...
    this to
%   remove the gravity vector from 2D accelerometer data.
%   x,y is accelerometer data in Gs (9.81 m/s^2)
%   g is gyro data in rad/s
%   t is time in s
%
% Author: Martin Henderson

interval = (t(end)-t(1))/(length(t)-1);

d1 = -atan2(x,y);
%move away from arctan transition
trans=0;
while d1(1)+trans<-pi/2
    trans = trans+pi/4;
end
while d1(1)+trans>pi/2
    trans = trans-pi/4;
end
d1 = d1+trans;
%correct arctan jumps
for i = 2:length(d1)
```

```
25      while d1(i)<-pi
26          d1(i) = d1(i)+2*pi;
27      end
28      while d1(i)>pi
29          d1(i) = d1(i)-2*pi;
30       end
31       while d1(i)-d1(i-1)>pi
32           d1(i) = d1(i) -2*pi;
33       end
34       while d1(i-1)-d1(i)>pi
35           d1(i) = d1(i) +2*pi;
36       end
37  end
38  d1 = d1-trans;
39
40  d2 = (cumsum(g)*interval);
41
42  th0 = mean(d1(1:101));
43  thf = mean(d1(end-100:end));
44  phiE1 = (thf-th0)/(t(end)-t(1));
45  phiE2 = (mean(d2(end-100:end))-mean(d2(1:101)))/(t(end)-t(1));
46
47  phiE = phiE2-phiE1;
48
49  %%%%%%%%%%%%%%%%%%%%%%%%%%%%%%%%%%%%%%%%%%%%%%%%
50  % Correction of th0, phiE and T
51  %%%%%%%%%%%%%%%%%%%%%%%%%%%%%%%%%%%%%%%%%%%%%%%%
52
53  phiEadj = 1;
54  th0adj = 0;
55  Tadj = 1;
```

```
56 T = interval;
57
58 function [] = calc_adj(h1,h2,h3, haxes)
59     str=get(h1,'String');
60     if isempty(str2num(str))
61         set(h1,'string','0');
62         str = '0';
63         warndlg('Input must be numerical');
64     end
65   th0adj = str2num(str);
66     str=get(h2,'String');
67     if isempty(str2num(str))
68         set(h2,'string','0');
69         str = '0';
70         warndlg('Input must be numerical');
71     end
72   phiEadj = str2num(str);
73     str=get(h3,'String');
74     if isempty(str2num(str))
75         set(h3,'string','0');
76         str = '0';
77         warndlg('Input must be numerical');
78     end
79   Tadj = str2num(str);
80
81   plot(haxes,t,d1,'r',t,(d2 - phiE*t*phiEadj)*Tadj + ...
        th0+th0adj,'b');
82   title('correctness of fit');
83 end
84
85 f = figure;
```

```
ax = axes('Parent',f,'position',[0.13 0.39  0.77 0.54]);
plot(ax,t,d1,'r',t,(d2 - phiE*t*phiEadj)*Tadj + th0+th0adj,'b');
title('correctness of fit');

b1 = uicontrol('Parent',f,'Style','edit','Position',...
    [81,134,419,23],'String',th0adj);
bgcolor = f.Color;
bl1 = uicontrol('Parent',f,'Style','text','Position',...
    [50,130,23,23],'String','-0.1','BackgroundColor',bgcolor);
bl2 = uicontrol('Parent',f,'Style','text','Position',...
    [500,130,23,23],'String','0.1','BackgroundColor',bgcolor);
bl3 = uicontrol('Parent',f,'Style','text','Position',...
    [215,100,150,23],'String','Adjustment for \theta_0',...
    'BackgroundColor',bgcolor);



b2 = ...
    uicontrol('Parent',f,'Style','edit','Position',[81,85,419,23],...
              'String',phiEadj);
bgcolor = f.Color;
bl5 = ...
    uicontrol('Parent',f,'Style','text','Position',[50,85,23,23],...
                'String','-2','BackgroundColor',bgcolor);
bl6 = ...
    uicontrol('Parent',f,'Style','text','Position',[500,85,23,23],...
                'String','2','BackgroundColor',bgcolor);
bl7 = ...
    uicontrol('Parent',f,'Style','text','Position',[215,64,150,23],...
                'String','Adjustment for \phi_E',...
                'BackgroundColor',bgcolor);
```

```
113
114
115
116 b3 = ...
        uicontrol('Parent',f,'Style','edit','Position',[81,30,419,23],...
117                 'String',Tadj);
118 bgcolor = f.Color;
119 uicontrol('Parent',f,'Style','text','Position',[50,30,23,23],...
120                   'String','0.7','BackgroundColor',bgcolor);
121 uicontrol('Parent',f,'Style','text','Position',[500,30,23,23],...
122                   'String','1.3','BackgroundColor',bgcolor);
123 uicontrol('Parent',f,'Style','text','Position',[215,0,150,23],...
124                   'String','Adjustment for ...
                         T','BackgroundColor',bgcolor);
125
126 b1.Callback = @(es,ed) calc_adj(b1,b2,b3, ax);
127 b2.Callback = @(es,ed) calc_adj(b1,b2,b3, ax);
128 b3.Callback = @(es,ed) calc_adj(b1,b2,b3, ax);
129
130
131 uiwait(f);
132
133 disp(th0adj);
134 disp(th0adj);
135
136 d2 = (d2 - phiE*t*phiEadj)*Tadj + th0+th0adj;
137 interval = T*Tadj;
138
139 %%%%%%%%%%%%%%%%%%%%%%%%%%%%%%%%%%%%%%%%%%%%%%%
140 % Correction of Accelerometer Scaling
141 %%%%%%%%%%%%%%%%%%%%%%%%%%%%%%%%%%%%%%%%%%%%%%%
```

```
142
143 Gx = 1;%9.81;
144 Gy = 1;%9.81;
145
146 d3 = sqrt(y.*y + x.*x);
147 d4 = [-d3.*sin(d1); d3.*cos(d1)];
148
149   th = 0:pi/50:2*pi;
150   xunit = Gx * sin(th);
151   yunit = Gy * cos(th);
152
153 function [] = calc_g(h1, h2, haxes)
154   Gx = get(h1,'value');
155   Gy = get(h2,'value');
156
157   xunit = Gx * sin(th);
158   yunit = Gy * cos(th);
159
160   plot(haxes,d4(1,:),d4(2,:),'b');
161   hold on
162   axis manual
163   plot(haxes,xunit,yunit,'r');
164   title('correctness of fit');
165   hold off
166
167   %disp('Gx');disp(Gx)
168   %disp('Gy');disp(Gy)
169 end
170
171 f = figure;
172 ax = axes('Parent',f,'position',[0.13 0.39  0.77 0.54]);
```

```
173
174   plot(ax,d4(1,:),d4(2,:),'b');
175   hold on
176   axis manual
177   plot(ax,xunit,yunit,'r');
178   title('correctness of fit');
179   hold off
180
181 b3 = uicontrol('Parent',f,'Style','slider','Position',...
182     [81,74,419,23],'value',Gx, 'min',0.8, 'max',1.2);
183 bgcolor = f.Color;
184 bl8 = uicontrol('Parent',f,'Style','text','Position',...
185     [50,74,23,23],'String','9','BackgroundColor',bgcolor);
186 bl9 = uicontrol('Parent',f,'Style','text','Position',...
187     [500,74,23,23],'String','12','BackgroundColor',bgcolor);
188 bl10 = uicontrol('Parent',f,'Style','text','Position',...
189     [215,45,150,23],'String','Adjustment for Gx',...
190     'BackgroundColor',bgcolor);
191
192
193 b4 = uicontrol('Parent',f,'Style','slider','Position',...
194     [81,30,419,23],'value',Gy, 'min',0.8, 'max',1.2);
195 bgcolor = f.Color;
196 bl5 = uicontrol('Parent',f,'Style','text','Position',...
197     [50,30,23,23],'String','9','BackgroundColor',bgcolor);
198 bl6 = uicontrol('Parent',f,'Style','text','Position',...
199     [500,30,23,23],'String','12','BackgroundColor',bgcolor);
200 bl7 = uicontrol('Parent',f,'Style','text','Position',...
201     [215,0,150,23],'String','Adjustment for Gy',...
202     'BackgroundColor',bgcolor);
203
```

```
204
205
206 b3.Callback = @(es,ed) calc_g(b3,b4, ax);
207 b4.Callback = @(es,ed) calc_g(b3,b4, ax);
208
209
210 uiwait(f);
211
212 %%%%%%%%%%%%%%%%%%%%%%%%%%%%%%%%%%%%%%%%%%%%%%%%
213
214 d5 = [-Gx.*sin(d2); Gy.*cos(d2)];
215
216 d6 = d4-d5;
217
218 corr_x = d6(1,:);
219 corr_y = d6(2,:);
220
221
222 %%%%%%%%%%%%%%%%%%%%%%%%%%%%%%%%%%%%%%%%%%%%%%%%%%%%%%%%%%%%%%%%%%%%%%%
223 % Transpose Acceleration to Reference Axes
224 %%%%%%%%%%%%%%%%%%%%%%%%%%%%%%%%%%%%%%%%%%%%%%%%%%%%%%%%%%%%%%%%%%%%%%%
225
226 abs_x = corr_x.*cos(-d2) - corr_y.*sin(-d2);
227 abs_y = corr_x.*sin(-d2) + corr_y.*cos(-d2);
228
229 %%%%%%%%%%%%%%%%%%%%%%%%%%%%%%%%%%%%%%%%%%%%%%%%%%%%%%%%%%%%%%%%%%%%%%%
230
231 tilt=d2*(180/pi);
232 end
```

Listing of MATLAB tool for marking the timings of swallowing events

```
% Marks events
% Author: Martin Henderson

load('swallowing_data.mat');

[N,M]=size(swallowing_data);

for m = 1:M
    t = swallowing_data{3,m}.t;
    for n = 1:2 % # of IMUs
        disp([swallowing_data{1,m},', ',swallowing_data{2,m},...
        ', imu', num2str(n)])
        tilt = swallowing_data{3+n,m}.tilt;
        T1 = 0;
        T2 = 0;

        events = [];% col1 = start ; col2 = end

        save('events.mat','events');

        f = figure;
        ax = axes('Parent',f,'position',[0.13 0.39  0.77 0.54]);

        plot(t,tilt,'b');
        hold on
        plot(t,tilt,'b');
        axis manual
        plot([T1,T1],[min(tilt),max(tilt)],'r');
        plot([T2,T2],[min(tilt),max(tilt)],'r');
```

```
30          title('Mark Eventing');
31          hold off
32
33          b3 = uicontrol('Parent',f,'Style','slider','Position',...
34              [81,90,419,23],'value',T1, 'min',min(t), 'max',max(t));
35          bgcolor = f.Color;
36          bl8 = uicontrol('Parent',f,'Style','text','Position',...
37              [50,90,23,23],'String',num2str(min(t)),...
38              'BackgroundColor',bgcolor);
39          bl9 = uicontrol('Parent',f,'Style','text','Position',...
40              [500,90,23,23],'String',num2str(max(t)),...
41              'BackgroundColor',bgcolor);
42          bl10 = uicontrol('Parent',f,'Style','text','Position',...
43              [215,66,150,23],'String','Start Marker',...
44              'BackgroundColor',bgcolor);
45
46
47          b4 = uicontrol('Parent',f,'Style','slider','Position',...
48              [81,50,419,23],'value',T2, 'min',min(t), 'max',max(t));
49          bgcolor = f.Color;
50          bl5 = uicontrol('Parent',f,'Style','text','Position',...
51              [50,50,23,23],'String',num2str(min(t)),...
52              'BackgroundColor',bgcolor);
53          bl6 = uicontrol('Parent',f,'Style','text','Position',...
54              [500,50,23,23],'String',num2str(max(t)),...
55              'BackgroundColor',bgcolor);
56          bl7 = uicontrol('Parent',f,'Style','text','Position',...
57              [215,26,150,23],'String','End Marker',...
58              'BackgroundColor',bgcolor);
59
60
```

```
61
62          b3.Callback = @(es,ed) disp_T(b3,b4, ax, [t;tilt]);
63          b4.Callback = @(es,ed) disp_T(b3,b4, ax, [t;tilt]);
64
65          btn = uicontrol(f,'Style', 'pushbutton', 'String',...
66              'Add Events','Position',[81,0,419,23],'Value',events);
67
68          btn.Callback = @(es,ed) set_T(b3,b4);
69
70          uiwait(f);
71          load('events.mat')
72          % save eventing
73          swallowing_data{3+n,m}.events=events;
74      end
75  end
76  % Redraw eventing marks
77  function [] = disp_T(h1, h2, haxes, graph)
78    T1 = get(h1,'value');
79    T2 = get(h2,'value');
80
81    plot(haxes,graph(1,:), graph(2,:),'b');
82    hold on
83    axis manual
84    plot(haxes,[T1,T1],[min(graph(2,:)),max(graph(2,:))],'r');
85    plot(haxes,[T2,T2],[min(graph(2,:)),max(graph(2,:))],'r');
86    title('Mark Eventing');
87    hold off
88  end
89  % Save timing of events
90  function [] = set_T(h1, h2)
91    T1 = get(h1,'value');
```

```
92    T2 = get(h2,'value');
93    load('events.mat');
94
95    events(end+1,:)=[T1,T2]
96
97    save('events.mat','events');
98  end
```